



**HAL**  
open science

## The Toxicity of a Novel Antifungal Compound Is Modulated by Endoplasmic Reticulum-Associated Protein Degradation (ERAD) Components

Shriya S Raj, Karthik Krishnan, David S Askew, Olivier S Helynck, Peggy Suzanne, Aurélien Lesnard, Sylvain Rault, Ute S Zeidler, Christophe d'Enfert, Jean-Paul S Latgé, et al.

### ► To cite this version:

Shriya S Raj, Karthik Krishnan, David S Askew, Olivier S Helynck, Peggy Suzanne, et al.. The Toxicity of a Novel Antifungal Compound Is Modulated by Endoplasmic Reticulum-Associated Protein Degradation (ERAD) Components. *Antimicrobial Agents and Chemotherapy*, 2016, 60 (3), pp.1438-1449. 10.1128/AAC.02239-15 . pasteur-01427574

**HAL Id: pasteur-01427574**

**<https://pasteur.hal.science/pasteur-01427574v1>**

Submitted on 5 Jan 2017

**HAL** is a multi-disciplinary open access archive for the deposit and dissemination of scientific research documents, whether they are published or not. The documents may come from teaching and research institutions in France or abroad, or from public or private research centers.

L'archive ouverte pluridisciplinaire **HAL**, est destinée au dépôt et à la diffusion de documents scientifiques de niveau recherche, publiés ou non, émanant des établissements d'enseignement et de recherche français ou étrangers, des laboratoires publics ou privés.



Distributed under a Creative Commons Attribution - NonCommercial - ShareAlike 4.0 International License

# Toxicity of a novel antifungal compound is modulated by ERAD components

1 Shriya Raj<sup>1</sup>, Karthik Krishnan<sup>2</sup>, David S. Askew<sup>2</sup>, Olivier Helync<sup>3,4</sup>, Peggy Suzanne<sup>5</sup>,  
2 Aureslien Lesnard<sup>5</sup>, Sylvain Rault<sup>5</sup>, Ute Zeidler<sup>6,7,@</sup>, Christophe d'Enfert<sup>6,7</sup>, Jean-Paul Latgé<sup>1,#</sup>,  
3 Hélène Munier-Lehmann<sup>3,4,#</sup>, Cosmin Saveanu<sup>8,9,#</sup>

4 <sup>1</sup> Institut Pasteur, Unité des Aspergillus, Département Mycologie, 25-28 rue du docteur Roux  
5 75015, Paris, France

6 <sup>2</sup> Department of Pathology & Laboratory Medicine, University of Cincinnati, Cincinnati, OH  
7 45267-0529, USA

8 <sup>3</sup> Institut Pasteur, Unité de Chimie et Biocatalyse, 25-28 rue du docteur Roux 75015, Paris,  
9 France

10 <sup>4</sup> CNRS UMR3523, F-75015, Paris, France

11 <sup>5</sup> Centre d'Etudes et de Recherche sur le Médicament de Normandie, EA4258, UFR des  
12 Sciences Pharmaceutiques, University of Caen Basse-Normandie, Caen, France

13 <sup>6</sup> Institut Pasteur, Unité Biologie et Pathogénicité Fongiques, Département Mycologie, 25-28  
14 rue du docteur Roux 75015, Paris, France

15 <sup>7</sup> INRA USC2019, F-75015 Paris, France

16 <sup>8</sup> Institut Pasteur, Unité de Génétique des Interactions Macromoléculaires, Département  
17 Génomes et Génétique, 25-28 rue du docteur Roux 75015, Paris, France

18 <sup>9</sup> CNRS UMR3525, F-75015 Paris, France

19 @ Current address: Sandoz, Unterach, Austria

20 # Corresponding authors: jean-paul.latge@pasteur.fr (JPL), helene.munier-lehmann@pasteur.fr  
21 (HML), cosmin.saveanu@pasteur.fr (CS)

22 **Running title:** Endoplasmic reticulum-related antifungal toxicity

## Abstract

In a search for new antifungal compounds, we screened a library of 4454 chemicals for toxicity against the human fungal pathogen *Aspergillus fumigatus*. We identified sr7575, a molecule that inhibits growth of the evolutionary distant fungi *A. fumigatus*, *Cryptococcus neoformans*, *Candida albicans*, and *Saccharomyces cerevisiae* but lacks acute toxicity for mammalian cells. To gain insight into the mode of inhibition, sr7575 was screened against 4885 *S. cerevisiae* mutants from the systematic collection of haploid deletion strains and 977 barcoded haploid DAMP strains in which the function of essential genes was perturbed by the introduction of a drug resistance cassette downstream of the coding sequence region. Comparisons with previously published chemogenomic screens revealed that the set of mutants conferring sensitivity to sr7575 was strikingly narrow, affecting components of the endoplasmic-associated protein degradation (ERAD) stress response and the ER membrane protein complex (EMC). ERAD-deficient mutants were hypersensitive to sr7575 in both *S. cerevisiae* and *A. fumigatus*, indicating a conserved mechanism of growth inhibition between yeast and filamentous fungi. Although the unfolded protein response (UPR) is linked to ERAD regulation, sr7575 did not trigger the UPR in *A. fumigatus* and UPR mutants showed no enhanced sensitivity to the compound. The data from this chemogenomic analysis demonstrate that sr7575 exerts its antifungal activity by disrupting ER protein quality control in a manner that requires ERAD intervention but bypasses the need for the canonical UPR. ER protein quality control is thus a specific vulnerability of fungal organisms that might be exploited for antifungal drug development.

## 44 **Introduction**

45           The burden of fungal infections in the human population is very high, with an estimated  
46 1.5 million annual deaths worldwide, despite antifungal prophylaxis (1–3). The evolutionary  
47 proximity between mammalian and fungal cells creates a challenge for the identification of  
48 selective drug targets. Consequently, there are only a few mechanistically distinct classes of  
49 antifungal agents. The major antifungal drugs in clinical use disrupt membrane homeostasis by  
50 targeting ergosterol (4), impair cell wall integrity by inhibiting  $\beta$ -(1,3)-glucan synthase (5), or  
51 perturb nucleic acid synthesis via a fluorinated nucleotide analogue (6). The limited number of  
52 therapeutic options impedes effective management of invasive fungal infections, particularly  
53 when resistance to a drug is either emerging or an intrinsic characteristic of the fungal  
54 pathogen.

55           The identification of novel drugs and their targets can follow several strategies, ranging  
56 from the inhibition of a known protein target with a panel of inhibitors to the analysis of  
57 mutant strain sensitivity to toxic compounds (7). Chemical genomic screens analyze large  
58 collections of genetically defined mutant strains for their sensitivity to chemical libraries in a  
59 systematic manner. Data from these screens can provide insight into candidate targets for a  
60 given drug, as well as the cellular pathways required to buffer drug toxicity (8–11). The  
61 interpretation of chemogenomic screens depends on the type of mutant collection utilized for  
62 the analysis. For example, the absence of a general dosage compensation mechanism in yeast  
63 (12) allows heterozygous deletion strains to be used as tools to determine how a reduction in  
64 the level of a gene product impacts drug sensitivity. However, since heterozygous deletion  
65 strains retain some level of gene function, compensatory mechanisms could mask changes in

66 drug sensitivity. Haploid deletion strains can circumvent this problem and increase the  
67 sensitivity of the screen. The resulting chemogenomic profile, or pattern of mutants that are  
68 affected by a given compound, is predictive of the mechanism of action and has been  
69 successfully applied to drug lead identification and target classification in yeast (13). Further  
70 insight into pathways that are modulated by a compound can be obtained by developing *in*  
71 *silico* comparison tools that link the results of a chemogenomic analysis to the data of other  
72 published large-scale chemogenomic or genetic interaction screens (14, 15, for examples).

73 Most of the large chemogenomic data sets currently available have investigated non-  
74 essential gene deletions in haploid strains (10, 16). Essential genes, representing about one  
75 sixth of all *S. cerevisiae* genes, are more difficult to study in haploid or heterozygous deletion  
76 strains, so an alternative approach is the use of Decreased Abundance by mRNA Perturbation  
77 (DAmP) strains. DAmP strains contain a drug resistance marker inserted into the 3'  
78 untranslated region (UTR) of a gene, resulting in defects in mRNA stability that can create  
79 hypomorphic alleles for phenotypic analysis of essential gene function (17). These strains have  
80 provided important insights into gene function, as well as the response of cells to stress (18,  
81 for example).

82 In this study, we report the identification of sr7575, a small molecule with fungistatic  
83 activity against *S. cerevisiae* and three genera of human fungal pathogens: *A. fumigatus*, *C.*  
84 *neoformans*, and *C. albicans*. We employed a genome-wide approach to characterize the mode  
85 of action of sr7575, using a systematic determination of *S. cerevisiae* deletion and DAmP  
86 mutant sensitivity to the drug, combined with extensive *in silico* comparisons with large-scale  
87 datasets from published chemogenomic and genetic interaction screens. The strategy led to the  
88 conclusion that *S. cerevisiae* and *A. fumigatus* mutants that are deficient in ER-associated

89 degradation (ERAD), a degradative pathway that disposes of misfolded proteins that arise in  
90 the ER membrane or lumen (19) are hypersensitive to sr7575. Collectively, these data  
91 implicate ER protein quality control as the target of sr7575 toxicity in evolutionarily distant  
92 fungi, and suggest that further analysis of compounds that disrupt ER homeostasis may  
93 provide novel avenues for antifungal drug development.

## 94 **Materials and Methods**

### 95 **Screening procedure of the CERMN chemical library.**

96 All robotic steps were performed on a Tecan Freedom EVO platform. Compounds were  
97 transferred from mother plates into clear, flat bottom, barcoded tissue culture 96-well plates  
98 (Greiner Bio One): 1  $\mu$ L of a DMSO solution containing 3.3 mg/mL of each compound was  
99 spiked into dry wells of daughter plates (80 compounds per plate). For each plate, columns 1  
100 and 12 served as controls: 8 positive controls spiked with DMSO alone provided the reference  
101 as 100% growth and 8 negative controls contained the antifungal drug amphotericin B at 15  
102  $\mu$ g/mL to kill all cells. 130  $\mu$ L of a mixture containing 10 volumes of conidial suspension  $10^5$   
103 conidia/mL (in RPMI with 0.1% Tween 20) and 3 volumes of resazurin 0.01% was added to  
104 each well. After 48 hours of incubation at 37°C, the absorbance at 570 nm (measurement  
105 wavelength) and 604 nm (reference wavelength) were measured on a Safire2 (Tecan)  
106 microplate reader. The data were normalized using the following formula: % viability = 100 x  
107 (sample value - average value of negative controls) / (average of positive controls - average of  
108 negative controls).

109 For analysis of toxicity to human cells, compounds were added to HeLa cells at a  
110 concentration of 10  $\mu$ M (2.8  $\mu$ g/mL for sr7575) and the release of cytoplasmic lactate

111 dehydrogenase was measured using the ELISA-based Cytotoxicity Detection Kit (Roche),  
112 according to the manufacturer's recommendations. Mutagenic activity was tested in the  
113 bacterial reverse mutation test, either in the presence or absence of a rat metabolizing system  
114 (performed by CiToxLAB Safety and Health Research Laboratories). To determine acute  
115 mouse toxicity, groups of four NMRI mice were given a single dose of sr7575 (100 mg/kg) by  
116 i.p. injection, and mortality was monitored for 3 days.

### 117 **Yeast strains, growth, and media.**

118 All strains used in this study are described in Table S4. The pooled haploid deletion  
119 library (MATa) contained deletions in 4885 non-essential genes along with DAmP  
120 modifications of 977 essential genes (20, 21). Wild type (WT) *S. cerevisiae* strain BY4741  
121 was routinely maintained on YPD agar (1% yeast extract, 2% peptone, 2% dextrose, 2% bacto  
122 agar; YPDA).

123 For *S. cerevisiae* serial dilution spot assays, fresh colonies from plates were used to  
124 inoculate overnight cultures in YPD. The next morning, cultures were washed once, diluted to  
125 OD<sub>600</sub> 1 in PBS and serial ten-fold dilutions were carried out in a 96-well plate. 10 µL of each  
126 dilution was spotted onto SC medium (containing 6.7 g/L yeast nitrogen base with ammonium  
127 sulfate, BD Difco, with all amino acids, 2% dextrose and 2% bacto agar) lacking or  
128 supplemented with 0.25 µg/mL sr7575. Plates were incubated at 30°C and growth was  
129 monitored every 24 h over three days. Spot assays on SC supplemented with the analog sr7576  
130 were conducted in a similar fashion.

131 The same serial dilution spot assay used to assess sensitivity in *S. cerevisiae* was used  
132 for *C. albicans* and *C. neoformans*, with the exception that the plates were supplemented with

133 sr7575 between 1-8  $\mu\text{g}/\text{mL}$  and were incubated at 37°C.

#### 134 **Verification of *S. cerevisiae* mutant strains.**

135 The following mutants were extracted from the gene deletion library maintained in the  
136 96-well format(8): *YBR283C* (*SSH1*), *YCL045C* (*EMC1*), *YDL020C* (*RPN4*), *YDL226C*  
137 (*GCS1*), *YER019C-A* (*SBH2*), *YER090W* (*TRP2*), *YKL126W* (*YPK1*), *YKL207W* (*EMC3*),  
138 *YML105C* (*SEC65*; DAmP strain), *YMR022W* (*UBC7*), *YMR264W* (*CUE1*), *YOL013C*  
139 (*HRD1*), *YOR008C* (*SLG1*), *YOR153W* (*PDR5*), *YPR060C* (*ARO7*), *YHR079C* (*IRE1*),  
140 *YFL031W* (*HAC1*), *YBR201W* (*DER1*), *YLR207W* (*HRD3*), *YIL030C* (*SSM4/DOA10*),  
141 *YDL190C* (*UFD2*), *YGL013C* (*PDR1*), *YNL181W* (DAmP strain), and *YML125C* (*PGA3*;  
142 DAmP strain). Genomic DNA was extracted using phenol-chloroform followed by ethanol  
143 precipitation. Mutants were verified by PCR amplification using a common forward primer  
144 annealing to the KanMX cassette (KaniF) and gene specific reverse primers (oligonucleotides  
145 listed in Table S5).

#### 146 **Complementation tests in *S. cerevisiae*.**

147 Complementation tests were performed with plasmids from the Molecular Barcoded  
148 Yeast ORF collection (MoBY-ORF) (22). *URA3* plasmids carrying ORFs corresponding to  
149 genes *ARO7*, *CUE1*, *EMC1*, *EMC3*, *HRD1*, *RPN4*, *SSH1*, and *UBC7* (Table S4) were  
150 recovered from *E.coli* grown in LB medium (1% tryptone, 0.5% yeast extract, 1% NaCl, 1.5%  
151 bacto agar) supplemented with chloramphenicol (60  $\mu\text{g}/\text{ml}$ ) and kanamycin (50  $\mu\text{g}/\text{ml}$ ) (22).  
152 500 ng of each plasmid was transformed into the appropriate yeast deletion parent following  
153 the lithium acetate protocol (23) and *URA3*-expressing transformants were selected on SC  
154 medium lacking uracil. The resulting transformants were purified by passaging onto fresh SC



155 (-URA) medium and four clones of each transformant-set were screened by colony PCR using  
156 a gene-specific primer pair (Table S5), generating product sizes ranging between 500-1000 bp.  
157 The deletion parent was always included as a negative control. Complemented strains were  
158 screened in parallel with the parental deletion strains in spot assays.

#### 159 **Overexpression tests in *S. cerevisiae*.**

160 2 micron-based *LEU2* plasmids from the systematic overexpression library (24)  
161 corresponding to regions of the yeast genome that contain the ORFs *PDR1*, *PDR5*, *PDR12*,  
162 and a control lacking intact genes (Table S4) were recovered from *E. coli* DH10B cultures  
163 grown in LB medium supplemented with kanamycin (50 µg/mL), transformed into wild type  
164 BY4741, and transformants selected on SC (-LEU) plates. Transformants were purified by  
165 passaging onto fresh SC (-LEU) plates. Overexpressing strains were screened by serial  
166 dilution spot assays on SC medium supplemented with increasing concentrations of sr7575.

#### 167 **Chemogenomic profiling.**

168 Concentrations of sr7575 that inhibit WT growth by 10-20% in liquid culture were  
169 determined using the haploid strain BY4741 (MATa; *his3Δ1*; *leu2Δ0*; *met15Δ0*; *ura3Δ0*).  
170 Single colonies from fresh YPDA plates were inoculated into 10 ml YPD and incubated at  
171 30°C for 14 h. Cultures were diluted to OD<sub>600</sub> of 0.01 and grown to an OD<sub>600</sub> of 0.05 prior to  
172 the addition of increasing concentrations of sr7575 (0.0625 µg/mL to 0.5 µg/mL). DMSO was  
173 used as a vehicle control but there was no observable difference in growth rate between the  
174 no-vehicle and DMSO-treated cultures. Growth was monitored by measuring the OD<sub>600</sub> every  
175 hour, starting from 0 h until 10 h (Fig. S2A).

176 Pooled 400 mL cultures of the haploid deletion library were grown for 12 generations in

177 the presence of sr7575 at 0.125  $\mu\text{g}/\text{mL}$  or DMSO vehicle-control. Amplified TAG products  
178 from the pooled cultures were hybridized to Agilent barcode-specific microarrays (platform  
179 GPL18088, GEO) as previously described (14). Images obtained with a GenePix 4200AL  
180 scanner were annotated by using GenePix Pro 7 (Molecular Devices, CA, USA). Gpr files  
181 were normalized separately for the UP and DOWN barcodes and aggregated for each mutant.  
182 Raw and normalized data were deposited in the GEO database under identifier GSE60934.  
183 Only results for which data were obtained in two independent biological replicates were  
184 further considered for analysis. A total of 4909 mutants, including both deletion and DAMP-  
185 modified strains, showed consistent growth measurements (Table S6), with a Pearson  
186 correlation coefficient between the two series of log-transformed values of 0.78.

#### 187 **Gene set enrichment analysis and correlations.**

188 Over-representation of GO terms in the chemogenomic screen results was analyzed  
189 using the web interface at <http://go.princeton.edu/cgi-bin/GOTermFinder> to the GO Term  
190 finder program (25). This program identifies enriched GO terms by calculating the frequency  
191 with which one expects to encounter a number of genes having the same annotation in a subset  
192 of genes (hypergeometric distribution). Correlations with published large-scale datasets were  
193 computed using the R project (<https://cran.r-project.org/>) function ‘cor.test’, using either  
194 “*pearson*” or “*spearman*” as comparison methods. Treatments or gene deletion perturbations  
195 were ranked in decreasing order of calculated correlation coefficients.

#### 196 ***A. fumigatus* strains, growth, and media.**

197 WT *A. fumigatus* strain kuA and deletion mutants *derA* $\Delta$ , *hacA* $\Delta$ , *hrdA* $\Delta$ , and  
198 *hrdA* $\Delta$ /*derA* $\Delta$  were maintained on malt slants (2% malt extract, 2% bacto agar) while strains

199 *ireA*Δ and *hacA*Δ/*derA*Δ were maintained on *Aspergillus* minimal medium (MM) with 5 mM  
200 ammonium tartrate as the nitrogen source and osmotically stabilized with 1.2 M sorbitol (26).  
201 G418 was obtained from Invitrogen and Sigma Aldrich was the source for ampicillin,  
202 kanamycin, and chloramphenicol.

203 Conidia from *ireA*Δ and *hacA*Δ/*hrdA*Δ strains were recovered from *Aspergillus* MM +  
204 1.2 M sorbitol slants, while that of the parental *kuA* strain and the remaining deletion strains  
205 were recovered from 10-day old malt slants in 0.05% Tween. Conidia were diluted to 10<sup>7</sup>  
206 conidia/mL and serial 10-fold dilutions were carried out in a 96-well plate prior to spotting 10  
207 μL of each dilution onto MOPS-buffered RPMI-1640 pH 7.0 plates in the presence or absence  
208 of 5 μg/mL sr7575. The analog sr7576 precipitated out of solution in RPMI-1640 media and  
209 was therefore not included in the analysis. Plates were incubated at 37°C and growth was  
210 monitored over four days.

#### 211 **MIC determination.**

212 Determination of the minimal inhibitory concentration (MIC) for yeast strains was  
213 carried out by the CLSI M27-A3 broth microdilution method (27). Growth inhibition of  
214 *Aspergillus* strains was monitored using a colorimetric test described earlier (28). The MIC of  
215 *A. fumigatus* strain that constitutively expresses DsRed fluorescent protein (29) was  
216 determined following growth for 24 h at 37°C by measuring fluorescence using a Biotek  
217 Synergy fluorescent microplate reader with an excitation wavelength of 254 nm and emission  
218 filter set at 291 nm. The relative fluorescence units were plotted against the compound  
219 concentrations to determine MIC.

220 **Measurement of fungistatic or fungicidal activity.**

221 For yeast, freshly growing YPD cultures were diluted to OD<sub>600</sub> 0.001. sr7575 was added  
222 at 0.625 µg/mL, amphotericin B at 0.5 µg/mL, and DMSO was used as a vehicle control.  
223 100 µL aliquots were recovered for plating on YPDA. Cultures were grown for 16 h, cells  
224 were washed once in 1X PBS and 100 µL of serially diluted samples were plated. Colonies  
225 were counted following 48 h and normalized to the OD<sub>600</sub>.

226 For *A. fumigatus*, 50 mL RPMI cultures with a starting cell number of 1x10<sup>5</sup> conidia/ml  
227 were setup in the presence or absence of 5 µg/mL sr7575 (in duplicate). 100 µL aliquots were  
228 recovered for enumeration of colony forming units. Following 16 h of growth, mycelia from  
229 one pair of flasks were filtered and mycelial dry weight estimated. From the second pair,  
230 100 µL from the drug-treated flask was serially diluted and plated to assess viability.

231 **qRT-PCR.**

232 *A. fumigatus* conidia were inoculated into YG medium (0.5% yeast extract, 2% glucose)  
233 and incubated overnight at 37°C, 200 rpm. The mycelium was treated with the indicated  
234 concentrations of sr7575 or dithiothreitol (DTT), along with appropriate vehicle controls, for  
235 1 h. The mycelia were harvested by filtration and lysed by crushing in liquid nitrogen. RNA  
236 was isolated using the TRIzol reagent, treated with DNase to remove traces of DNA, and  
237 reverse-transcribed using M-MuLV reverse transcriptase (NEB) together with an oligo-d(T)  
238 primer. Quantitation of *bipA* and *tigA* mRNA expression was performed by qRT-PCR, as  
239 previously described (30).

## 240 **Results**

### 241 **Identification of a new inhibitor of fungal growth**

242 In a search for new antifungals, we tested the toxicity of 4454 chemicals from the  
243 CERMN compound library against *A. fumigatus* using the strategy outlined in Fig. 1A. The  
244 CERMN library is part of the French national collection of chemicals (31) and was built since  
245 1998 to be used in the framework of partnerships with public research laboratories. The  
246 dynamic range and degree of separation between positive and negative controls in the screen  
247 was evaluated by computing the  $Z'$  score (32). The average  $Z'$  value was  $0.92 \pm 0.03$ ,  
248 indicating a robust and reliable assay. Data analysis identified 76 hits showing greater than  
249 90% fungal growth inhibition, which were clustered into 7 chemical families and 29 singletons  
250 (Table S1). Compounds with known effects on human physiology (33), or which showed  
251 cytotoxicity for HeLa cells in a lactate dehydrogenase release assay, were eliminated from  
252 further consideration. The compound sr1810 was active against *A. fumigatus* and was selected  
253 for further analysis. Since sr1810 consisted of a mixture of two isomers, 75% of sr7575 (1)  
254 (Fig. 1A) and 25% of sr7576 (2), we synthesized each isomer (Fig S1, A and B) and found that  
255 it was only sr7575 that was responsible for the antifungal activity. The sr7575 compound  
256 showed no mutagenic activity in the bacterial reverse mutation test, and no acute toxicity was  
257 observed in mice at a dose of 100 mg/kg.

258 To gain insight into the structural basis for sr7575 antifungal activity, we prepared thirty  
259 analogues using aniline derivatives with different substitutions in the first reaction  
260 (compounds 3-32, Tables S2 and S3, synthesis detailed in Text S1). Growth inhibition tests  
261 with these compounds showed that at least two features of sr7575 were required for its  
262 antifungal potency: the chlorine at position 4 of the phenyl group and the positioning of the

263 nitro group in relation to the pyrrole moiety (Table S2).

264 In addition to its effects on *A. fumigatus*, sr7575 was active against *A. flavus* (Fig. 1B),  
265 *C. neoformans*, *C. albicans* (Fig. 1C), and *S. cerevisiae* (Fig. 1D) on plates and in liquid  
266 medium at inhibitory concentrations ranging from 0.6 to 10  $\mu\text{g}/\text{mL}$  (Fig. S2A, B, C, D). More  
267 than 90% of either *S. cerevisiae* or *A. fumigatus* cells were able to resume growth after a 16 h  
268 incubation in the presence of sr7575 (0.625  $\mu\text{g}/\text{mL}$  and 5  $\mu\text{g}/\text{mL}$ , respectively) indicating that  
269 the compound exerts a fungistatic effect.

#### 270 **ERAD-deficient mutants of *S. cerevisiae* are hypersensitive to sr7575**

271 To gain insight into the mechanism by which sr7575 perturbs fungal physiology, the  
272 effect of sr7575 was tested on the growth rate of each of 4885 haploid yeast deletion strains in  
273 the systemic deletion collection (20). In addition, sr7575 activity was measured on 977 locus  
274 tagged barcoded DAmP (17) mutants of essential genes that were previously generated in our  
275 laboratory (21). This collection of gene knockout and DAmP strains contains molecular  
276 barcodes to facilitate detection and quantitation of DNA by custom Agilent microarrays (34,  
277 35). Following the strategy outlined in Fig. 1A, the normalized ratio of the hybridization  
278 signal in the presence or absence of treatment was used as an estimate of relative growth rate  
279 in pools of mutants. Only a fraction of mutant strains showed hypersensitivity to sr7575, as  
280 indicated by the left tail of the distribution for sensitivity values (Fig. 2A). The strain that  
281 showed the most dramatic increase in sr7575 sensitivity harbors a deletion of the *PDR1* gene,  
282 encoding the main regulator of multidrug resistance in yeast (36). Pdr1 is a transcriptional  
283 activator for xenobiotic efflux transporter genes, thereby governing resistance to numerous  
284 toxic compounds. It is likely that the effect of *PDR1* deletion on sensitivity to sr7575 is

285 mediated through the plasma membrane ATP-binding cassette (ABC) transporter Pdr5, since  
286 *PDR5* is a known target of Pdr1 (37) and the *pdr5* mutant was ranked 6<sup>th</sup> among deletion  
287 strains that were most affected by *sr7575*.

288 To identify cellular pathways or protein complexes that allow cells to counteract *sr7575*  
289 effects, we used a gene set enrichment analysis on 89 mutant strains that showed an average  
290 increase in generation time of at least 10% relative to WT in the presence of *sr7575*. The most  
291 over-represented pathway in the dataset was ER-associated protein degradation (ERAD),  
292 specifically the GO term “ER-associated ubiquitin-dependent protein catabolic process”  
293 (GO:0030433), with a p-value corrected for multiple hypotheses testing of  $1.5 \times 10^{-6}$ . This set  
294 included *CUE1*, *UBC7*, *HRD1*, *HRD3*, *UFD2*, *UBX4*, *SSM4 (DOA10)*, *DSK2*, and *UBX2*,  
295 encompassing one fifth of the total number of genes annotated to this term (Fig. 2B). The  
296 second most over-represented GO term was “aromatic amino acid family biosynthetic  
297 process” (GO:0009073). However, strains deficient in this pathway are known to exhibit a  
298 multidrug response signature (9), so the study of the corresponding strains was not pursued  
299 further.

300 Cellular component enrichment analysis was used to determine whether any of the 89  
301 proteins selected in the screen were linked to the same protein complex or intracellular  
302 location. The ER membrane protein complex (EMC) was the most over-represented group by  
303 this analysis, with a p-value of  $2 \times 10^{-7}$ . In addition to gene deletions directly affecting *EMC1*,  
304 *EMC3*, *EMC4* and *EMC5*, deletions affecting dubious ORFs which overlap with *EMC2*  
305 (*YJR087W*) and *EMC1 (YCL046W)* that are distinct mutants of these genes, were also present  
306 in this dataset. Members of the EMC complex are required for efficient protein folding in the  
307 ER (38), potentially through roles in phospholipid metabolism at the ER membrane (39).

308 Other components of the ER membrane showed enrichment, including 10 of 58 genes  
309 annotated as "intrinsic components of the ER membrane" (GO:0031227) and two DAmP-  
310 modified essential genes of uncharacterized function (*YNL181W* and *PGA3*). In addition,  
311 several genes encoding components of the signal recognition particle (SRP) involved in co-  
312 translational targeting of proteins into the ER showed enrichment: *sec65*-DAmP, *srp21*-DAmP,  
313 *shr3*-DAmP, *ssh1* $\Delta$ , and *sbh2* $\Delta$ . Taken together, these findings indicate that sensitivity to the  
314 inhibitory effects of *sr7575* is exacerbated by defects in the ERAD stress response, as well as  
315 by alterations in ER membrane composition that affect optimal ER protein translocation and  
316 folding.

#### 317 **The *sr7575* sensitivity profile suggests a UPR-independent stress response**

318 The effects of *sr7575* on haploid yeast deletion strains were compared to profiles  
319 obtained from 1,824 different chemicals in a recently published large-scale chemogenomic  
320 screen (16). The compound CMB4166 had the highest Spearman correlation coefficient in this  
321 comparison (Fig. 2C,  $r=0.44$ ) and showed a remarkably similar profile to that of *sr7575*  
322 (Fig. 2D). Most of the strains showing sensitivity to *sr7575* were also sensitive to CMB4166  
323 (Fig. 2E), suggesting that the two compounds trigger similar cellular responses. However,  
324 CMB4166 is a macrolide (D. Hoepfner, personal communication) and shares no structural  
325 homology to *sr7575*.

326 To acquire insights into the specificity of the response to *sr7575*, we compared its  
327 sensitivity profile to published results on 3,356 other chemical compounds (10). The pattern of  
328 *sr7575* sensitive mutants revealed little-to-no similarity to profiles obtained from the other  
329 compounds in this comparison. For example, the maximum computed Pearson correlation



330 coefficient was 0.27 for the compound k048-0007 (screen SGTC\_352, Fig. S3A). However,  
331 this correlation was due to strains with deletions in *PDR1*, *RPN4*, or *GCSI*, which confer  
332 sensitivity to multiple stresses (Fig. S3C). To avoid the typically large effect of outliers on the  
333 Pearson correlation, we also tested correlation via the Spearman non-parametric test that uses  
334 ranks rather than values. The maximum correlation by this approach was also low (0.18),  
335 identifying the compound 4245-1575 used in screen SGTC\_513 (Fig. S3B). Most of the  
336 correlation in this case could be attributed to the hypersensitivity of the *ubc7Δ* and *cue1Δ*  
337 ERAD mutants (Fig. S3D). Since this second compound was annotated as having an unfolded  
338 protein response (UPR) signature (10), we also tested the correlation between the profile of  
339 sr7575 and tunicamycin, a well-known and widely used inducer of the UPR (40, 41, for  
340 review). However, no similarity was found (Fig. S3E). Collectively, these comparisons suggest  
341 that while many sensitivity profiles are related and indicate the most frequent types of cellular  
342 responses to chemical toxicity (10), the profile obtained for sr7575 was specific, with  
343 similarity to only one compound out of over 5000 chemicals analyzed.

344 Large-scale chemical toxicity screens are complementary to synthetic genetic array  
345 analyses (SGA), in which double deletion mutant strains are used to determine functional  
346 interactions between genes. We compared the sensitivity profile of sr7575 with the results  
347 from 1711 SGA screens (42). The closest hit was the profile shown by a strain harboring a  
348 DAmP modification of the essential gene *PGA3* (17) (Fig. S4A). The correlation between the  
349 sr7575 and *PGA3* profiles was robust, since it also ranked 5<sup>th</sup> when estimated using Spearman  
350 correlation (Fig. S4B). Despite the low value of the correlation coefficient (0.23), several  
351 strains containing gene deletions were affected by both sr7575 treatment and replacement of  
352 *PGA3* with the *pga3*-DAmP allele, including the ERAD-associated genes *cue1Δ*, *ubc7Δ*,

353 *ufd2Δ*, *ssm4Δ*, and EMC complex components (Fig. S4C). A role in newly synthesized protein  
354 trafficking has been proposed for Pga3 (43), raising the possibility that its presence in our  
355 dataset is due to a function that impacts ER homeostasis.

356 The gene deletion that ranked second in terms of correlation with the *sr7575* profile  
357 involved *CHO2*, encoding a phosphatidyl N-methyltransferase required for phosphatidyl-  
358 choline synthesis. The absence of *CHO2* renders yeast cells dependent on the UPR for survival  
359 (42, 44), suggesting that *CHO2* contributes to ER homeostasis. Consistent with this, *CHO2*  
360 deletion shows an aggravating interaction with the loss of EMC genes in terms of yeast growth  
361 (39).

362 A summary of the correlations between *sr7575* sensitivity profiles and those derived  
363 from published chemogenomic screens is shown in Fig. 3. Since the numerical values reported  
364 for genetic and chemogenomic screens are not readily comparable, the ranking of the different  
365 mutants in each screen was used to generate a meaningful graphical display. The resulting  
366 heatmap (Fig. 3A) highlights the unique ERAD signature of *sr7575* relative to currently  
367 published screens. A schematic illustrating the ER membrane proteins involved in the ERAD  
368 pathway is shown for perspective (Fig. 3B). Since ERAD is known to work in concert with the  
369 UPR to relieve ER stress, it is interesting to note that hypersensitivity to *sr7575* was observed  
370 for ERAD mutants, but not for the UPR-inactivated strains *ire1Δ* and *hac1Δ*. Taken together,  
371 these data are consistent with a model in which *sr7575* toxicity is counteracted by a functional  
372 ERAD machinery, independent of signaling through the UPR pathway.

### 373 **Specific ERAD deficiencies enhance *sr7575* toxicity in *S. cerevisiae***

374 Seventeen *S. cerevisiae* mutant strains were selected to validate the results of the

375 chemogenomic screen, encompassing strains with deletions in components of the ERAD and  
376 proteasome pathways, the EMC, the Ssh1 co-translocase, the PDR network, aromatic acid  
377 biosynthesis, and DAmP modifications of *YNL181W* and *PGA3*. Each strain was analyzed  
378 individually for sr7575 susceptibility, using a subinhibitory concentration for WT (Fig. 4A and  
379 Fig. S5). A strain deleted for aromatic amino acid biosynthesis (*aro7Δ*) showed increased  
380 sr7575 sensitivity (Fig. 4A), consistent with the pleiotropic effects of this mutation on stress  
381 response.

382 As predicted by the chemogenomic screen, mutants in the *PDR5* multidrug transporter  
383 and its transcriptional activator *PDR1* were hypersensitive to sr7575 (Fig. S5). Conversely,  
384 overexpression of *PDR1* and *PDR5*, but not *PDR12* rendered *S. cerevisiae* cells tolerant to  
385 high concentrations of sr7575 (Fig. S6A). This phenotype was conserved across fungal  
386 species, since clinical isolates and laboratory *C. albicans* strains that overexpress *CDR1*, the  
387 ortholog of *S. cerevisiae* *PDR5*, were also tolerant to sr7575 (Fig. S6B).

388 Deletions of genes coding for EMC members, *EMC1* and *EMC3*, and the co-  
389 translational translocase *SSH1* conferred increased sensitivity to sr7575, as suggested by the  
390 chemogenomic screen. However, a mutant in *SBH2*, which functions in the Ssh1 translocase  
391 complex (45), did not show increased sensitivity at least at this concentration (Fig. S5).  
392 Hypersensitivity to sr7575 was confirmed for components of the ERAD complex, including  
393 the Hrd1 E3 ubiquitin ligase, the E2 ubiquitin conjugating enzyme Ubc7, and the ER  
394 membrane-resident recruiter Cue1 (46–48) (Fig. 4A). Although the ERAD component Der1  
395 (49) was not identified in our chemogenomic screen, a mild increase in sr7575 sensitivity was  
396 observed for this mutant (Fig. S5), consistent with ERAD involvement in sr7575 effects.  
397 sr7575 hypersensitivity was also validated for a strain lacking *RPN4*, encoding a

398 transcriptional activator of proteasome genes (Fig. 4A). Since proteasomal degradation is the  
399 final step in the disposal of misfolded proteins by ERAD, this finding is consistent with the  
400 notion that sr7575 affects protein quality control in the ER. In conclusion, these findings  
401 demonstrate that components of the ERAD pathway are necessary to protect yeast cells from  
402 the toxic effects of sr7575 in *S. cerevisiae*, suggesting a mechanism of action that involves  
403 perturbation of ER protein quality control.

#### 404 **ERAD protects against sr7575 toxicity in *A. fumigatus*, but is UPR-independent**

405 The UPR is a stress response pathway that communicates information on ER  
406 homeostasis to the nucleus (40, 41). The pathway is triggered by misfolded proteins, which  
407 accumulate in the ER when the demand for secretion exceeds ER folding capacity, or when the  
408 cell encounters adverse environmental conditions. Unfolded proteins are sensed by the ER-  
409 transmembrane sensor Ire1, which triggers the synthesis of Hac1, a transcription factor. Hac1  
410 translocates to the nucleus and upregulates the expression of chaperones, folding enzymes, and  
411 other proteins that support ER function (44, 50). Since ERAD mutants are hypersensitive to  
412 sr7575, and ERAD capacity can be regulated by the UPR, we were surprised to find that  
413 neither *HAC1* nor *IRE1* were identified in the sr7575 chemogenomic screen. The UPR  
414 independence of this response was confirmed by susceptibility testing: yeast *ire1Δ* and *hac1Δ*  
415 mutants were not affected by sr7575 at concentrations of up to 0.5 μg/mL (Fig. 4C). These  
416 findings suggest that ERAD protects against sr7575 toxicity through a mechanism that is  
417 independent of the UPR in *S. cerevisiae*.

418 Consistent with the results obtained in *S. cerevisiae*, UPR mutants of *A. fumigatus* that  
419 lack either the ER sensor IreA or the transcription factor HacA showed no hypersensitivity to

420 sr7575 (Fig. 5A). As in yeast, the *hrdA*Δ mutant, which lacks the ortholog of *S. cerevisiae*  
421 *HRD1*, showed increased sensitivity to sr7575. A *derA*Δ mutant that is deficient in the DerA  
422 component of the HrdA ERAD complex showed no increase in sr7575 sensitivity. However, a  
423 double deletion mutant lacking both DerA and HrdA showed greater sensitivity to sr7575 than  
424 a mutant lacking HrdA alone, underscoring the importance of the Hrd1 complex in the  
425 response to sr7575 toxicity. We conclude that sr7575 action involves the inhibition of an  
426 evolutionarily conserved target, necessitating the intervention of the ERAD complex  
427 Hrd1/HrdA in both *S. cerevisiae* and *A. fumigatus*.

428 The ERAD-enriched signature for sr7575 suggested that some aspect of ER protein  
429 quality control is adversely affected by this compound. However, since UPR deficient strains  
430 of *S. cerevisiae* or *A. fumigatus* showed no increase in sr7575 sensitivity, the results suggest  
431 that a UPR-independent mechanism of ERAD activity is involved in the sr7575 response. To  
432 confirm UPR independence, qRT-PCR was used to measure mRNA levels for two well-known  
433 UPR target genes: the ER chaperone *bipA* and the protein disulfide isomerase *tigA*. As  
434 expected, the expression of both genes was strongly induced by treatment with a sub-  
435 inhibitory concentration of dithiothreitol (DTT, 1 mM), a well-known inducer of the UPR  
436 (Fig. 5B). By contrast, no increase in expression was observed following treatment with a sub-  
437 inhibitory concentration of sr7575 (0.1 μg/mL). In addition, pretreatment with sr7575 for 1 h  
438 prior to DTT exposure failed to block UPR activation. These results indicate that while  
439 exposure to sr7575 does not trigger the UPR, it was also unable to prevent UPR activation by  
440 DTT. We conclude that sr7575 is unlikely to target UPR signaling for its toxic effects in  
441 *A. fumigatus* or *S. cerevisiae*, consistent with the UPR-independent response suggested by the  
442 chemogenomic screen.

## 443 **Discussion**

444 In this study, we describe the identification of a novel antifungal compound, sr7575 that  
445 was active against species from four fungal genera. Chemogenomic profiling in *S. cerevisiae*  
446 demonstrated that the set of genes required for protection against sr7575 was markedly  
447 narrow, involving components of the ERAD stress response and other components of the ER  
448 membrane. The function of the ERAD pathway is to maintain protein quality control in the ER  
449 by eliminating toxic unfolded proteins that may accumulate in the fungus during periods of  
450 high secretory activity, or when the organism encounters adverse environmental conditions.  
451 This disposal mechanism centers on a multi-protein complex in the ER membrane that  
452 selectively identifies misfolded proteins in the ER lumen or membrane and transports them  
453 back into the cytoplasm for degradation by the proteasome. The results from our  
454 chemogenomic screen demonstrate that mutants of this complex, either in *S. cerevisiae* or  
455 *A. fumigatus*, are hypersensitive to sr7575 inhibition, suggesting that the antifungal effects of  
456 this compound involves a disruption of ER protein quality control.

457 ER protein quality control is also affected by the UPR, a signaling pathway that counters  
458 the accumulation of unfolded proteins in the ER by increasing the expression of chaperones  
459 and other proteins involved in protein folding when the demand for secretion exceeds the  
460 folding capacity of the organelle. A tight coordination between the UPR and ERAD pathways  
461 was demonstrated in yeast where UPR mutants have decreased ERAD activity whereas ERAD  
462 mutants exhibit constitutive UPR upregulation (50). In addition, although ERAD is sufficient  
463 to eliminate misfolded proteins that continually arise during normal growth, it requires the  
464 UPR for optimal degradative capacity under conditions of severe ER stress (51). Basal ERAD  
465 activity is thus sufficient to handle low levels of unfolded proteins and is UPR-independent.

466 However, upregulation of ERAD activity by the UPR is needed when the level of unfolded  
467 proteins reaches a critical threshold of toxicity. The connection between these pathways is also  
468 evident in *A. fumigatus*, where mutants deficient in both the UPR and ERAD are less fit than  
469 those lacking the UPR or ERAD alone (52).

470 In view of the link between the UPR and ERAD pathways, we were surprised to find  
471 that neither *ire1Δ* nor *hac1Δ* were among the strains most affected by sr7575 in our  
472 chemogenomic screen, and that these strains showed no increase in sr7575 sensitivity when  
473 tested individually. In addition, our experiments revealed that sr7575 did not trigger the UPR,  
474 nor did it prevent the UPR from being activated by DTT, a strong inducer of unfolded  
475 proteins. These observations suggest that sr7575 does not cause the widespread protein  
476 unfolding that is typical of strong ER stress aggravators such as DTT and tunicamycin.  
477 Specific ER stress can be induced, for example, by expressing topologically abnormal ERAD-  
478 targeted integral membrane proteins without inducing the canonical UPR pathway in yeast  
479 (53).

480 The ability of sr7575 to inhibit the growth of fungi but not human cells raises the  
481 possibility that it targets a fungal-specific process. Our chemogenomic screen identified  
482 *ynl181w*-DAmP as one of the top 10 strains most affected by sr7575 toxicity. *YNL181W*  
483 encodes an essential ER-membrane protein, the function of which is currently unknown, but is  
484 speculated to involve an oxido-reductase activity (54, 55). The Ynl181w protein is conserved  
485 among fungi (Fig. 6A) and has no metazoan orthologue, as defined in the OrthoMCL database  
486 (56). Since the protein is essential, a heterozygous *YNL181W/ynl181wΔ* deletion strain was  
487 previously used to study its function in chemogenomic investigations (10, 16). We were  
488 especially interested in the effects of chemical CMB4166 in these studies because our data

489 revealed that the strain sensitivity profile for that compound (16) most closely resembled that  
490 of sr7575 (Fig. 2C, D, E). A striking finding from this comparison was that the heterozygous  
491 deletion strain of *YNL181W* was among the strains most affected by CMB4166 (Fig. 3A),  
492 indicating that the absence of Ynl181w sensitizes yeast to both sr7575 and CMB4166.

493 A DAmP modification of *YNL181W* has been previously combined with a large-scale  
494 genetic screen to identify mutations that synergize with loss of *YNL181W* function (42). A  
495 comparison of the sr7575 sensitivity profile with the results of this genetic screen identified  
496 several ERAD mutants that were affected by both DAmP modification of *YNL181W* and by  
497 treatment with sr7575, including *UBC7*, *CUE1*, and *RPN4* (Fig. 6B). The connection to *UBC7*  
498 was particularly remarkable because a similar synergistic growth defect associated with  
499 *ynl181w*-DAmP and *ubc7* $\Delta$  mutation was observed in two other large-scale studies (17, 57).  
500 The correlation between Ynl181w mutation and sr7575 sensitivity obtained by  
501 chemogenomics was confirmed on plates by showing that a *ynl181w*-DAmP mutant was  
502 hypersensitive to sr7575 (Fig. 6C). We speculate that Ynl181w could be involved in processes  
503 that are targeted by sr7575.

504 In conclusion, we report the identification of a novel compound that has activity against  
505 both *S. cerevisiae* and *A. fumigatus*. The data are consistent with a model for sr7575 action in  
506 which the compound disrupts the structure of one or more proteins in the ER lumen or  
507 membrane, resulting in a situation that necessitates ERAD intervention to eliminate the  
508 abnormal protein(s) but does not require UPR activation. These findings underscore the  
509 importance of ER homeostasis to the growth fungi and suggest the presence of fungal-specific  
510 ER processes that could represent new opportunities for antifungal intervention.



## 511 **Funding information**

512 Funding was provided by AVIESAN *A. fumigatus* grant BAP109, Institut Carnot Pasteur  
513 Maladies Infectieuses grant FUNGI, Institut Pasteur, CNRS, and INSERM. The funders had  
514 no role in study design, data collection and interpretation, or the decision to submit the work  
515 for publication.

## 516 **Acknowledgments**

517 We thank Pr. Michel Boulouard (Groupe Mémoire et Plasticité Comportementale,  
518 GMPc, EA4259) for the *in vivo* toxicity tests on mice, Dominique Sanglard (CHUV Laussane,  
519 Switzerland) for the *C. albicans* strains, Françoise Dromer (CNRMA, Institut Pasteur) for the  
520 *A. fumigatus* clinical isolates, and Alain Jacquier (Unité de Génétique des Interactions  
521 Macromoléculaires, Institut Pasteur) for support and critical reading of the manuscript,.

## 522 **References**

- 523 1. **Brown GD, Denning DW, Levitz SM.** 2012. Tackling human fungal infections.  
524 Science **336**:647.
- 525 2. **Lai C-C, Tan C-K, Huang Y-T, Shao P-L, Hsueh P-R.** 2008. Current challenges in  
526 the management of invasive fungal infections. J Infect Chemother Off J Jpn Soc Chemother  
527 **14**:77–85.
- 528 3. **Park BJ, Wannemuehler KA, Marston BJ, Govender N, Pappas PG, Chiller TM.**  
529 2009. Estimation of the current global burden of cryptococcal meningitis among persons  
530 living with HIV/AIDS. AIDS Lond Engl **23**:525–530.
- 531 4. **Odds FC, Brown AJP, Gow NAR.** 2003. Antifungal agents: mechanisms of action.  
532 Trends Microbiol **11**:272–279.
- 533 5. **Perlin DS.** 2011. Current perspectives on echinocandin class drugs. Future Microbiol  
534 **6**:441–457.
- 535 6. **Hope WW, Taberner L, Denning DW, Anderson MJ.** 2004. Molecular  
536 mechanisms of primary resistance to flucytosine in *Candida albicans*. Antimicrob Agents  
537 Chemother **48**:4377–4386.
- 538 7. **Schenone M, Dančík V, Wagner BK, Clemons PA.** 2013. Target identification and  
539 mechanism of action in chemical biology and drug discovery. Nat Chem Biol **9**:232–240.
- 540 8. **Giaever G, Nislow C.** 2014. The Yeast Deletion Collection: A Decade of Functional

541 Genomics. *Genetics* **197**:451–465.

542 9. Hillenmeyer ME, Fung E, Wildenhain J, Pierce SE, Hoon S, Lee W, Proctor M, St  
543 Onge RP, Tyers M, Koller D, Altman RB, Davis RW, Nislow C, Giaever G. 2008. The  
544 chemical genomic portrait of yeast: uncovering a phenotype for all genes. *Science* **320**:362–  
545 365.

546 10. Lee AY, St Onge RP, Proctor MJ, Wallace IM, Nile AH, Spagnuolo PA, Jitkova Y,  
547 Gronda M, Wu Y, Kim MK, Cheung-Ong K, Torres NP, Spear ED, Han MKL, Schlecht  
548 U, Suresh S, Duby G, Heisler LE, Surendra A, Fung E, Urbanus ML, Gebbia M, Lissina  
549 E, Miranda M, Chiang JH, Aparicio AM, Zeghouf M, Davis RW, Cherfils J, Boutry M,  
550 Kaiser CA, Cummins CL, Trimble WS, Brown GW, Schimmer AD, Bankaitis VA, Nislow  
551 C, Bader GD, Giaever G. 2014. Mapping the cellular response to small molecules using  
552 chemogenomic fitness signatures. *Science* **344**:208–211.

553 11. Parsons AB, Lopez A, Givoni IE, Williams DE, Gray CA, Porter J, Chua G,  
554 Sopko R, Brost RL, Ho C-H, Wang J, Ketela T, Brenner C, Brill JA, Fernandez GE,  
555 Lorenz TC, Payne GS, Ishihara S, Ohya Y, Andrews B, Hughes TR, Frey BJ, Graham  
556 TR, Andersen RJ, Boone C. 2006. Exploring the mode-of-action of bioactive compounds by  
557 chemical-genetic profiling in yeast. *Cell* **126**:611–625.

558 12. Springer M, Weissman JS, Kirschner MW. 2010. A general lack of compensation  
559 for gene dosage in yeast. *Mol Syst Biol* **6**:368.

560 13. Hillenmeyer ME, Ericson E, Davis RW, Nislow C, Koller D, Giaever G. 2010.  
561 Systematic analysis of genome-wide fitness data in yeast reveals novel gene function and drug  
562 action. *Genome Biol* **11**:R30.

563 14. Decourty L, Saveanu C, Zemam K, Hantraye F, Frachon E, Rousselle J-C,  
564 Fromont-Racine M, Jacquier A. 2008. Linking functionally related genes by sensitive and  
565 quantitative characterization of genetic interaction profiles. *Proc Natl Acad Sci U S A*  
566 **105**:5821–5826.

567 15. Tong AHY, Lesage G, Bader GD, Ding H, Xu H, Xin X, Young J, Berriz GF, Brost  
568 RL, Chang M, Chen Y, Cheng X, Chua G, Friesen H, Goldberg DS, Haynes J,  
569 Humphries C, He G, Hussein S, Ke L, Krogan N, Li Z, Levinson JN, Lu H, Ménard P,  
570 Munyana C, Parsons AB, Ryan O, Tonikian R, Roberts T, Sdicu A-M, Shapiro J, Sheikh  
571 B, Suter B, Wong SL, Zhang LV, Zhu H, Burd CG, Munro S, Sander C, Rine J,  
572 Greenblatt J, Peter M, Bretscher A, Bell G, Roth FP, Brown GW, Andrews B, Bussey H,  
573 Boone C. 2004. Global mapping of the yeast genetic interaction network. *Science* **303**:808–  
574 813.

575 16. Hoepfner D, Helliwell SB, Sadlish H, Schuierer S, Filipuzzi I, Brachat S, Bhullar  
576 B, Plikat U, Abraham Y, Altorfer M, Aust T, Baeriswyl L, Cerino R, Chang L, Estoppey  
577 D, Eichenberger J, Frederiksen M, Hartmann N, Hohendahl A, Knapp B, Krastel P,  
578 Melin N, Nigsch F, Oakeley EJ, Petitjean V, Petersen F, Riedl R, Schmitt EK, Staedtler  
579 F, Studer C, Tallarico JA, Wetzel S, Fishman MC, Porter JA, Movva NR. 2014. High-  
580 resolution chemical dissection of a model eukaryote reveals targets, pathways and gene  
581 functions. *Microbiol Res* **169**:107–120.

582 17. Schuldiner M, Collins SR, Thompson NJ, Denic V, Bhamidipati A, Punna T,  
583 Ihmels J, Andrews B, Boone C, Greenblatt JF, Weissman JS, Krogan NJ. 2005.  
584 Exploration of the function and organization of the yeast early secretory pathway through an  
585 epistatic miniarray profile. *Cell* **123**:507–519.

- 586 18. **Berry DB, Guan Q, Hose J, Haroon S, Gebbia M, Heisler LE, Nislow C, Giaever**  
587 **G, Gasch AP.** 2011. Multiple means to the same end: the genetic basis of acquired stress  
588 resistance in yeast. *PLoS Genet* **7**:e1002353.
- 589 19. **Thibault G, Ng DTW.** 2012. The endoplasmic reticulum-associated degradation  
590 pathways of budding yeast. *Cold Spring Harb Perspect Biol* **4**.
- 591 20. **Giaever G, Chu AM, Ni L, Connelly C, Riles L, Véronneau S, Dow S, Lucau-**  
592 **Danila A, Anderson K, André B, Arkin AP, Astromoff A, El-Bakkoury M, Bangham R,**  
593 **Benito R, Brachat S, Campanaro S, Curtiss M, Davis K, Deutschbauer A, Entian K-D,**  
594 **Flaherty P, Foury F, Garfinkel DJ, Gerstein M, Gotte D, Güldener U, Hegemann JH,**  
595 **Hempel S, Herman Z, Jaramillo DF, Kelly DE, Kelly SL, Kötter P, LaBonte D, Lamb**  
596 **DC, Lan N, Liang H, Liao H, Liu L, Luo C, Lussier M, Mao R, Menard P, Ooi SL,**  
597 **Revuelta JL, Roberts CJ, Rose M, Ross-Macdonald P, Scherens B, Schimmack G, Shafer**  
598 **B, Shoemaker DD, Sookhai-Mahadeo S, Storms RK, Strathern JN, Valle G, Voet M,**  
599 **Volckaert G, Wang C, Ward TR, Wilhelmy J, Winzeler EA, Yang Y, Yen G, Youngman**  
600 **E, Yu K, Bussey H, Boeke JD, Snyder M, Philippsen P, Davis RW, Johnston M.** 2002.  
601 Functional profiling of the *Saccharomyces cerevisiae* genome. *Nature* **418**:387–391.
- 602 21. **Decourty L, Doyen A, Malabat C, Frachon E, Rispal D, Séraphin B, Feuerbach F,**  
603 **Jacquier A, Saveanu C.** 2014. Long open reading frame transcripts escape nonsense-  
604 mediated mRNA decay in yeast. *Cell Rep* **6**:593–598.
- 605 22. **Ho CH, Magtanong L, Barker SL, Gresham D, Nishimura S, Natarajan P, Koh**  
606 **JLY, Porter J, Gray CA, Andersen RJ, Giaever G, Nislow C, Andrews B, Botstein D,**  
607 **Graham TR, Yoshida M, Boone C.** 2009. A molecular barcoded yeast ORF library enables  
608 mode-of-action analysis of bioactive compounds. *Nat Biotechnol* **27**:369–377.
- 609 23. **Schiestl RH, Gietz RD.** 1989. High efficiency transformation of intact yeast cells  
610 using single stranded nucleic acids as a carrier. *Curr Genet* **16**:339–346.
- 611 24. **Jones GM, Stalker J, Humphray S, West A, Cox T, Rogers J, Dunham I, Prelich**  
612 **G.** 2008. A systematic library for comprehensive overexpression screens in *Saccharomyces*  
613 *cerevisiae*. *Nat Methods* **5**:239–241.
- 614 25. **Boyle EI, Weng S, Gollub J, Jin H, Botstein D, Cherry JM, Sherlock G.** 2004.  
615 GO::TermFinder--open source software for accessing Gene Ontology information and finding  
616 significantly enriched Gene Ontology terms associated with a list of genes. *Bioinforma Oxf*  
617 *Engl* **20**:3710–3715.
- 618 26. **Richie DL, Hartl L, Amanianda V, Winters MS, Fuller KK, Miley MD, White S,**  
619 **McCarthy JW, Latgé J-P, Feldmesser M, Rhodes JC, Askew DS.** 2009. A role for the  
620 unfolded protein response (UPR) in virulence and antifungal susceptibility in *Aspergillus*  
621 *fumigatus*. *PLoS Pathog* **5**:e1000258.
- 622 27. 2008. Reference method for broth dilution antifungal susceptibility testing of yeasts;  
623 Approved Standard-Third Edition. CLSI document M27-A3. Clinical and Laboratory  
624 Standards Institute, Wayne, PA.
- 625 28. **Clavaud C, Beauvais A, Barbin L, Munier-Lehmann H, Latgé J-P.** 2012. The  
626 composition of the culture medium influences the  $\beta$ -1,3-glucan metabolism of *Aspergillus*  
627 *fumigatus* and the antifungal activity of inhibitors of  $\beta$ -1,3-glucan synthesis. *Antimicrob*  
628 *Agents Chemother* **56**:3428–3431.
- 629 29. **Jhingran A, Mar KB, Kumasaka DK, Knoblauch SE, Ngo LY, Segal BH, Iwakura**  
630 **Y, Lowell CA, Hamerman JA, Lin X, Hohl TM.** 2012. Tracing conidial fate and measuring

631 host cell antifungal activity using a reporter of microbial viability in the lung. *Cell Rep*  
632 **2**:1762–1773.

633 30. **Feng X, Krishnan K, Richie DL, Amanianda V, Hartl L, Grahl N, Powers-**  
634 **Fletcher MV, Zhang M, Fuller KK, Nierman WC, Lu LJ, Latgé J-P, Woollett L,**  
635 **Newman SL, Cramer RA, Rhodes JC, Askew DS.** 2011. HacA-Independent Functions of  
636 the ER Stress Sensor IreA Synergize with the Canonical UPR to Influence Virulence Traits in  
637 *Aspergillus fumigatus*. *PLoS Pathog* **7**.

638 31. **Hibert MF.** 2009. French/European academic compound library initiative. *Drug*  
639 *Discov Today* **14**:723–725.

640 32. **Zhang J-H, Chung TDY, Oldenburg KR.** 1999. A Simple Statistical Parameter for  
641 Use in Evaluation and Validation of High Throughput Screening Assays. *J Biomol Screen*  
642 **4**:67–73.

643 33. **Prunier H, Rault S, Lancelot JC, Robba M, Renard P, Delagrance P, Pfeiffer B,**  
644 **Caignard DH, Misslin R, Guardiola-Lemaitre B, Hamon M.** 1997. Novel and selective  
645 partial agonists of 5-HT<sub>3</sub> receptors. 2. Synthesis and biological evaluation of  
646 piperazinopyridopyrrolopyrazines, piperazinopyrroloquinoxalines, and  
647 piperazinopyridopyrroloquinoxalines. *J Med Chem* **40**:1808–1819.

648 34. **Smith AM, Heisler LE, Mellor J, Kaper F, Thompson MJ, Chee M, Roth FP,**  
649 **Giaever G, Nislow C.** 2009. Quantitative phenotyping via deep barcode sequencing. *Genome*  
650 *Res* **19**:1836–1842.

651 35. **Eason RG, Pourmand N, Tongprasit W, Herman ZS, Anthony K, Jejelowo O,**  
652 **Davis RW, Stolc V.** 2004. Characterization of synthetic DNA bar codes in *Saccharomyces*  
653 *cerevisiae* gene-deletion strains. *Proc Natl Acad Sci U S A* **101**:11046–11051.

654 36. **Cannon RD, Lamping E, Holmes AR, Niimi K, Baret PV, Keniya MV, Tanabe K,**  
655 **Niimi M, Goffeau A, Monk BC.** 2009. Efflux-mediated antifungal drug resistance. *Clin*  
656 *Microbiol Rev* **22**:291–321, Table of Contents.

657 37. **Meyers S, Schauer W, Balzi E, Wagner M, Goffeau A, Golin J.** 1992. Interaction of  
658 the yeast pleiotropic drug resistance genes PDR1 and PDR5. *Curr Genet* **21**:431–436.

659 38. **Jonikas MC, Collins SR, Denic V, Oh E, Quan EM, Schmid V, Weibezahn J,**  
660 **Schwappach B, Walter P, Weissman JS, Schuldiner M.** 2009. Comprehensive  
661 characterization of genes required for protein folding in the endoplasmic reticulum. *Science*  
662 **323**:1693–1697.

663 39. **Lahiri S, Chao JT, Tavassoli S, Wong AKO, Choudhary V, Young BP, Loewen**  
664 **CJR, Prinz WA.** 2014. A conserved endoplasmic reticulum membrane protein complex  
665 (EMC) facilitates phospholipid transfer from the ER to mitochondria. *PLoS Biol* **12**:e1001969.

666 40. **Hampton RY.** 2000. ER stress response: getting the UPR hand on misfolded proteins.  
667 *Curr Biol CB* **10**:R518–521.

668 41. **Schröder M.** 2008. Endoplasmic reticulum stress responses. *Cell Mol Life Sci CMLS*  
669 **65**:862–894.

670 42. **Costanzo M, Baryshnikova A, Bellay J, Kim Y, Spear ED, Sevier CS, Ding H, Koh**  
671 **JLY, Toufighi K, Mostafavi S, Prinz J, St Onge RP, VanderSluis B, Makhnevych T,**  
672 **Vizeacoumar FJ, Alizadeh S, Bahr S, Brost RL, Chen Y, Cokol M, Deshpande R, Li Z,**  
673 **Lin Z-Y, Liang W, Marback M, Paw J, San Luis B-J, Shuteriqi E, Tong AHY, van Dyk**  
674 **N, Wallace IM, Whitney JA, Weirauch MT, Zhong G, Zhu H, Houry WA, Brudno M,**  
675 **Ragibzadeh S, Papp B, Pál C, Roth FP, Giaever G, Nislow C, Troyanskaya OG, Bussey**

676 **H, Bader GD, Gingras A-C, Morris QD, Kim PM, Kaiser CA, Myers CL, Andrews BJ,**  
677 **Boone C.** 2010. The genetic landscape of a cell. *Science* **327**:425–431.

678 43. **Yu L, Peña Castillo L, Mnaimneh S, Hughes TR, Brown GW.** 2006. A survey of  
679 essential gene function in the yeast cell division cycle. *Mol Biol Cell* **17**:4736–4747.

680 44. **Thibault G, Shui G, Kim W, McAlister GC, Ismail N, Gygi SP, Wenk MR, Ng**  
681 **DTW.** 2012. The membrane stress response buffers lethal effects of lipid disequilibrium by  
682 reprogramming the protein homeostasis network. *Mol Cell* **48**:16–27.

683 45. **Finke K, Plath K, Panzner S, Prehn S, Rapoport TA, Hartmann E, Sommer T.**  
684 1996. A second trimeric complex containing homologs of the Sec61p complex functions in  
685 protein transport across the ER membrane of *S. cerevisiae*. *EMBO J* **15**:1482–1494.

686 46. **Biederer T, Volkwein C, Sommer T.** 1997. Role of Cue1p in ubiquitination and  
687 degradation at the ER surface. *Science* **278**:1806–1809.

688 47. **Bordallo J, Plemper RK, Finger A, Wolf DH.** 1998. Der3p/Hrd1p is required for  
689 endoplasmic reticulum-associated degradation of misfolded luminal and integral membrane  
690 proteins. *Mol Biol Cell* **9**:209–222.

691 48. **Hampton RY, Gardner RG, Rine J.** 1996. Role of 26S proteasome and HRD genes  
692 in the degradation of 3-hydroxy-3-methylglutaryl-CoA reductase, an integral endoplasmic  
693 reticulum membrane protein. *Mol Biol Cell* **7**:2029–2044.

694 49. **Mehnert M, Sommer T, Jarosch E.** 2014. Der1 promotes movement of misfolded  
695 proteins through the endoplasmic reticulum membrane. *Nat Cell Biol* **16**:77–86.

696 50. **Travers KJ, Patil CK, Wodicka L, Lockhart DJ, Weissman JS, Walter P.** 2000.  
697 Functional and Genomic Analyses Reveal an Essential Coordination between the Unfolded  
698 Protein Response and ER-Associated Degradation. *Cell* **101**:249–258.

699 51. **Friedlander R, Jarosch E, Urban J, Volkwein C, Sommer T.** 2000. A regulatory  
700 link between ER-associated protein degradation and the unfolded-protein response. *Nat Cell*  
701 *Biol* **2**:379–384.

702 52. **Richie DL, Feng X, Hartl L, Amanianda V, Krishnan K, Powers-Fletcher MV,**  
703 **Watson DS, Galande AK, White SM, Willett T, Latgé J-P, Rhodes JC, Askew DS.** 2011.  
704 The virulence of the opportunistic fungal pathogen *Aspergillus fumigatus* requires cooperation  
705 between the endoplasmic reticulum-associated degradation pathway (ERAD) and the unfolded  
706 protein response (UPR). *Virulence* **2**:12–21.

707 53. **Buck TM, Jordan R, Lyons-Weiler J, Adelman JL, Needham PG, Kleyman TR,**  
708 **Brodsky JL.** 2015. Expression of three topologically distinct membrane proteins elicits  
709 unique stress response pathways in the yeast *Saccharomyces cerevisiae*. *Physiol Genomics*  
710 **47**:198–214.

711 54. **Hazbun TR, Malmström L, Anderson S, Graczyk BJ, Fox B, Riffle M, Sundin**  
712 **BA, Aranda JD, McDonald WH, Chiu C-H, Snydsman BE, Bradley P, Muller EGD,**  
713 **Fields S, Baker D, Yates JR, Davis TN.** 2003. Assigning function to yeast proteins by  
714 integration of technologies. *Mol Cell* **12**:1353–1365.

715 55. **Huh W-K, Falvo JV, Gerke LC, Carroll AS, Howson RW, Weissman JS, O’Shea**  
716 **EK.** 2003. Global analysis of protein localization in budding yeast. *Nature* **425**:686–691.

717 56. **Chen F, Mackey AJ, Stoeckert CJ, Roos DS.** 2006. OrthoMCL-DB: querying a  
718 comprehensive multi-species collection of ortholog groups. *Nucleic Acids Res* **34**:D363–368.

719 57. **Hoppins S, Collins SR, Cassidy-Stone A, Hummel E, Devay RM, Lackner LL,**  
720 **Westermann B, Schuldiner M, Weissman JS, Nunnari J.** 2011. A mitochondrial-focused

721 genetic interaction map reveals a scaffold-like complex required for inner membrane  
722 organization in mitochondria. *J Cell Biol* **195**:323–340.

## 723 **Figure legends**

724 **Fig. 1:** Identification of a compound with broad antifungal activity. **(A)** Selection of a  
725 new antifungal, sr7575, through a chemical library screen of *A. fumigatus* growth inhibition  
726 was followed by chemogenomic profiling in *S. cerevisiae* to identify a potential mechanism of  
727 action. sr7575 inhibited growth of various fungi, including *A. flavus* (48 h, 37°C, RPMI  
728 medium, 5 µg/mL) **(B)**; *C. albicans* and *C. neoformans* (24 h, 37°C, SC medium, 2 µg/mL)  
729 **(C)**; *S. cerevisiae* (48 h, 30°C, SC medium, 1 µg/mL) **(D)**.

730 **Fig. 2:** Chemogenomic profiling reveals an ERAD-enriched signature for sr7575  
731 toxicity. **(A)** Distribution of relative growth values for *S. cerevisiae* mutant strains grown in  
732 the presence of sr7575. Colors indicate functional categories from the pooled library with  
733 genes annotated as ERAD (violet), protein translocation (grey), ER membrane complex  
734 (EMC; pink), and vesicular traffic (green) showing the most sensitivity to sr7575 when  
735 mutated. Note: *YML012C-A\** overlaps *UBX2* and “#” indicates a DAmP strain; **(B)**  
736 Distribution of sensitivity values for deletion strains affected for genes annotated with the GO  
737 term 0030433, ERAD; **(C)** Pearson correlation coefficients between results obtained with  
738 sr7575 and a published large scale chemogenomics data set identifies chemical 4166 as having  
739 a profile that is most similar to sr7575. Only the scores for the top 100 correlated treatments  
740 are displayed; **(D)** Same as **(C)** but with the Spearman rank correlation; **(E)** Comparison of the  
741 fitness defect scores between sr7575 and chemical 4166; gene names are color coded as in  
742 **(A)**.

743 **Fig. 3:** Summary of mutations conferring increased susceptibility to sr7575. **(A)**  
744 Heatmap showing the unique ERAD signature of sr7575 compared with published  
745 chemogenomic and SGA growth defect profiles; **(B)** Model showing the two main pathways  
746 responsible for ERAD in fungi- Doa10 pathway (green) for clearing misfolded proteins with  
747 cytosolic lesions, and the Hrd1 pathway (violet), which degrades misfolded proteins with  
748 luminal or transmembrane lesions. Shared components (Ubx2, Ubc7, Cue1, and the Cdc48  
749 complex) are denoted in gray or black.

750 **Fig. 4:** Sensitivity to sr7575 depends on EMC and ERAD components. **(A)** Serial 10-  
751 fold dilutions of the WT and selected haploid deletion mutants were grown on SC plates in the  
752 absence or presence of 0.25  $\mu\text{g/mL}$  sr7575 for 48 h at 30°C; **(B)** Complementation of sr7575  
753 sensitivity for the strains shown in panel **(A)** was tested by using single copy plasmids  
754 carrying the corresponding genes; **(C)** Strains lacking core UPR components, *HAC1* and *IRE1*  
755 were tested for sensitivity against sr7575 at 0.5  $\mu\text{g/mL}$ .

756 **Fig. 5:** The hypersensitivity of ERAD mutants to sr7575 is conserved in *A. fumigatus*.  
757 **(a)** Conidia from *A. fumigatus* WT and deletion mutants were recovered in 0.05% Tween-  
758 water and serial dilutions were spotted onto sr7575-containing RPMI 1640, pH 7.0. Plates  
759 were incubated at 37°C for 72 h; **(B)** Analysis of UPR target gene expression (*bipA* and *tigA*)  
760 by qRT-PCR. Cultures were treated with sr7575, DTT, or sr7575 for 1 h followed by DTT.  
761 RNA was extracted and analyzed by qRT-PCR, using *tubA* mRNA for normalization. The  
762 results of treated vs untreated samples from three independent experiments are shown.

763 **Fig. 6:** Ynl181w is an ER protein conserved in fungi and involved in adaptation to  
764 sr7575. **(A)** T-Coffee alignment of the conserved short chain dehydrogenase region within Sc  
765 Ynl181w (PFAM 54-187) and its orthologs in pathogenic fungi. Gene annotations with

766 number range indicate the position of the PFAM domain: *A. fumigatus* (Afu5g10790; 54-205),  
767 *C. albicans* (orf19.6233; 58-204), *C. glabrata* (XP\_448202; 54-193); **(B)** Scatter plot showing  
768 the correlation between sr7575 sensitivity values and the previously published SGA scores for  
769 ynl181w-DAmP; **(C)** Spot assays showing the difference in sensitivity to sr7575 and UPR  
770 inducer tunicamycin (TM) for *ynl181w*-DAmP as compared with a strain defective for UPR  
771 (*hac1Δ*).

## 772 **Supplementary Data synopsis**

773 **Fig. S1:** Synthetic pathways for sr7575 and related compounds.

774 **Fig. S2:** Growth of *A. fumigatus*, *A. flavus*, *S. cerevisiae*, *C. albicans* and *C. neoformans*  
775 cells in liquid medium in the presence of various concentrations of sr7575.

776 **Fig. S3:** sr7575 profile shows little correlation with a previously published large-scale  
777 chemogenomics dataset.

778 **Fig. S4:** Perturbation of PGA3 function shows similarities with the sensitivity profile for  
779 sr7575.

780 **Fig. S5:** Susceptibility testing of yeast strains against sr7575.

781 **Fig. S6:** Susceptibility of multidrug resistant *S. cerevisiae* strains and azole resistant *C.*  
782 *albicans* strains to sr7575.

783 **Table S1:** List of 76 compounds from the CERMN chemical library showing 90% or  
784 more growth inhibition of *A.fumigatus* at 25 µg/mL.

785 **Table S2:** Analogues of sr7575 and MIC<sub>100</sub> values against *A. fumigatus*.

786 **Table S3:** Analogues of sr7576 and MIC<sub>100</sub> values against *A. fumigatus*.

787 **Table S4:** List of strains used in this study.



788           **Table S5:** List of oligonucleotides used in this study.

789           **Table S6** (provided as a separate xls file): Sensitivity of *S. cerevisiae* deletion and

790           DAmP strains to 0.125 µg/mL sr7575.

791           **Text S1:** Synthesis of sr7575 and related compounds.

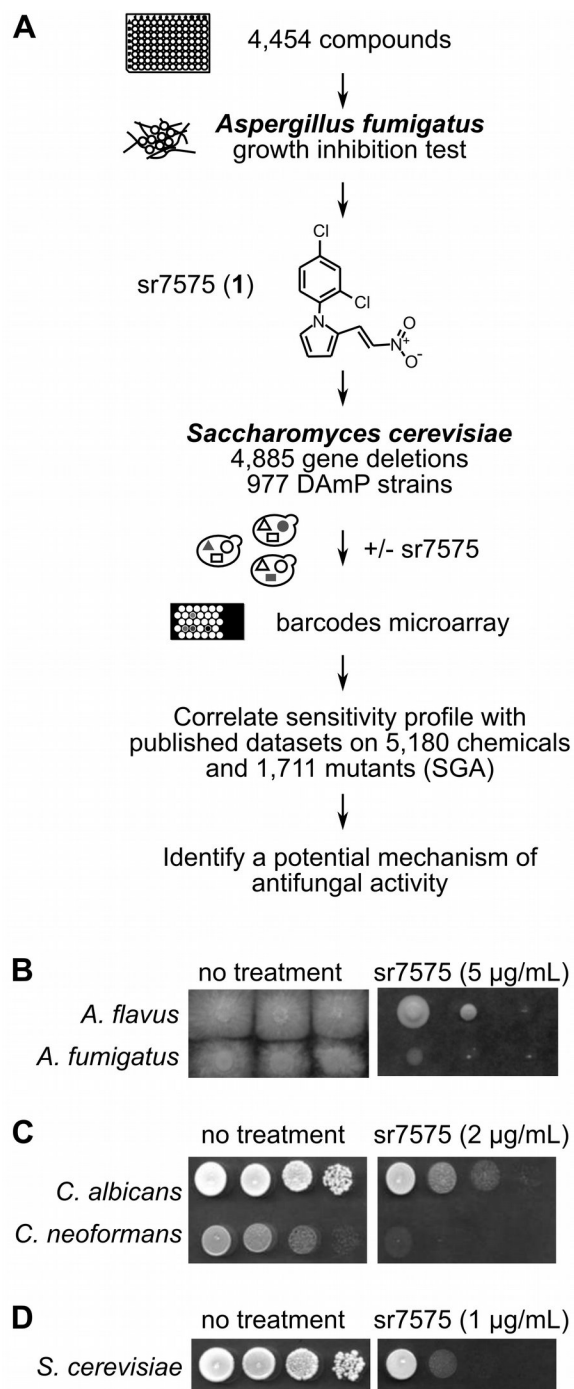


**Fig. 1:** Identification of a compound with broad antifungal activity. **(A)** Selection of a new antifungal, sr7575, through a chemical library screen of *A. fumigatus* growth inhibition was followed by chemogenomic profiling in *S. cerevisiae* to identify a potential mechanism of action. sr7575 inhibited growth of various fungi, including *A. flavus* (48 h, 37°C, RPMI medium, 5  $\mu\text{g/mL}$ ) **(B)**; *C. albicans* and *C. neoformans* (24 h, 37°C, SC medium, 2  $\mu\text{g/mL}$ ) **(C)**; *S. cerevisiae* (48 h, 30°C, SC medium, 1  $\mu\text{g/mL}$ ) **(D)**.

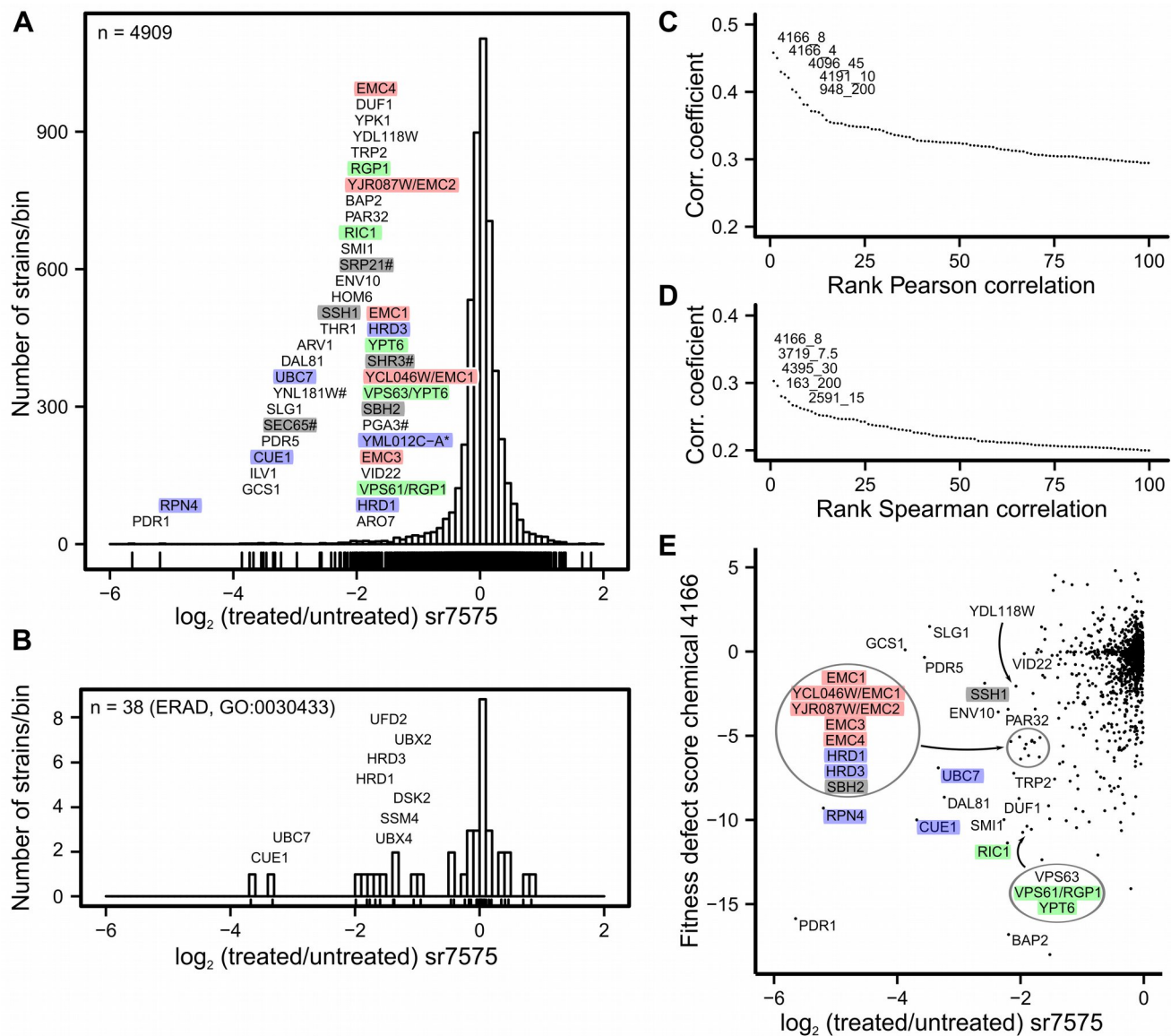


**Fig. 2:** Chemogenomic profiling reveals an ERAD-enriched signature for sr7575 toxicity. **(A)** Distribution of relative growth values for *S. cerevisiae* mutant strains grown in the presence of sr7575. Colors indicate functional categories from the pooled library with genes annotated as ERAD (violet), protein translocation (grey), ER membrane complex (EMC; pink), and vesicular traffic (green) showing the most sensitivity to sr7575 when mutated. Note: *YML012C-A\** overlaps *UBX2* and “#” indicates a DAmP strain; **(B)** Distribution of sensitivity values for deletion strains affected for genes annotated with the GO term 0030433, ERAD; **(C)** Pearson correlation coefficients between results obtained with sr7575 and a published large scale chemogenomics data set identifies chemical 4166 as having a profile that is most similar to sr7575. Only the scores for the top 100 correlated treatments are displayed; **(D)** Same as **(C)** but with the Spearman rank correlation; **(E)** Comparison of the fitness defect scores between sr7575 and chemical 4166; gene names are color coded as in **(A)**.

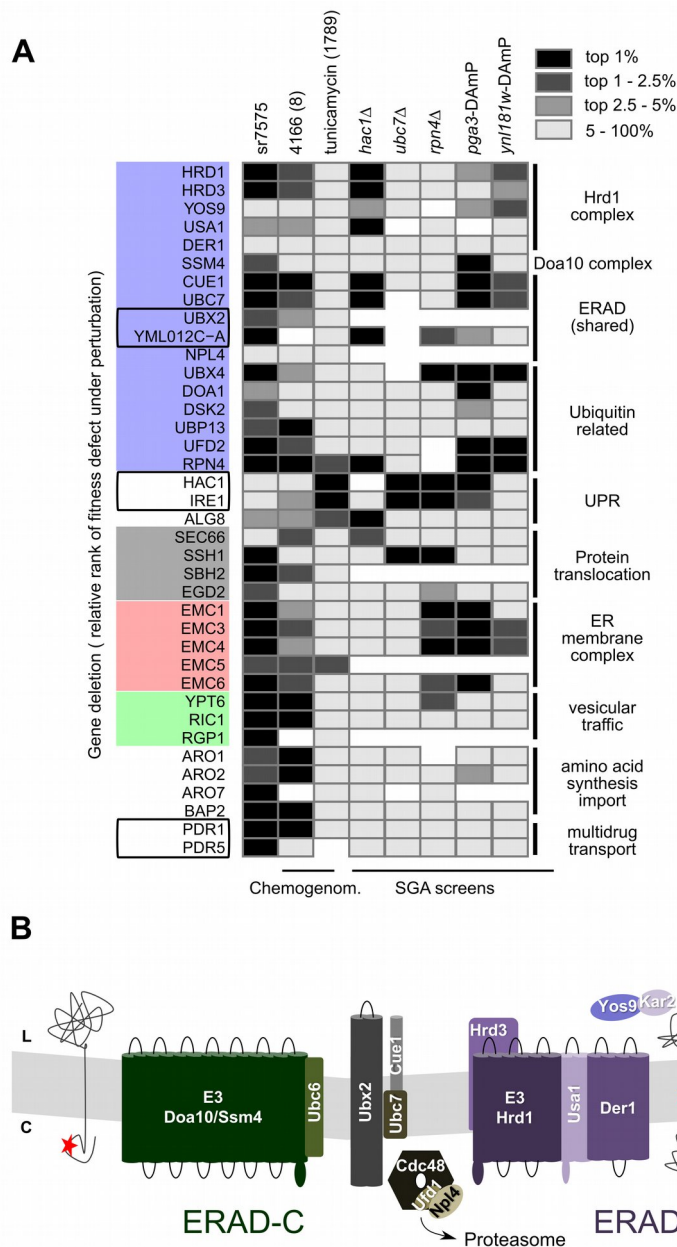


**Fig. 3:** Summary of mutations conferring increased susceptibility to *sr7575*. **(A)** Heatmap showing the unique ERAD signature of *sr7575* compared with published chemogenomic and SGA growth defect profiles; **(B)** Model showing the two main pathways responsible for ERAD in fungi- Doa10 pathway (green) for clearing misfolded proteins with cytosolic lesions, and the Hrd1 pathway (violet), which degrades misfolded proteins with luminal or transmembrane lesions. Shared components (Ubc2, Ubc7, Cue1, and the Cdc48 complex) are denoted in grey or black.

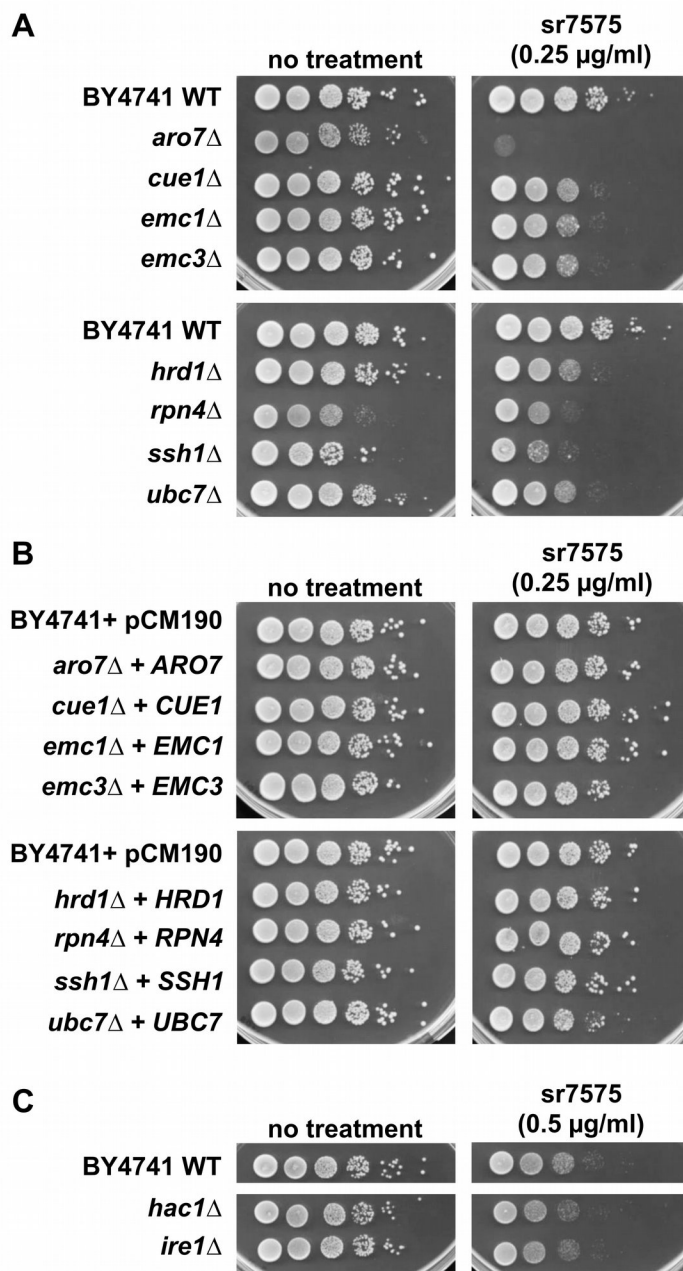


**Fig. 4:** Sensitivity to sr7575 depends on EMC and ERAD components. **(A)** Serial 10-fold dilutions of the WT and selected haploid deletion mutants were grown on SC plates in the absence or presence of 0.25 µg/mL sr7575 for 48 h at 30°C; **(B)** Complementation of sr7575 sensitivity for the strains shown in panel **(A)** was tested by using single copy plasmids carrying the corresponding genes; **(C)** Strains lacking core UPR components, *HAC1* and *IRE1* were tested for sensitivity against sr7575 at 0.5 µg/mL.

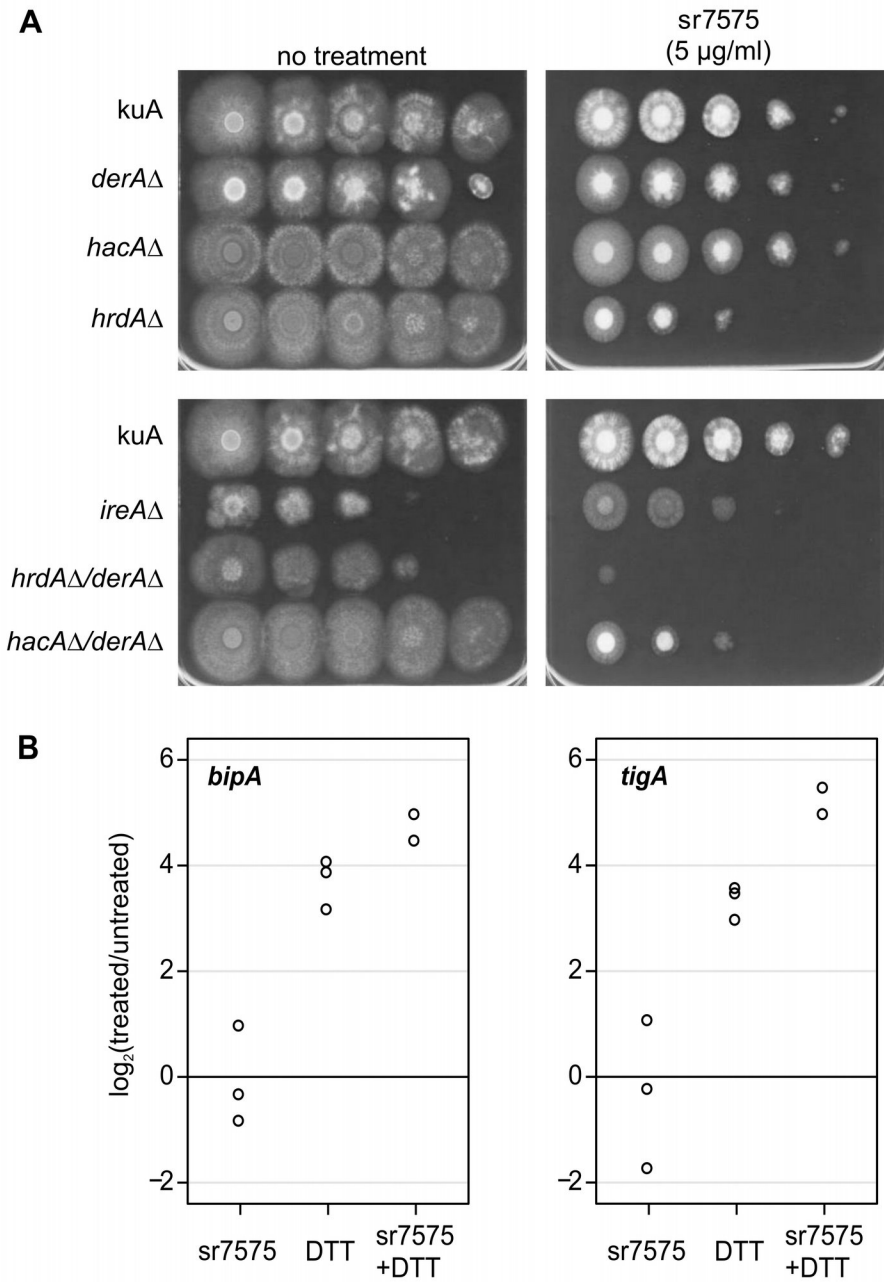


**Fig. 5:** The hypersensitivity of ERAD mutants to sr7575 is conserved in *A. fumigatus*. **(a)** Conidia from *A. fumigatus* WT and deletion mutants were recovered in 0.05% Tween-water and serial dilutions were spotted onto sr7575-containing RPMI 1640, pH 7.0. Plates were incubated at 37°C for 72 h; **(B)** Analysis of UPR target gene expression (*bipA* and *tigA*) by qRT-PCR. Cultures were treated with sr7575, DTT, or sr7575 for 1 h followed by DTT. RNA was extracted and analyzed by qRT-PCR, using *tubA* mRNA for normalization. The results of treated vs untreated samples from three independent experiments are shown.

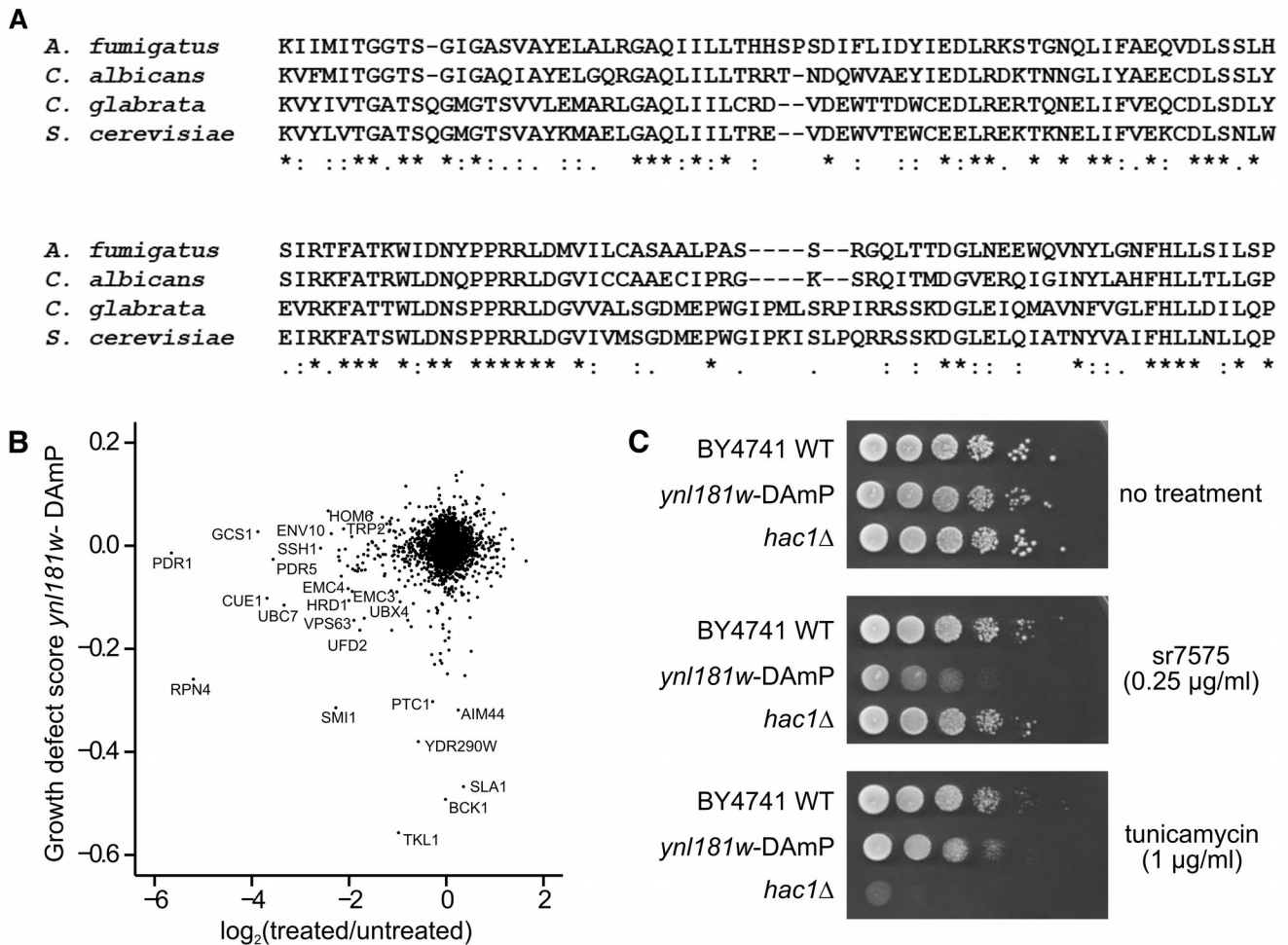


**Fig. 6:** Ynl181w is an ER protein conserved in fungi and involved in adaptation to sr7575. **(A)** T-Coffee alignment of the conserved short chain dehydrogenase region within Sc Ynl181w (PFAM 54-187) and its orthologs in pathogenic fungi. Gene annotations with number range indicate the position of the PFAM domain: *A. fumigatus* (Afu5g10790; 54-205), *C. albicans* (orf19.6233; 58-204), *C. glabrata* (XP\_448202; 54-193); **(B)** Scatter plot showing the correlation between sr7575 sensitivity values and the previously published SGA scores for *ynl181w*-DAmP; **(C)** Spot assays showing the difference in sensitivity to sr7575 and UPR inducer tunicamycin (TM) for *ynl181w*-DAmP as compared with a strain defective for UPR (*hac1Δ*).

Supplementary Material for Publication of manuscript "Toxicity of a novel antifungal compound is modulated by ERAD components", by Raj et al.

**Fig. S1:** Synthetic pathways for sr7575 and related compounds.

**Fig. S2:** Growth of *A. fumigatus*, *A. flavus*, *S. cerevisiae*, *C. albicans* and *C. neoformans* cells in liquid medium in the presence of various concentrations of sr7575.

**Fig. S3:** sr7575 profile shows little correlation with a previously published large-scale chemogenomics dataset.

**Fig. S4:** Perturbation of PGA3 function shows similarities with the sensitivity profile for sr7575.

**Fig. S5:** Susceptibility testing of yeast strains against sr7575.

**Fig. S6:** Susceptibility of multidrug resistant *S. cerevisiae* strains and azole resistant *C. albicans* strains to sr7575.

**Table S1:** List of 76 compounds from the CERMN chemical library showing 90% or more growth inhibition of *A. fumigatus* at 25 µg/mL.

**Table S2:** Analogues of sr7575 and MIC<sub>100</sub> values against *A. fumigatus*.

**Table S3:** Analogues of sr7576 and MIC<sub>100</sub> values against *A. fumigatus*.

**Table S4:** List of strains and plasmids used in this study.

**Table S5:** List of oligonucleotides used in this study.

**Table S6** (provided as a separate xls file): Sensitivity of *S. cerevisiae* deletion and DAmP strains to 0.125 µg/mL sr7575.

**Text S1:** Synthesis of sr7575 and related compounds.



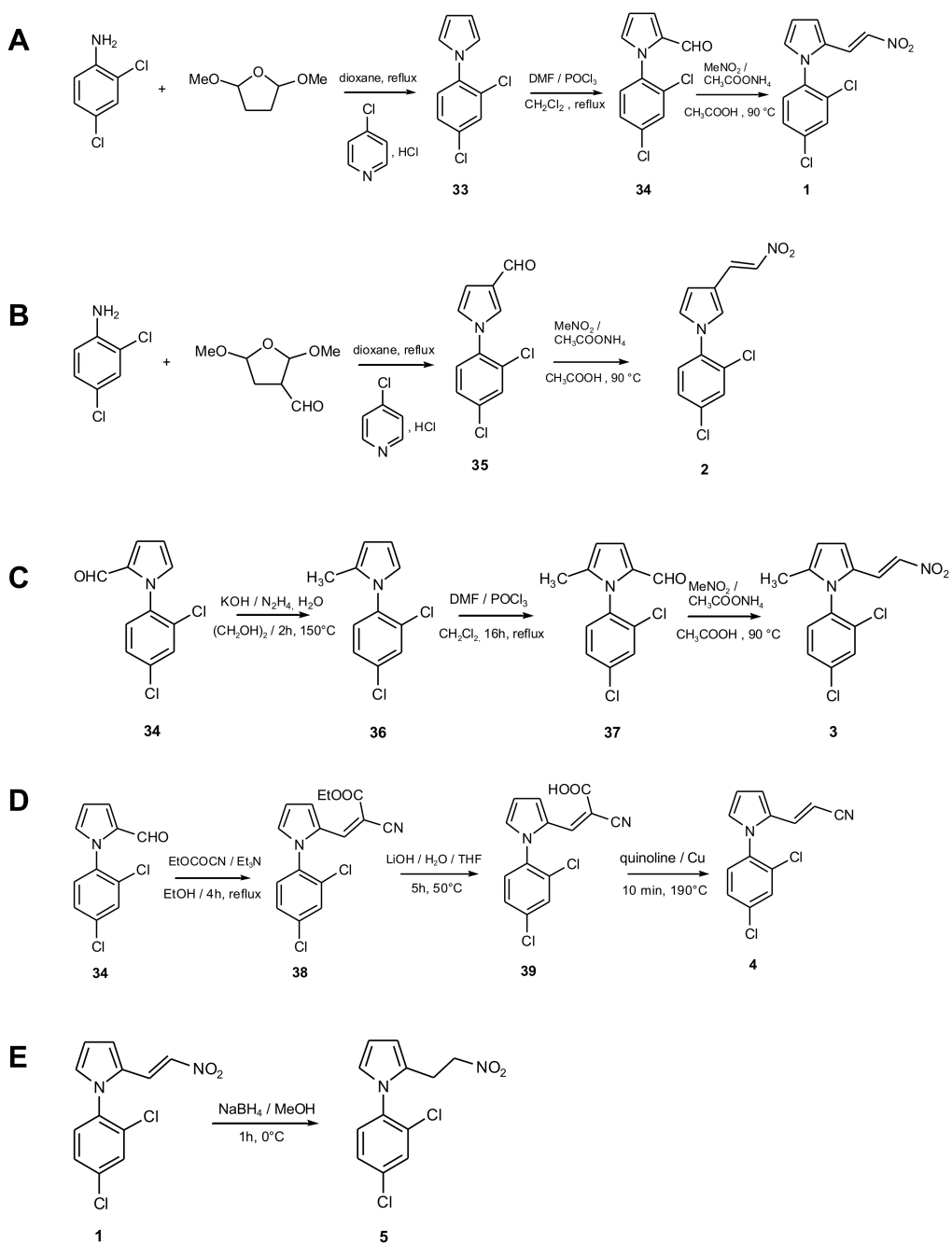


**Figure S1. Synthetic pathways for sr7575 and related compounds.** Pathways detailing the synthesis of sr7575 and analogues 2-5.

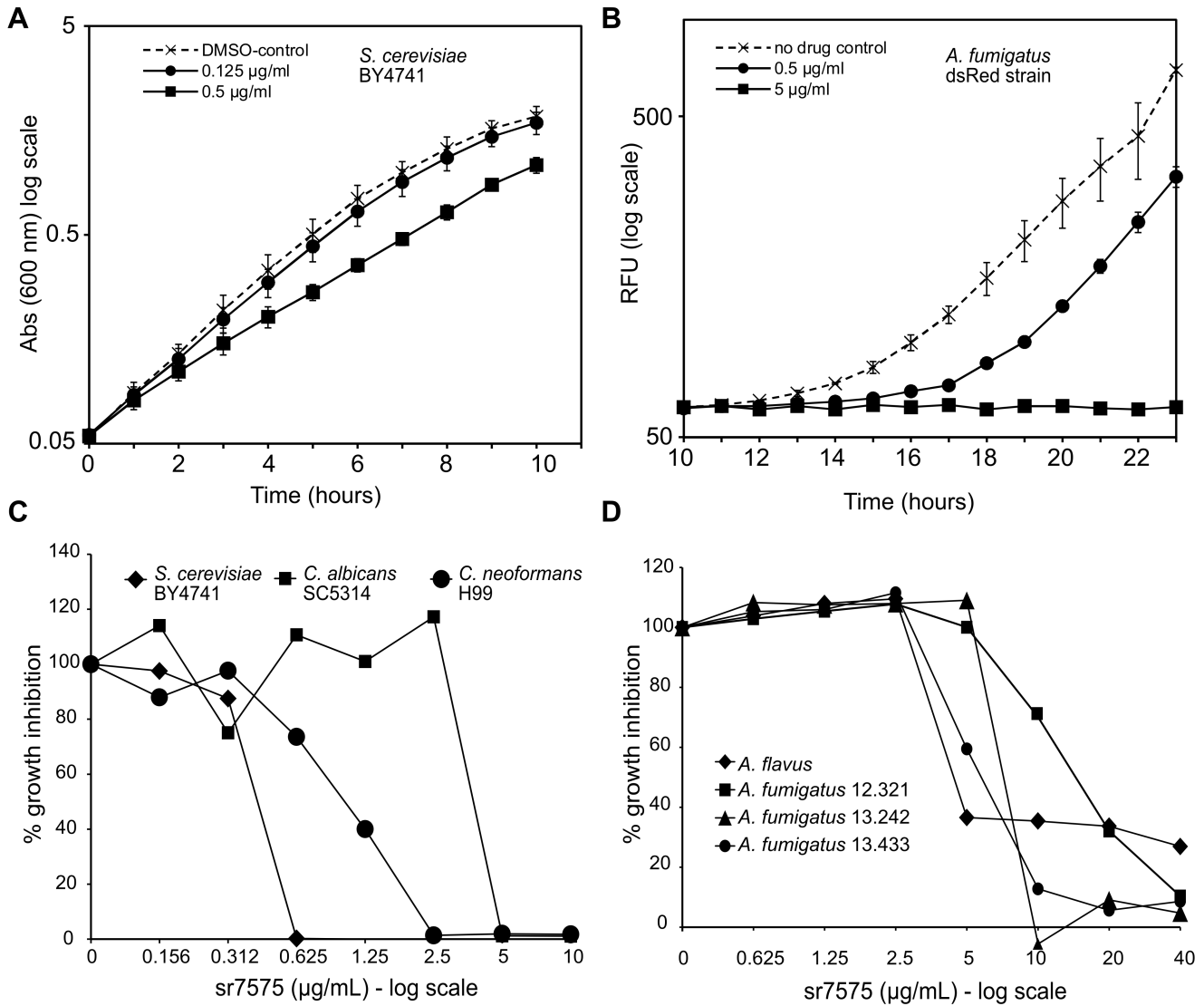


**Figure S2. Growth of *A. fumigatus*, *A. flavus*, *S. cerevisiae*, *C. albicans* and *C. neoformans* cells in liquid medium in the presence of various concentrations of sr7575. (A) Log-phase cultures of *S. cerevisiae* WT strain BY4741 were grown in the presence of increasing concentrations of sr7575 with DMSO as vehicle control. The Abs<sub>600</sub> was determined every hour for 10 h. (B) *A. fumigatus* strain Af293-dsRed was grown for 23 h in RPMI-1640 medium in the presence of increasing concentrations of sr7575. Fluorescence (ex 254 nm/ em 291 nm) was measured and relative fluorescence units (RFU) plotted against time. (C) Growth inhibition estimates were obtained at various concentrations of sr7575 by measuring absorbance at 600 nm for *S. cerevisiae* (BY4741, YPD, 30°C, 48 h), *C. albicans* (SC5314, RPMI, 37°C, 48 h) and *C. neoformans* (H99, RPMI, 37°C, 72 h). (D) Growth inhibition estimates for *A. flavus* and three *A. fumigatus* clinical isolates (12.321, 13.242, 13.433) were obtained by the resazurin reduction assay in RPMI medium, 37°C, 39 h at concentrations of sr7575 up to 40  $\mu\text{g/ml}$ .**

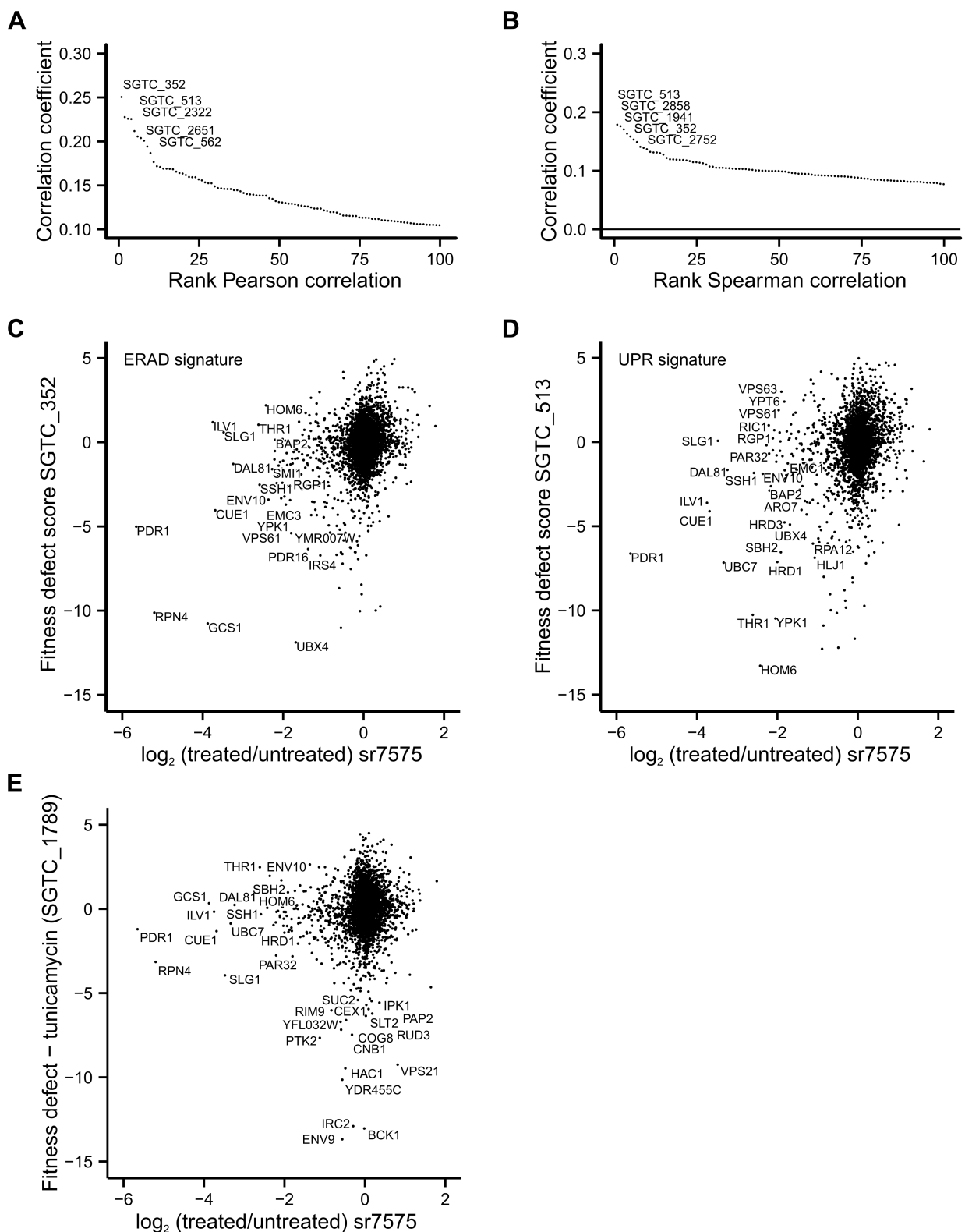


**Figure S3. sr7575 profile shows little correlation with a previously published large-scale chemogenomics dataset.** Computed Pearson (A) and Spearman (B) correlation coefficients between sr7575 values and previously published growth scores obtained with 3,356 compounds were ranked in descending order and the top 100 values are indicated. Among the highest correlations, we identified SGTC 352, a drug showing an ERAD signature (C) and SGTC 513, a compound with a UPR signature

**(D)** as being closest to the sr7575 profile. (E) The sr7575 profile showed no correlation with the one published for tunicamycin.

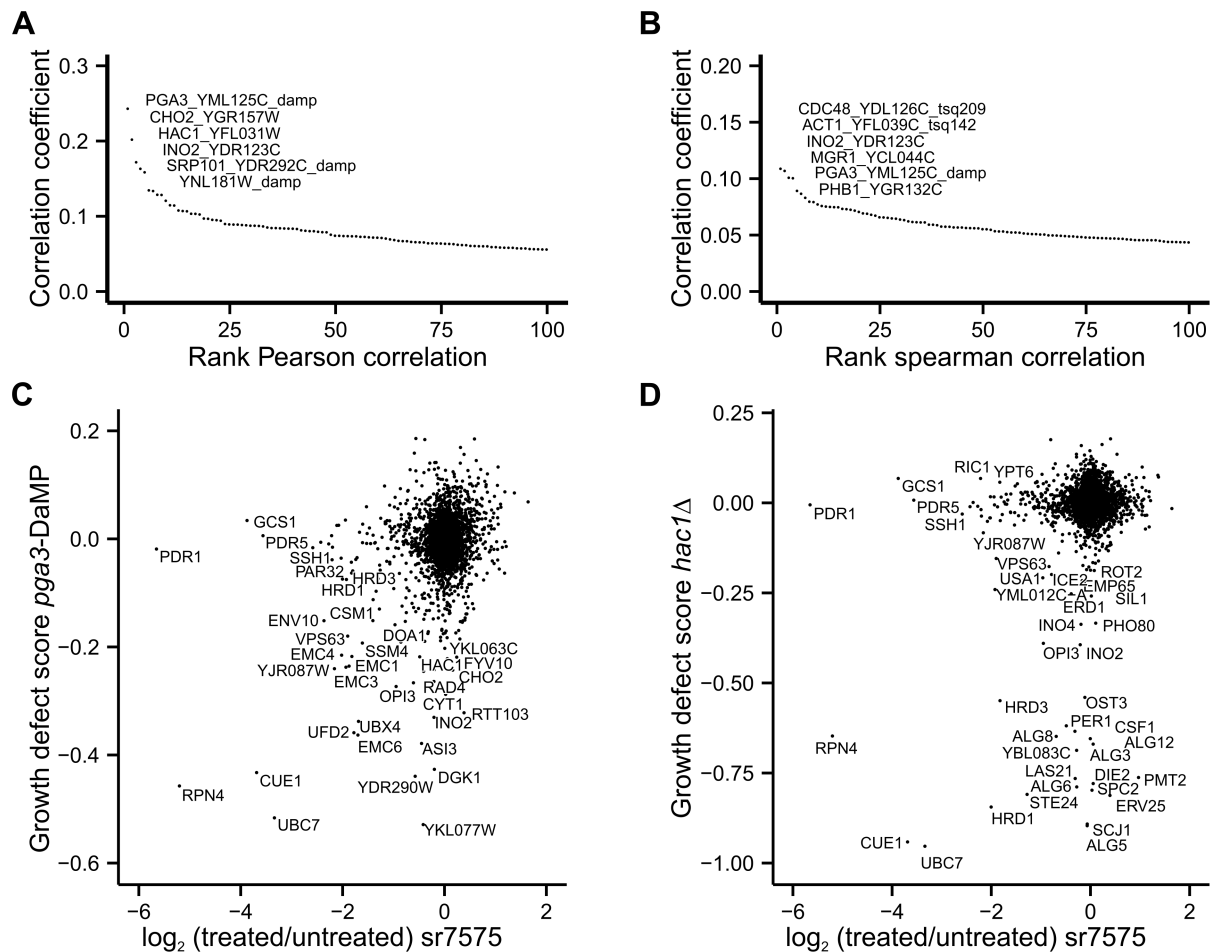


**Figure S4. Perturbation of *PGA3* function shows similarities with the sensitivity profile for *sr7575*.** Pearson (A) and Spearman (B) correlations between the *sr7575* profile and 1711 previously published SGA profiles. Fitness defect scores for DAMP modification of *PGA3* are shown in (C), while the interactions of *hac1* $\Delta$  and ERAD depleted strains are depicted in (D).

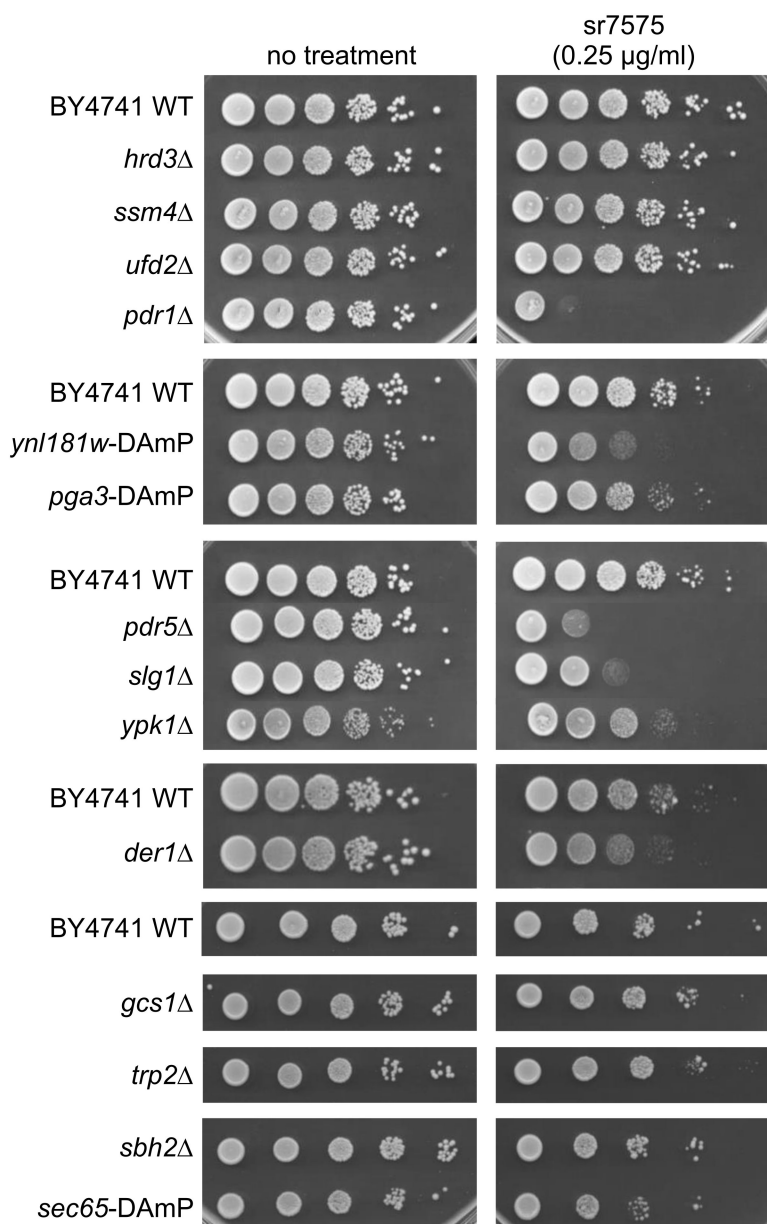


**Figure S5. Susceptibility testing of yeast strains against sr7575.** Mutants from the haploid deletion background were serially spotted onto SC plates supplemented with sr7575. Plates were incubated at 30°C for 48 h.

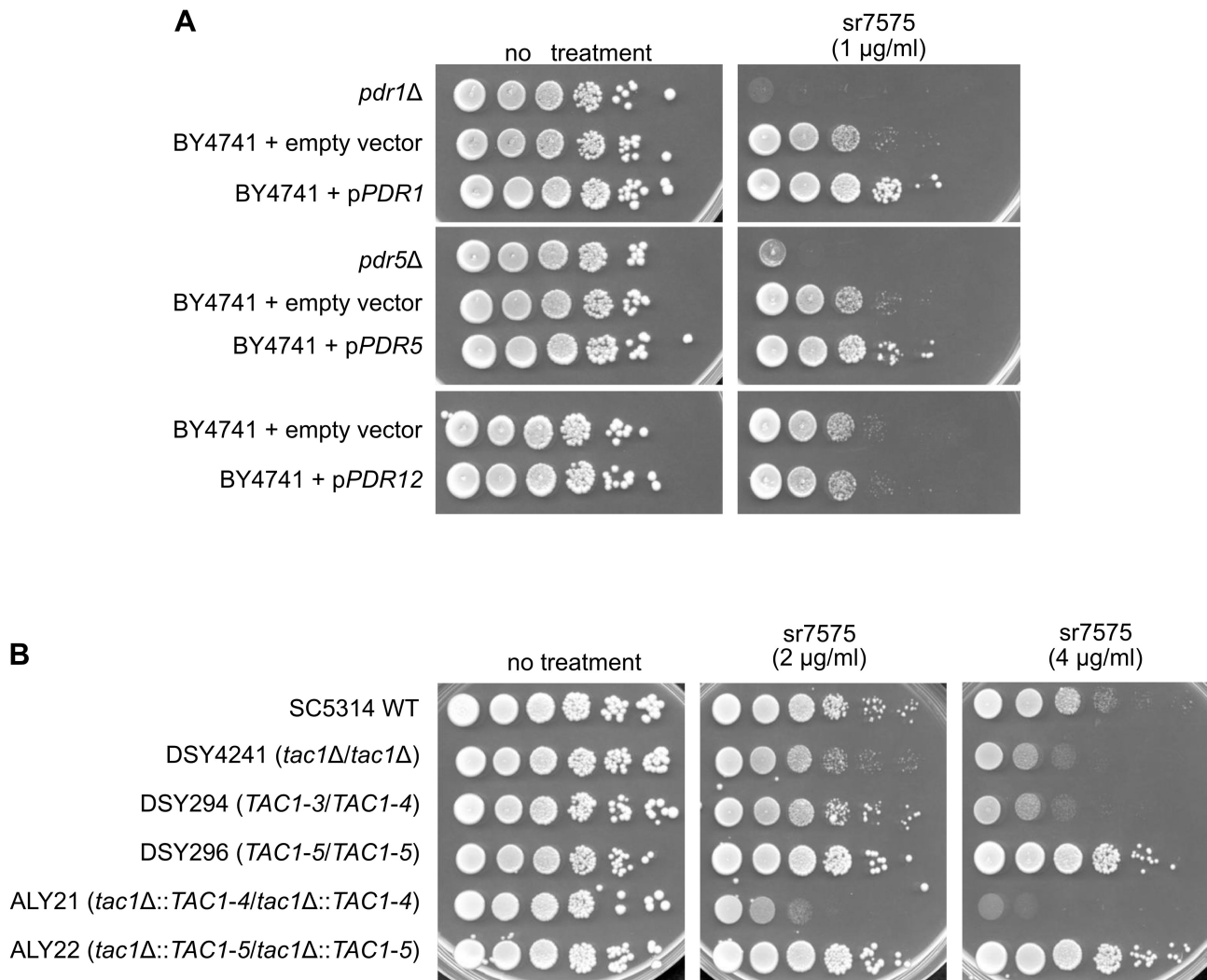


**Figure S6. Susceptibility of multidrug resistant *S. cerevisiae* strains and azole resistant *C. albicans* strains to sr7575.** (A) *S. cerevisiae* strains with deletions of or overexpressing *PDR1*, *PDR5* and *PDR12* were tested for susceptibility to sr7575 (1 µg/mL, SC medium, 30°C, 48 h). (B) Comparison of growth inhibition of *C. albicans* strains: WT (SC5314), *TAC1* transcription factor homozygous deletion strain (DSY4241), azole susceptible clinical isolate DSY294, azole resistant clinical isolate DSY296, azole susceptible laboratory generated strain ALY21 and azole resistant laboratory generated strain ALY22 (SC medium in the presence of 2 and 4 µg/mL sr7575, 37°C, 48 h).

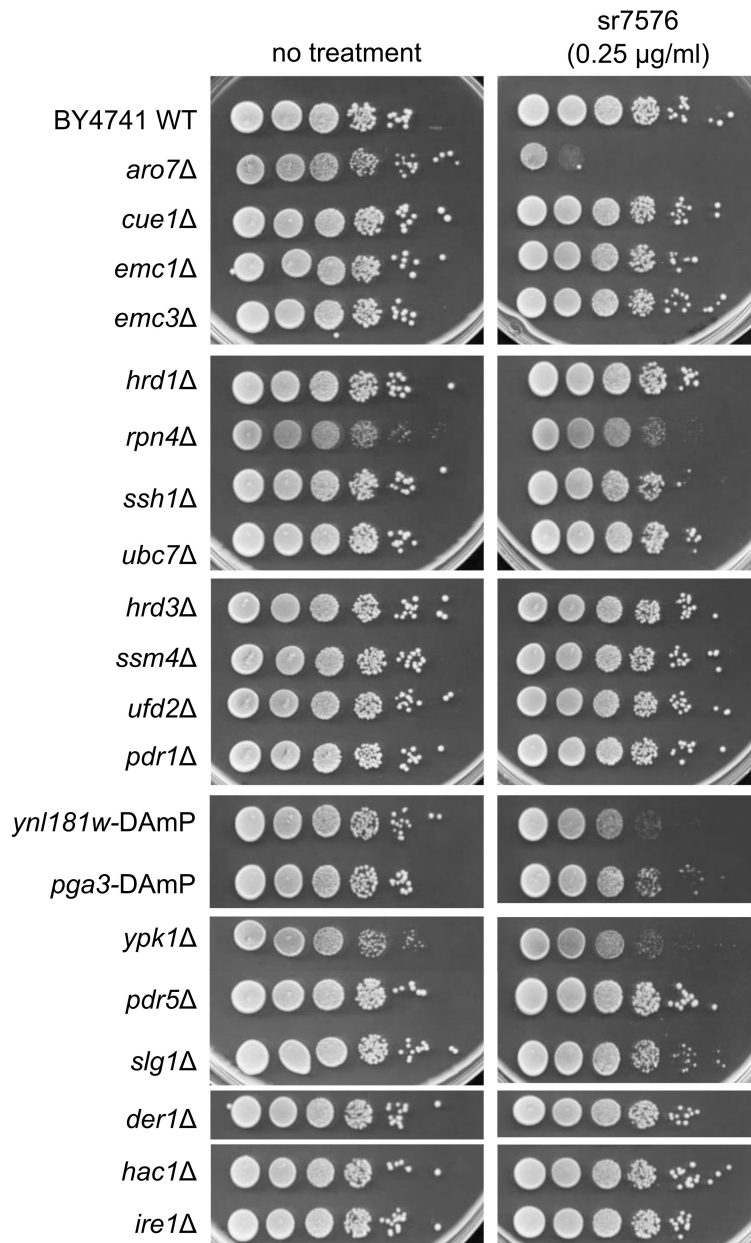


**Figure S7. Response of yeast mutants against sr7576.** Serial 10-fold dilutions of the WT and haploid deletion mutants were spotted onto SC plates supplemented with sr7576 (0.25  $\mu\text{g/mL}$ ). Plates were monitored for growth at 30°C for 48 h.



**Supplementary Table S4 - Strains and plasmids used in this study**

Strain	Genotype	Reference
BY4741	MATa;his3Δ 1;leu2Δ 0;met15Δ 0;ura3Δ 0	Brachmann et al, 1998

**(Deletion mutants were generated in the Sc BY4741 background)**

Strain	Genotype	Reference
aro7Δ	aro7::KanMX4	Giaever et al, 2002
cue1Δ	cue1::KanMX4	
der1Δ	der1::KanMX4	
doa10Δ	doa10::KanMX4	
emc1Δ	emc1::KanMX4	
emc3Δ	emc3::KanMX4	
gcs1Δ	gcs1::KanMX4	
hac1Δ	hac1::KanMX4	
hrd1Δ	hrd1::KanMX4	
hrd3Δ	hrd3::KanMX4	
ire1Δ	ire1::KanMX4	
pdr1Δ	pdr1::KanMX4	
pdr5Δ	pdr5::KanMX4	
pga3-DAmP	pga3-DAmP (KanMX4)	
rpn4Δ	rpn4::KanMX4	
sbh2Δ	sbh2::KanMX4	
sec65-DAMP	sec65-DAmP (KanMX4)	
slg1Δ	slg1::KanMX4	
ssh1Δ	ssh1::KanMX4	
trp2Δ	trp2::KanMX4	
ubc7Δ	ubc7::KanMX4	
ufd2Δ	ufd2::KanMX4	
ynl181w-DAmP	ynl181w-DAmP (KanMX4)	
yph1Δ	yph1::KanMX4	

**A. fumigatus strains used in this study:**

Strain	Genotype	Reference
kuA	akuA::ptrA	Krappmann et al, 2006
derAΔ	akuA::ptrA, derA::hph	Richie DL et al 2011
hacAΔ	akuA::ptrA, hacA::hph	Richie DL et al 2009
hrdAΔ	akuA::ptrA, hrdA::hph	Krishnan K et al 2013
ireAΔ	akuA::ptrA, ireA::ble	Jeng X et al 2011
derAΔ/hacAΔ	akuA::ptrA, hacA::hph, derA::ble	Richie DL et al 2011
derAΔ/hrdAΔ	akuA::ptrA, hrdA::hph, derA::ble	Krishnan K et al 2013

**Other yeast strains used in this study:**

Strain	Genotype	Reference
<i>C. albicans</i> SC5314	wild type	Lohberger et al, 2014
DSY4241	tac1Δ::FRT/tac1Δ::FRT	
DSY294	azole susceptible clinical isolate ( <i>TAC1-3/TAC1-4</i> )	
DSY296	azole resistant clinical isolate ( <i>TAC1-5/TAC1-5</i> ; N977D mutation)	
ALY21	tac1Δ::TAC1-4-FRT/tac1Δ::TAC1-4-FRT	
ALY22	tac1Δ::TAC1-5-FRT/tac1Δ::TAC1-5-FRT	
<i>C. neoformans</i> H99	wild type	

**MoBY plasmid (library v1.1) complemented *S. cerevisiae* strains:**

Strain	Genotype+ MoBY clone identifier	Reference
aro7Δ+ARO7	aro7::KanMX4+ YPR060C::29NP_C9	Ho et al, 2009
cue1Δ+CUE1	cue1::KanMX4+ YMR264W::33NP_H12	
emc1Δ+EMC1	emc1::KanMX4+ YCL045C::41NP_D8	
emc3Δ+EMC3	emc3::KanMX4+ YKL207W::8NP_A12	
hrd1Δ+HRD1	hrd1::KanMX4+ YOL013C::12NP_G12	
rpn4Δ+RPN4	rpn4::KanMX4+ YDL020C::30NP_F2	
ssh1Δ+SSH1	ssh1::KanMX4+ YBR283C::37NP_A11	
ubc7Δ+UBC7	ubc7::KanMX4+ YMR022W::36NP_G3	

**YGPM systematic overexpression library in *S. cerevisiae* strains:**

Strain	Genotype+ YGPM clone identifier	Reference
Control	BY4741+ YGPM22k06 chrIII:151898...152647	Jones et al, 2008
PDR1	BY4741+ YGPM26h12 chrVII:466658...477209	
PDR5	BY4741+ YGPM33k24 chrXV:619141...631341	
PDR12	BY4741+ YGPM8p07 chrXVI:444386...454435	

**References :**

- Brachmann CB, Davies A, Cost GJ, Caputo E, Li J, Hieter P, Boeke JD. Yeast. 1998 14(2):115-32.
- Krappmann S, Sasse C, Braus GH. Eukaryot Cell. 2006 5(1):212-5.
- Jones GM, Stalker J, Humphray S, West A, Cox T, Rogers J, Dunham I, Prelich G. Nature Methods. 2008 5:239-241
- Lohberger A, Coste AT, Sanglard D. Eukaryot Cell. 2014 13(1):127-42
- Perfect, JR, Lang SDR, and Durack DT. Am. J. Pathol. 1980 101:177-194.

Supplementary Material for Publication of manuscript "Toxicity of a novel antifungal compound is modulated by ERAD components", by Raj et al.

**Fig. S1:** Synthetic pathways for sr7575 and related compounds.

**Fig. S2:** Growth of *A. fumigatus*, *A. flavus*, *S. cerevisiae*, *C. albicans* and *C. neoformans* cells in liquid medium in the presence of various concentrations of sr7575.

**Fig. S3:** sr7575 profile shows little correlation with a previously published large-scale chemogenomics dataset.

**Fig. S4:** Perturbation of PGA3 function shows similarities with the sensitivity profile for sr7575.

**Fig. S5:** Susceptibility testing of yeast strains against sr7575.

**Fig. S6:** Susceptibility of multidrug resistant *S. cerevisiae* strains and azole resistant *C. albicans* strains to sr7575.

**Table S1:** List of 76 compounds from the CERMN chemical library showing 90% or more growth inhibition of *A. fumigatus* at 25 µg/mL.

**Table S2:** Analogues of sr7575 and MIC<sub>100</sub> values against *A. fumigatus*.

**Table S3:** Analogues of sr7576 and MIC<sub>100</sub> values against *A. fumigatus*.

**Table S4:** List of strains and plasmids used in this study.

**Table S5:** List of oligonucleotides used in this study.

**Table S6** (provided as a separate xls file): Sensitivity of *S. cerevisiae* deletion and DAmP strains to 0.125 µg/mL sr7575.

**Text S1:** Synthesis of sr7575 and related compounds.

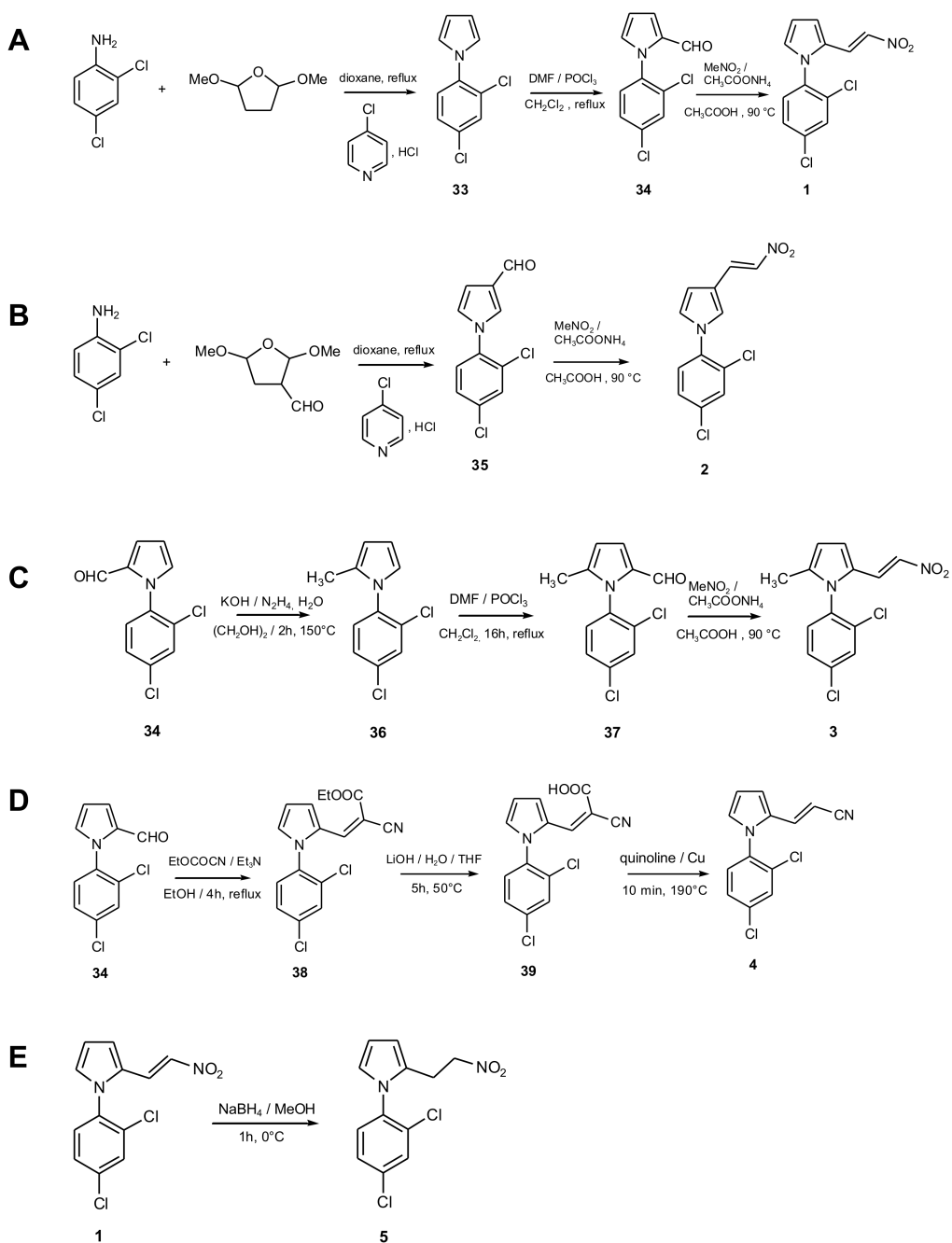


**Figure S1. Synthetic pathways for sr7575 and related compounds.** Pathways detailing the synthesis of sr7575 and analogues 2-5.

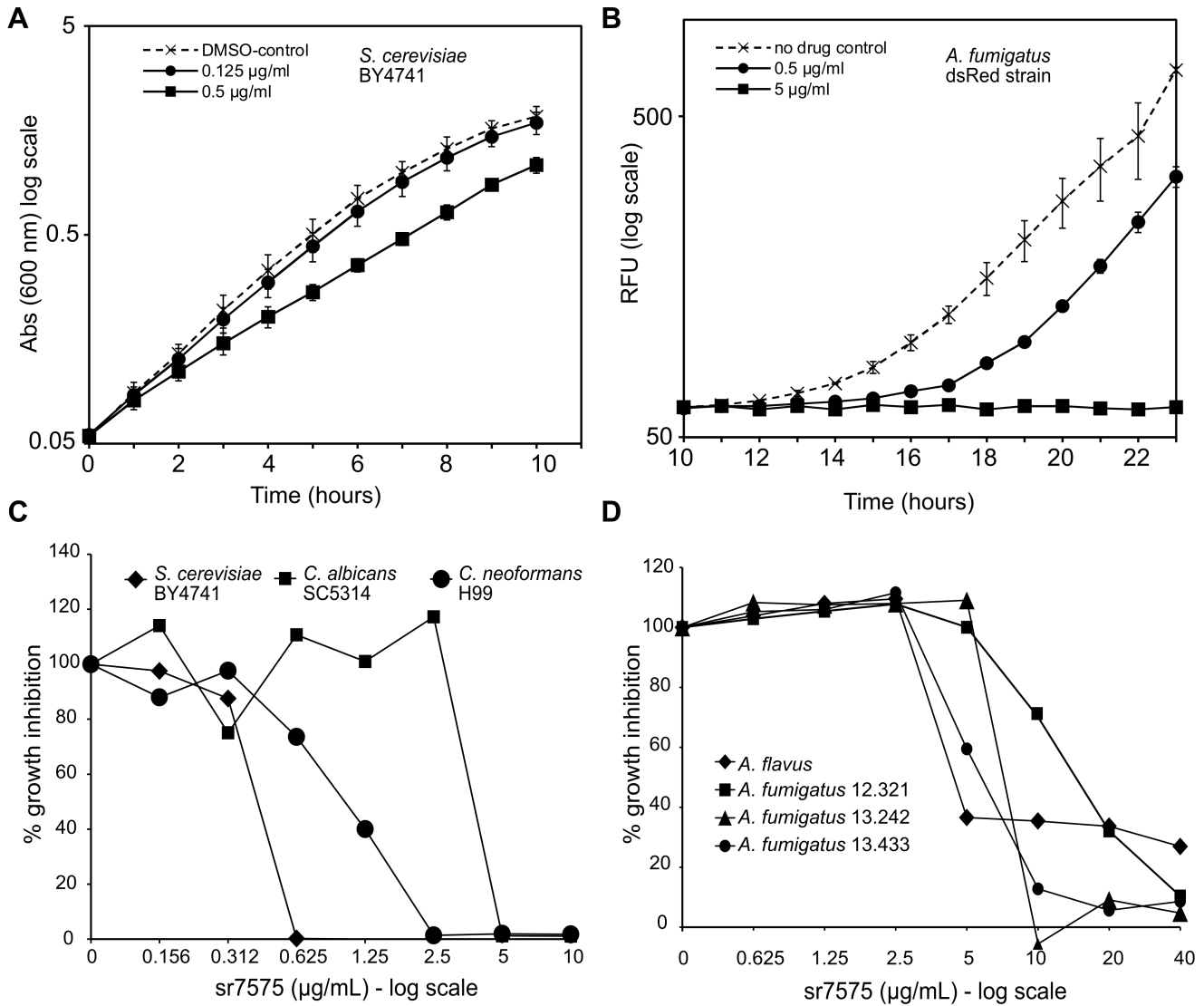


**Figure S2. Growth of *A. fumigatus*, *A. flavus*, *S. cerevisiae*, *C. albicans* and *C. neoformans* cells in liquid medium in the presence of various concentrations of sr7575. (A) Log-phase cultures of *S. cerevisiae* WT strain BY4741 were grown in the presence of increasing concentrations of sr7575 with DMSO as vehicle control. The Abs<sub>600</sub> was determined every hour for 10 h. (B) *A. fumigatus* strain Af293-dsRed was grown for 23 h in RPMI-1640 medium in the presence of increasing concentrations of sr7575. Fluorescence (ex 254 nm/ em 291 nm) was measured and relative fluorescence units (RFU) plotted against time. (C) Growth inhibition estimates were obtained at various concentrations of sr7575 by measuring absorbance at 600 nm for *S. cerevisiae* (BY4741, YPD, 30°C, 48 h), *C. albicans* (SC5314, RPMI, 37°C, 48 h) and *C. neoformans* (H99, RPMI, 37°C, 72 h). (D) Growth inhibition estimates for *A. flavus* and three *A. fumigatus* clinical isolates (12.321, 13.242, 13.433) were obtained by the resazurin reduction assay in RPMI medium, 37°C, 39 h at concentrations of sr7575 up to 40  $\mu\text{g/ml}$ .**

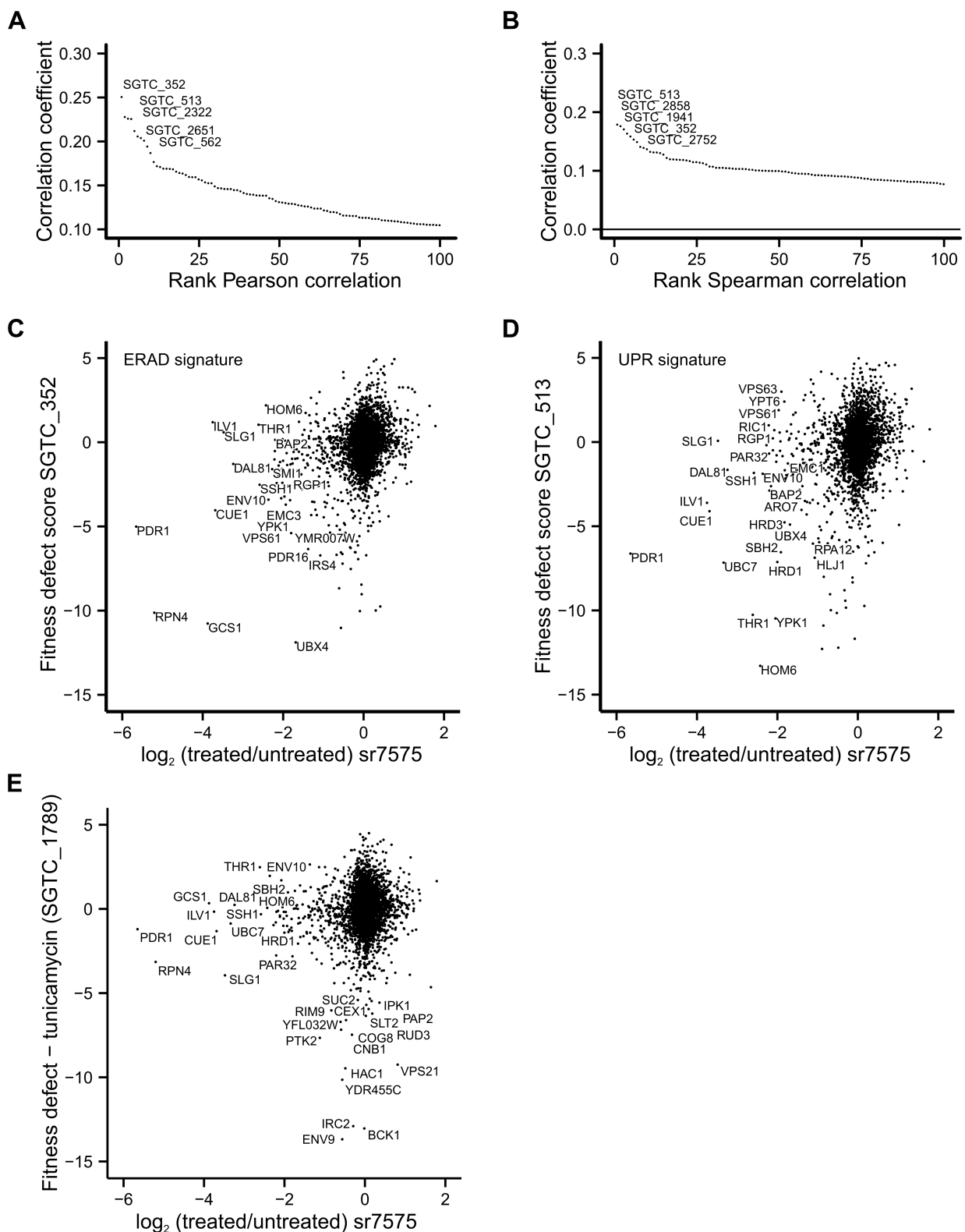


**Figure S3. sr7575 profile shows little correlation with a previously published large-scale chemogenomics dataset.** Computed Pearson (A) and Spearman (B) correlation coefficients between sr7575 values and previously published growth scores obtained with 3,356 compounds were ranked in descending order and the top 100 values are indicated. Among the highest correlations, we identified SGTC 352, a drug showing an ERAD signature (C) and SGTC 513, a compound with a UPR signature

**(D)** as being closest to the sr7575 profile. (E) The sr7575 profile showed no correlation with the one published for tunicamycin.

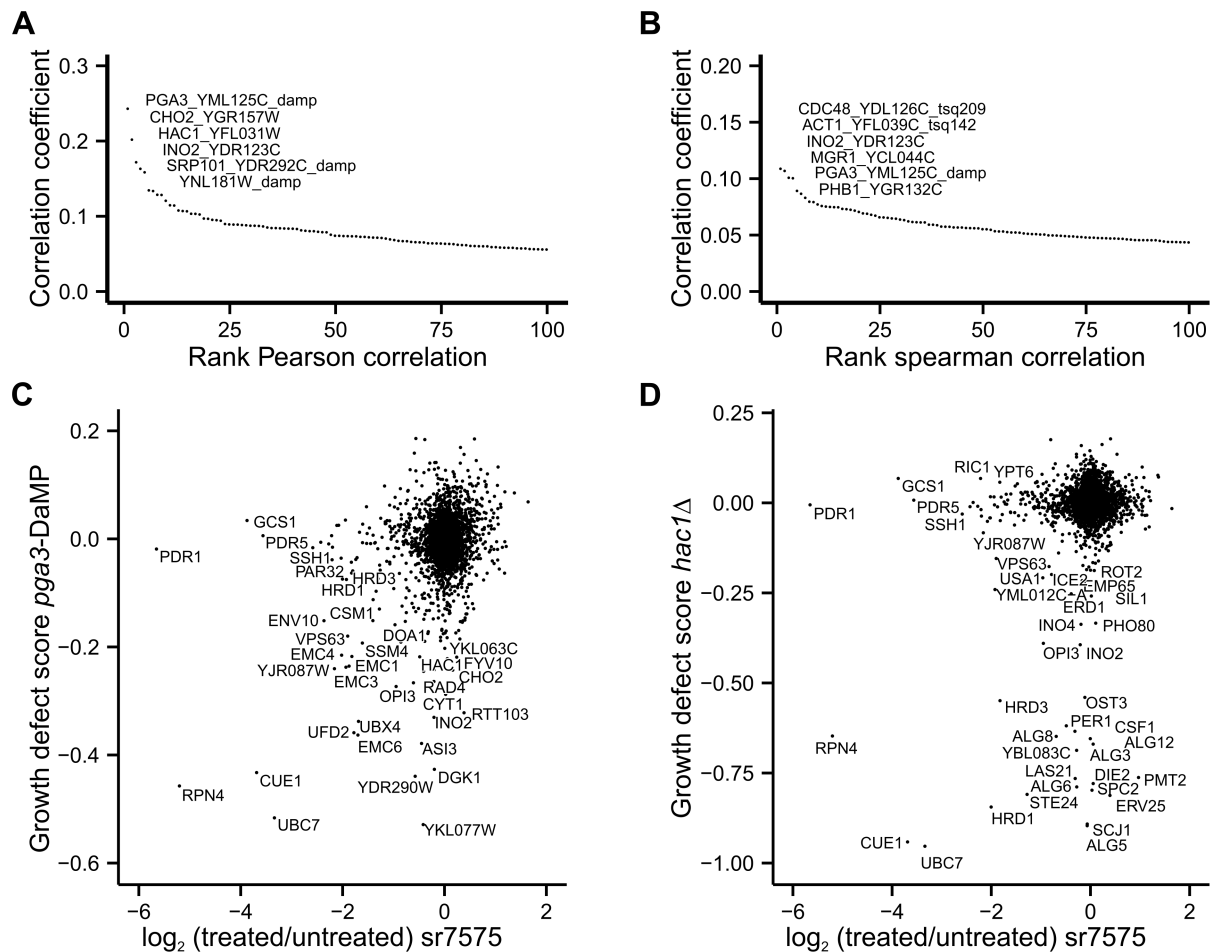


**Figure S4. Perturbation of *PGA3* function shows similarities with the sensitivity profile for *sr7575*.** Pearson (A) and Spearman (B) correlations between the *sr7575* profile and 1711 previously published SGA profiles. Fitness defect scores for DAMP modification of *PGA3* are shown in (C), while the interactions of *hac1* $\Delta$  and ERAD depleted strains are depicted in (D).

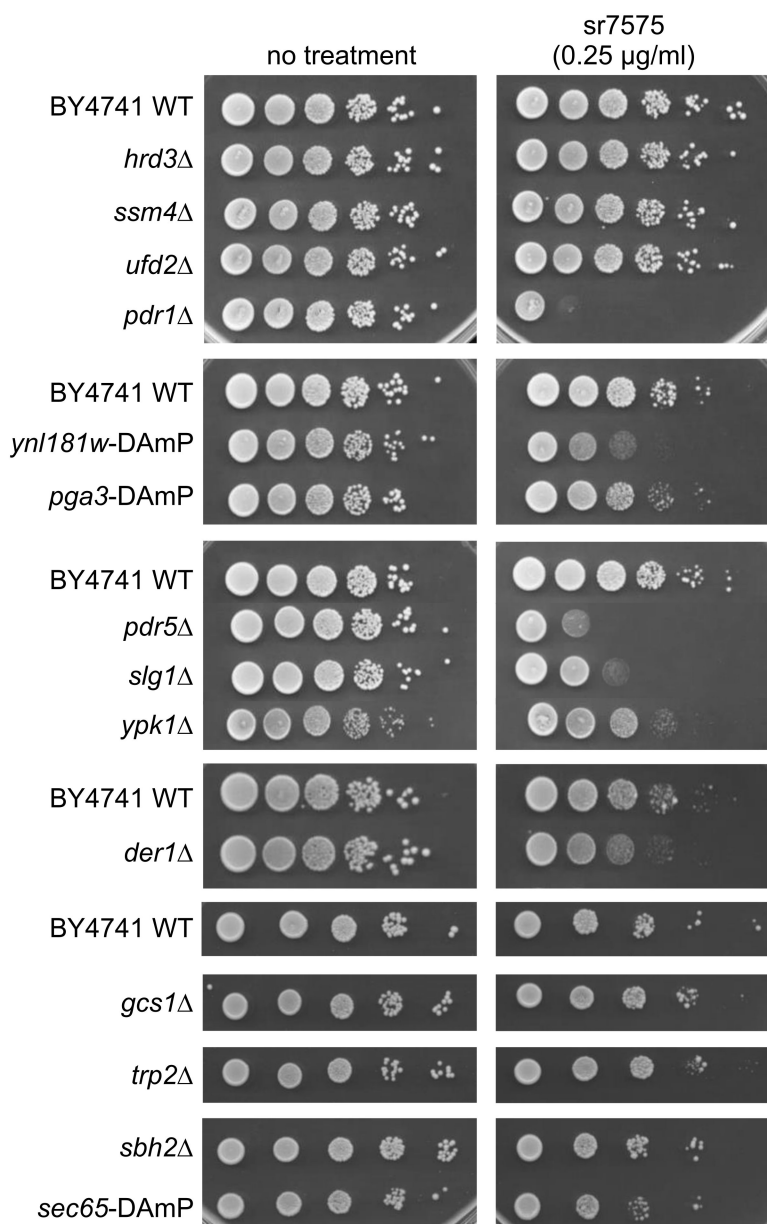


**Figure S5. Susceptibility testing of yeast strains against sr7575.** Mutants from the haploid deletion background were serially spotted onto SC plates supplemented with sr7575. Plates were incubated at 30°C for 48 h.



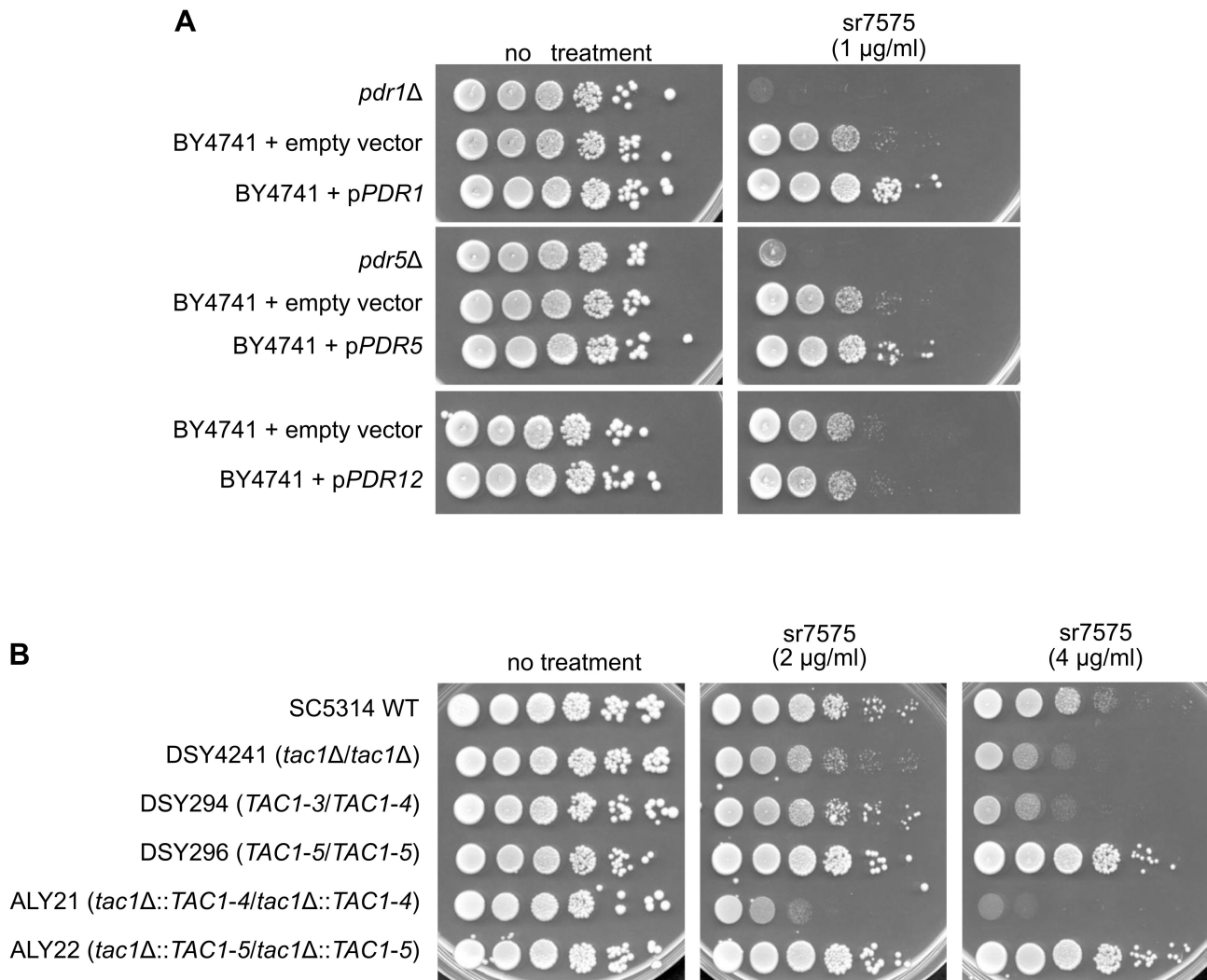
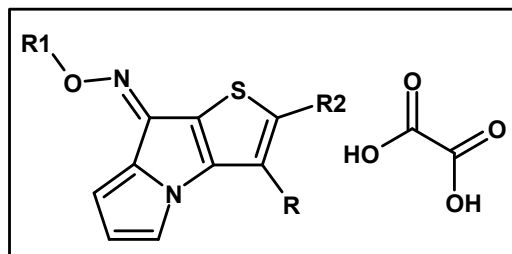


**Figure S6. Susceptibility of multidrug resistant *S. cerevisiae* strains and azole resistant *C. albicans* strains to sr7575.** (A) *S. cerevisiae* strains with deletions of or overexpressing *PDR1*, *PDR5* and *PDR12* were tested for susceptibility to sr7575 (1 µg/mL, SC medium, 30°C, 48 h). (B) Comparison of growth inhibition of *C. albicans* strains: WT (SC5314), *TAC1* transcription factor homozygous deletion strain (DSY4241), azole susceptible clinical isolate DSY294, azole resistant clinical isolate DSY296, azole susceptible laboratory generated strain ALY21 and azole resistant laboratory generated strain ALY22 (SC medium in the presence of 2 and 4 µg/mL sr7575, 37°C, 48 h).

**Supplementary Table S1 - list of 76 compounds from the CERMN chemical library showing 90% or more growth inhibition of *Aspergillus fumigatus* at 25 µg/mL.**

→ **Family A:**



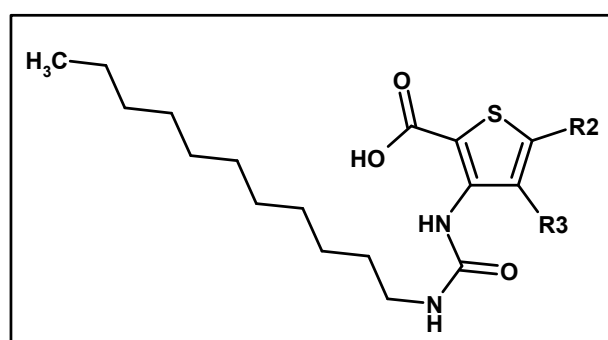
Compound	R	R1	R2	% viability
sr1304 <sup>1</sup>	-H			2
sr1308 <sup>2</sup>	-H			0
sr3163 <sup>2</sup>	-H			0
sr3164 <sup>2</sup>	-H			0
sr3168 <sup>3</sup>	-H			0
sr3169 <sup>2</sup>	-H			0

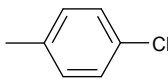
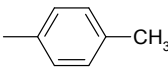
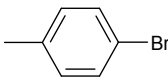
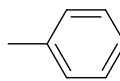
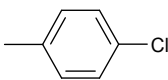
<sup>1</sup>S. Rault, S. Lemaître, F. Dauphin, A. Kervabon, M. Boulouard, J.-C. Lancelot, PCT Int. Appl., WO2001014381, (2001).

<sup>2</sup>Dual Histamine H3R/Serotonin 5-HT4R Ligands with Antiamnesic Properties: Pharmacophore-Based Virtual Screening and Polypharmacology, Lepailleur, Alban; Freret, Thomas; Lemaître, Stéphane; Boulouard, Michel; Dauphin, François; Hinschberger, Antoine; Dulin, Fabienne; Lesnard, Aurelien; Bureau, Ronan; Rault, Sylvain; Journal of Chemical Information and Modeling (2014), 54(6), 1773-1784.

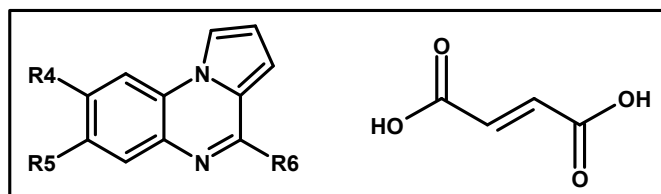
sr3172 <sup>1</sup>	-H		-OCH <sub>3</sub>	0
sr3174 <sup>3</sup>	-H			0
sr3179 <sup>2</sup>			-H	0
sr3180 <sup>2</sup>			-H	0
sr3181 <sup>3</sup>			-H	0
sr3182 <sup>2</sup>			-H	0
sr3185 <sup>3</sup>			-H	0
sr3186 <sup>1</sup>			-H	0
sr3188 <sup>2</sup>	-H			0

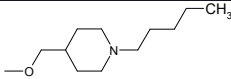
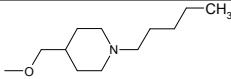
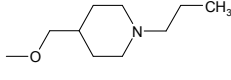
→ **Family B:**



Compound	R2	R3	% viability
sr4045 <sup>1</sup>	-H		2
sr4046 <sup>1</sup>		-H	0
sr4049 <sup>1</sup>		-H	0
sr4050 <sup>3</sup>	-H		0
sr4051 <sup>1</sup>		-H	0
sr4052 <sup>4</sup>	-H	-H	0

→ **Family C:** \_\_\_\_\_

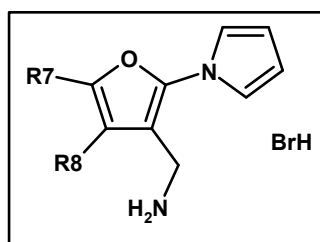


Compound	R4	R5	R6	% viability
mr22450 <sup>2</sup>	-H	-CH <sub>3</sub>		0
mr22442 <sup>2</sup>	-H	-Cl		0
mr22455 <sup>2</sup>	-H	-Cl		0

<sup>3</sup> Solution-phase parallel synthesis of a 1140-member ureidothiophene carboxylic acid library, Le Foulon, Francois-Xavier; Braud, Emmanuelle; Fabis, Frederic; Lancelot, Jean-Charles; Rault, Sylvain, Journal of Combinatorial Chemistry (2005), 7(2), 253-257.

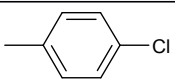
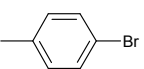
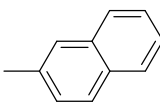
mr22461 <sup>2</sup>	-H	-Cl		0
mr22478 <sup>2</sup>	-H	-Cl		4
mr18993 <sup>4</sup>	-Cl	-Cl		4
mr23269 <sup>3</sup>	-H	-H		1
mr23270 <sup>1</sup>	-H	-F		0
mr24316 <sup>1</sup>	-H	-Cl		0
mr24344 <sup>3</sup>	-H	-H		3
sr1832 <sup>5</sup>	-H	-H		0
sr2823 <sup>1</sup>	-H	-CH3		0

→ **Family D:**

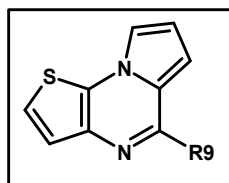


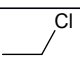
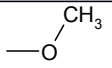
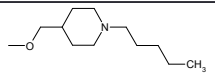
4 Synthesis of new pyrrolo[1,2-a]quinoxalines: potential non-peptide glucagon receptor antagonists, Guillon, Jean; Dallemagne, Patrick; Pfeiffer, Bruno; Renard, Pierre; Manechez, Dominique; Kervran, Alain; Rault, Sylvain, *European Journal of Medicinal Chemistry* (1998), 33(4), 293-308

5 Novel and Selective Partial Agonists of 5-HT<sub>3</sub> Receptors. 2. Synthesis and Biological Evaluation of Piperazinopyridopyrrolopyrazines, Piperazinopyrroloquinoxalines, and Piperazinopyridopyrroloquinoxalines Prunier, Herve; Rault, Sylvain; Lancelot, Jean-Charles; Robba, Max; Renard, Pierre; Delagrang, Philippe; Pfeiffer, Bruno; Caignard, Daniel-Henri; Misslin, Rene; Guardiola-Lemaitre, Beatrice; et al, *Journal of Medicinal Chemistry* (1997), 40(12), 1808-1819.

Compound	R7	R8	% viability
sr1457 <sup>1</sup>		-H	0
sr1460 <sup>1</sup>		-H	0
sr1462 <sup>1</sup>		-H	2

→ **Family E:**

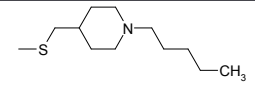
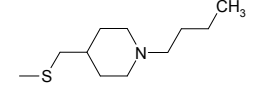


Compound	R9	% viability
sr2845 <sup>6</sup>		0
sr3584 <sup>7</sup>		0
mr22410 <sup>8</sup>		6

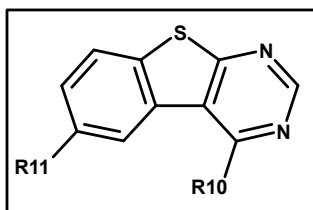
<sup>6</sup> Novel Selective and Partial Agonists of 5-HT<sub>3</sub> Receptors. Part 1. Synthesis and Biological Evaluation of Piperazinopyrrolothienopyrazines, Rault, Sylvain; Lancelot, Jean-Charles; Prunier, Herve; Robba, Max; Renard, Pierre; Delagrang, Philippe; Pfeiffer, Bruno; Caignard, Daniel-Henri; Guardiola-Lemaitre, Beatrice; Hamon, Michel, *Journal of Medicinal Chemistry* (1996), 39(10), 2068-80.

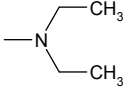
<sup>7</sup> Pyrrolo[1,2-a]thieno[3,2-e]pyrazines, Rault, Sylvain; Cugnon de Sevracourt, Michel; Nguyen-Huy Dung; Robba, Max, *Journal of Heterocyclic Chemistry* (1981), 18(4), 739-42.

<sup>8</sup> Novel antagonists of serotonin-4 receptors: Synthesis and biological evaluation of pyrrolothienopyrazines, Lemaitre, Stephane; Lepailleur, Alban; Bureau, Ronan; Butt-Gueulle, Sabrina; Lelong-Boulouard, Veronique; Duchatelle, Pascal; Boulouard, Michel; Dumuis, Aline; Daveu, Cyril; Lezoualc'h, Frank; et al, *Bioorganic & Medicinal Chemistry* (2009), 17(6), 2607-2622.

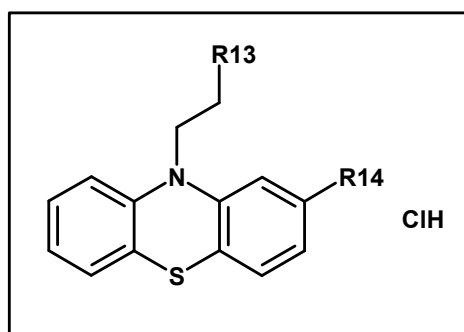
mr22422 <sup>1</sup>		0
mr24356 <sup>1</sup>		3

→ **Family F:**



Compound	R10	R11	% viability
sr2205 <sup>9</sup>		-H	3
sr2210 <sup>1</sup>	-NH <sub>2</sub>	-H	3
sr2634 <sup>1</sup>	-Cl	-NO <sub>2</sub>	0

→ **Family G:**



Compound	R13	R14	% viability

pa2 <sup>10</sup>		-CF <sub>3</sub>	0
pa18 <sup>11</sup>		-Cl	0

→ [Singletons:](#)

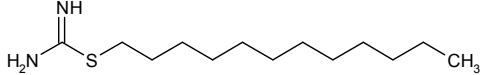
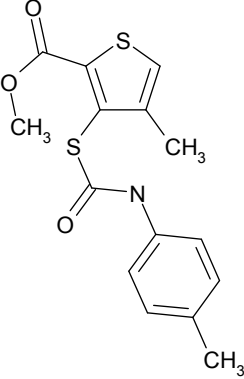
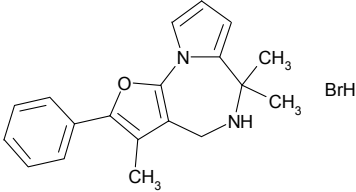
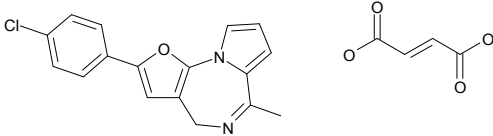
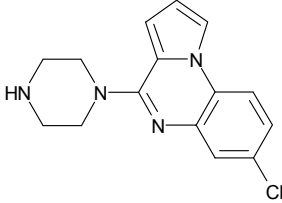
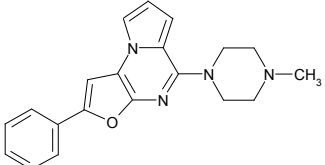
Compound	Structure	% viability
mr19807 <sup>1</sup>		0
mr15010a <sup>1</sup>		4
mr15059 <sup>12</sup>		4

<sup>10</sup>Trifluoperazine (DCI) dihydrochloride; New (trifluoromethyl)phenothiazine derivatives, Craig, P. N.; Nodiff, E. A.; Lafferty, J. J.; Ulliyot, G. E., *Journal of Organic Chemistry* (1957), 22, 709-11.

<sup>11</sup>Chlorpromazine (DCI) hydrochloride; Substituted 10-(dimethylaminopropyl)phenothiazines, Charpentier, Paul; Gailliot, Paul; Jacob, Robert; Gaudechon, Jacques; Buisson, Paul, *Compt. rend.* (1952), 235, 59-60.

<sup>12</sup>Anti-tumor heterocycles. Part 13. The syntheses of two new pyridocarbazoles (ellipticines) and some pyrrolocarbazole analogs, Chunchatprasert, Laddawan; Dharmasena, Priyanthi; Oliveira-Campos, Ana M. F.; Queiroz, Maria J. R. P.; Raposo, Maria M. M.; Shannon, Patrick V. R. *Journal of Chemical Research, Synopses* (1996), (2), 84-5.



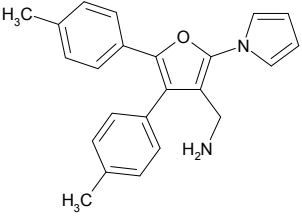
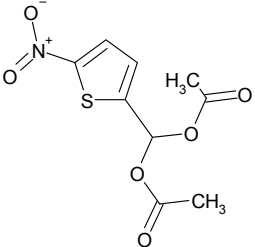
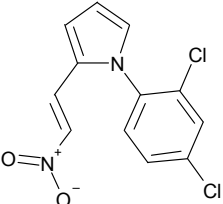
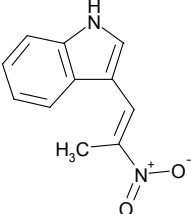
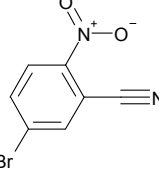
mr22633 <sup>13</sup>		0
mr16310 <sup>14</sup>		2
mr21034 <sup>15</sup>		10
mr21018 <sup>1</sup>		8
mr18499 <sup>16</sup>		0
sr1429 <sup>1</sup>		0

<sup>13</sup> Comparative effect of a family of substituted thiopseudoureas on protein synthesis by rat liver and Walker carcinoma ribosomes, Carmona, Andres; Gonzalez-Cadavid, Nestor F., *Chemico-Biological Interactions* (1978), 22(2-3), 309-27.

<sup>14</sup> Preparation of 3-mercapto-2-thiophenecarboxylic acid derivatives as intermediates for herbicides, Rault, Sylvain; Lancelot, Jean Charles; Letois, Bertrand; Robba, Max; Labat, Yves Fr. *Demande* (1993), FR 2689129 A1 19931001.

<sup>15</sup> First synthesis of 5,6-dihydro-4H-furo[3,2-f]pyrrolo[1,2-a][1,4]diazepines, Feng, Xiao; Lancelot, Jean-Charles; Gillard, Alain-Claude; Landelle, Henriette; Rault, Sylvain, *Journal of Heterocyclic Chemistry* (1998), 35(6), 1313-1316.

<sup>16</sup> Preparation of pyrrolopyrazines as 5-HT<sub>3</sub> ligands, Lancelot, Jean-Charles; Prunier, Herve; Robba, Max; Delagrang, Philippe; Renard, Pierre; Adam, Gerard, *Eur. Pat. Appl.* (1994), EP 623620 A1 19941109.

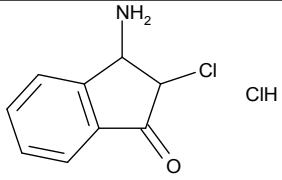
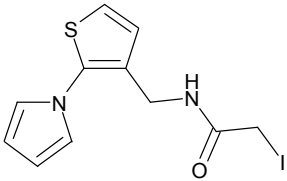
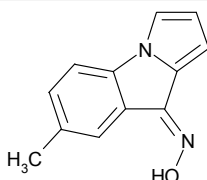
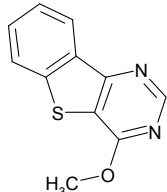
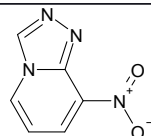
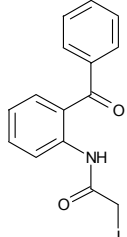
sr1461 <sup>17</sup>		1
sr1475 <sup>18</sup>		0
sr1810 <sup>1</sup>		9
sr1821 <sup>19</sup>		0
sr1922 <sup>20</sup>		0

<sup>17</sup> First synthesis of 4H-furo[3,2-f]pyrrolo[1,2-a][1,4]diazepines, Feng, Xiao; Lancelot, Jean-Charles; Prunier, Herve; Rault, Sylvain, *Journal of Heterocyclic Chemistry* (1996), 33(6), 2007-2011.

<sup>18</sup> Synthesis and in vitro antibacterial evaluation of N-[5-(5-nitro-2-thienyl)-1,3,4-thiadiazol-2-yl] piperazinylquinolones, Foroumadi, Alireza; Mansouri, Shahla; Kiani, Zahra; Rahmani, Afsaneh, *European Journal of Medicinal Chemistry* (2003), 38(9), 851-854.

<sup>19</sup> Alpha-ethyltryptamines as dual dopamine-serotonin releasers, Blough, Bruce E.; Landavazo, Antonio; Partilla, John S.; Decker, Ann M.; Page, Kevin M.; Baumann, Michael H.; Rothman, Richard B., *Bioorganic & Medicinal Chemistry Letters* (2014), 24(19), 4754-4758.

<sup>20</sup> Synthesis of nitrile and benzoyl substituted poly(biphenylene oxide)s via nitro displacement reaction In, Insik; Kim, Sang Youl, *Polymer* (2006), 47(13), 4549-4556

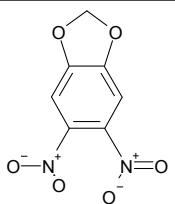
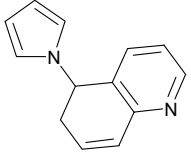
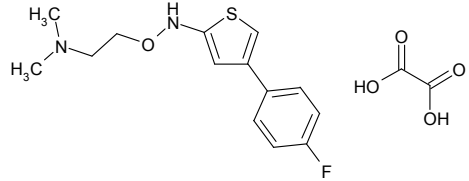
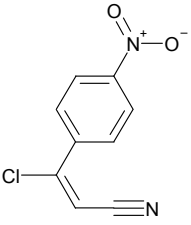
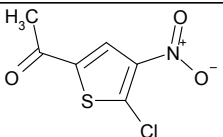
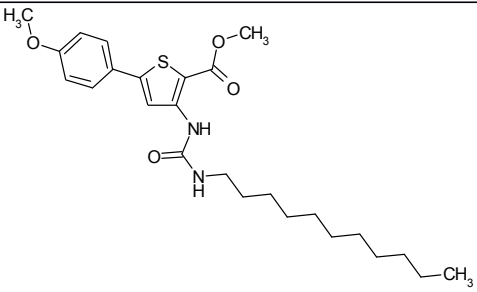
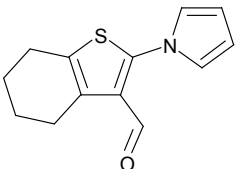
sr2223		8
sr2323 <sup>1</sup>		0
sr2565 <sup>21</sup>		5
sr2627 <sup>22</sup>		1
sr2970 <sup>23</sup>		6
sr2809 <sup>24</sup>		0

<sup>21</sup> First tricyclic oximino derivatives as 5-HT<sub>3</sub> ligands, Baglin, I.; Daveu, C.; Lancelot, J. C.; Bureau, R.; Dauphin, F.; Pfeiffer, B.; Renard, P.; Delagrangé, P.; Rault, S., *Bioorganic & Medicinal Chemistry Letters* (2001), 11(4), 453-457.

<sup>22</sup> [1]Benzothienopyrimidines. I. Study of 3H-benzothieno[3,2-d]pyrimidin-4-one, Robba, Max; Touzot, Paulette; El-Kashef, Hussein, *Journal of Heterocyclic Chemistry* (1980), 17(5), 923-8.

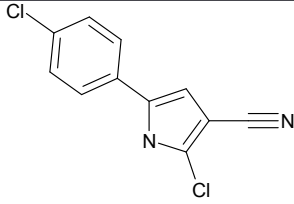
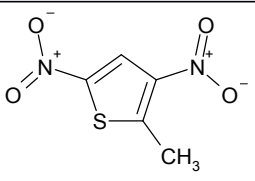
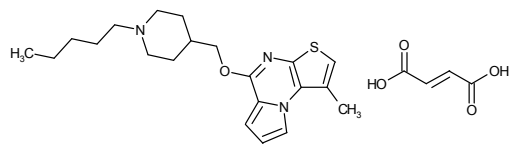
<sup>23</sup> Synthesis and physicochemical study of 1,2,4-triazolo[4,3-a]pyridines and of 1,2,4-triazolo[2,3-a]pyridines, Bouteau, Brigitte; Lancelot, Jean Charles; Robba, Max, *Journal of Heterocyclic Chemistry* (1990), 27(6), 1649-51.

<sup>24</sup> Method of producing 2-iodoacetylaminobenzophenones, Mazurov, A. A.; Andronati, S. A.; Yakubovskaya, L. N. U.S.S.R. (1991), SU 1622365 A1 19910123.

sr2967 <sup>25</sup>		3
mr12044 <sup>1</sup>		3
sr3184 <sup>1</sup>		0
sr3456 <sup>2</sup>		0
sr3355 <sup>26</sup>		0
sr5443 <sup>1</sup>		6
sr4274 <sup>1</sup>		2

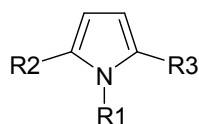
<sup>25</sup> Synthesis, in vitro cytotoxic and in vivo antitumor activities of new pyrrolo[2,1-c][1,4]benzodiazepines. Part I Foloppe, M. P.; Caballero, E.; Rault, S.; Robba, M., European Journal of Medicinal Chemistry (1992), 27(3), 291-5.

<sup>26</sup> Selective Dual Inhibitors of the Cancer-Related Deubiquitylating Proteases USP7 and USP47, Weinstock, Joseph; Wu, Jian; Cao, Ping; Kingsbury, William D.; McDermott, Jeffrey L.; Kodrasov, Matthew P.; McKelvey, Devin M.; Suresh Kumar, K. G.; Goldenberg, Seth J.; Mattern, Michael R.; et al, ACS Medicinal Chemistry Letters (2012), 3(10), 789-792.

sr4080 <sup>27</sup>		8
sr4211 <sup>28</sup>		8
mr24355 <sup>10</sup>		0

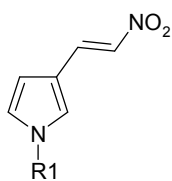
<sup>27</sup> Insecticidal action and mitochondrial uncoupling activity of AC-303,630 and related halogenated pyrroles, Black, Bruce C.; Hollingworth, Robert M.; Ahammadsahib, Kabeer I.; Kukel, Christine D.; Donovan, Stephen *Pesticide Biochemistry and Physiology* (1994), 50(2), 115-28.

<sup>28</sup> Synthesis of dinitro-substituted furans, thiophenes, and azoles, Katritzky, Alan R.; Vakulenko, Anatoliy V.; Sivapackiam, Jothilingam; Draghici, Bogdan; Damavarapu, Reddy *Synthesis* (2008), (5), 699-706.



Compound	R1	R2	R3	MIC <sub>100</sub> ( $\mu\text{g/ml}$ )
sr7575 (1)	2,4-dichlorophenyl	H		2.4-4.8
3	2,4-dichlorophenyl	CH <sub>3</sub>		> 26-32
4	2,4-dichlorophenyl	H		> 26-32
5	2,4-dichlorophenyl	H		> 26-32
6	4-chlorophenyl	H		2.4-4.8
7	3-chlorophenyl	H		9.6
8	2-chlorophenyl	H		13 - 26
9	3,4-dichlorophenyl	H		9.6
10	2,3-dichlorophenyl	H		19.2
11	2,5-dichlorophenyl	H		> 38.5
12	3,5-dichlorophenyl	H		9.6
13	2,6-dichlorophenyl	H		19.2
14	2,4,5-trichlorophenyl	H		9.6
15	2,4,6-trichlorophenyl	H		26 - 32
16	2-fluoro-4-chlorophenyl	H		13 - 26
17	2-chloro-4-fluorophenyl	H		13
18	2,4-dibromophenyl	H		13 - 26
19	2-bromo-4-chlorophenyl	H		13 - 26
20	2-chloro-4-bromophenyl	H		13
21	2-iodo-4-chlorophenyl	H		26
22	2-chloro-4-iodophenyl	H		26

**Supplementary Table S2: Analogues of sr7575 and MIC values against *A. fumigatus*.**



<b>Compound</b>	<b>R1</b>	<b>MIC<sub>100</sub> (<math>\mu\text{g/ml}</math>)</b>
<b>sr7576 (2)</b>	2,4-dichlorophenyl	> 38.5
<b>23</b>	3-chlorophenyl	26 - 32
<b>24</b>	3,4-dichlorophenyl	26 - 32
<b>25</b>	3,5-dichlorophenyl	26 - 32
<b>26</b>	2,6-dichlorophenyl	38.5
<b>27</b>	2,4,6-trichlorophenyl	38.5
<b>28</b>	2-bromo-4-chlorophenyl	> 26 - 32
<b>29</b>	2-chloro-4-bromophenyl	> 26 - 32
<b>30</b>	2,4-dibromophenyl	> 26 - 32
<b>31</b>	2-iodo-4-chlorophenyl	> 26 - 32
<b>32</b>	2-chloro-4-iodophenyl	>26 - 32

**Supplementary Table S3: Analogues of sr7576 and MIC values against *A. fumigatus*.**

**Supplementary Table S4 - Strains and plasmids used in this study**

Strain	Genotype	Reference
BY4741	MATa;his3Δ 1;leu2Δ 0;met15Δ 0;ura3Δ 0	Brachmann et al, 1998

**(Deletion mutants were generated in the Sc BY4741 background)**

Strain	Genotype	Reference
aro7Δ	aro7::KanMX4	Giaever et al, 2002
cue1Δ	cue1::KanMX4	
der1Δ	der1::KanMX4	
doa10Δ	doa10::KanMX4	
emc1Δ	emc1::KanMX4	
emc3Δ	emc3::KanMX4	
gcs1Δ	gcs1::KanMX4	
hac1Δ	hac1::KanMX4	
hrd1Δ	hrd1::KanMX4	
hrd3Δ	hrd3::KanMX4	
ire1Δ	ire1::KanMX4	
pdr1Δ	pdr1::KanMX4	
pdr5Δ	pdr5::KanMX4	
pga3-DAmP	pga3-DAmP (KanMX4)	
rpn4Δ	rpn4::KanMX4	
sbh2Δ	sbh2::KanMX4	
sec65-DAMP	sec65-DAmP (KanMX4)	
slg1Δ	slg1::KanMX4	
ssh1Δ	ssh1::KanMX4	
trp2Δ	trp2::KanMX4	
ubc7Δ	ubc7::KanMX4	
ufd2Δ	ufd2::KanMX4	
ynl181w-DAmP	ynl181w-DAmP (KanMX4)	
ypk1Δ	ypk1::KanMX4	

**A. fumigatus strains used in this study:**

Strain	Genotype	Reference
kuA	akuA::ptrA	Krappmann et al, 2006
derAΔ	akuA::ptrA, derA::hph	Richie DL et al 2011
hacAΔ	akuA::ptrA, hacA::hph	Richie DL et al 2009
hrdAΔ	akuA::ptrA, hrdA::hph	Krishnan K et al 2013
ireAΔ	akuA::ptrA, ireA::ble	Jeng X et al 2011
derAΔ/hacAΔ	akuA::ptrA, hacA::hph, derA::ble	Richie DL et al 2011
derAΔ/hrdAΔ	akuA::ptrA, hrdA::hph, derA::ble	Krishnan K et al 2013

**Other yeast strains used in this study:**

Strain	Genotype	Reference
<i>C. albicans</i> SC5314	wild type	Lohberger et al, 2014
DSY4241	tac1Δ::FRT/tac1Δ::FRT	
DSY294	azole susceptible clinical isolate ( <i>TAC1-3/TAC1-4</i> )	
DSY296	azole resistant clinical isolate ( <i>TAC1-5/TAC1-5</i> ; N977D mutation)	
ALY21	tac1Δ::TAC1-4-FRT/tac1Δ::TAC1-4-FRT	
ALY22	tac1Δ::TAC1-5-FRT/tac1Δ::TAC1-5-FRT	
<i>C. neoformans</i> H99	wild type	Perfect et al, 1980

**MoBY plasmid (library v1.1) complemented *S. cerevisiae* strains:**

Strain	Genotype+ MoBY clone identifier	Reference
aro7Δ+ARO7	aro7::KanMX4+ YPR060C::29NP_C9	Ho et al, 2009
cue1Δ+CUE1	cue1::KanMX4+ YMR264W::33NP_H12	
emc1Δ+EMC1	emc1::KanMX4+ YCL045C::41NP_D8	
emc3Δ+EMC3	emc3::KanMX4+ YKL207W::8NP_A12	
hrd1Δ+HRD1	hrd1::KanMX4+ YOL013C::12NP_G12	
rpn4Δ+RPN4	rpn4::KanMX4+ YDL020C::30NP_F2	
ssh1Δ+SSH1	ssh1::KanMX4+ YBR283C::37NP_A11	
ubc7Δ+UBC7	ubc7::KanMX4+ YMR022W::36NP_G3	

**YGPM systematic overexpression library in *S. cerevisiae* strains:**

Strain	Genotype+ YGPM clone identifier	Reference
Control	BY4741+ YGPM22k06 chrIII:151898...152647	Jones et al, 2008
PDR1	BY4741+ YGPM26h12 chrVII:466658...477209	
PDR5	BY4741+ YGPM33k24 chrXV:619141...631341	
PDR12	BY4741+ YGPM8p07 chrXVI:444386...454435	

**References :**

- Brachmann CB, Davies A, Cost GJ, Caputo E, Li J, Hieter P, Boeke JD. Yeast. 1998 14(2):115-32.
- Krappmann S, Sasse C, Braus GH. Eukaryot Cell. 2006 5(1):212-5.
- Jones GM, Stalker J, Humphray S, West A, Cox T, Rogers J, Dunham I, Prelich G. Nature Methods. 2008 5:239-241
- Lohberger A, Coste AT, Sanglard D. Eukaryot Cell. 2014 13(1):127-42
- Perfect, JR, Lang SDR, and Durack DT. Am. J. Pathol. 1980 101:177-194.



**Supplementary Table S5 - list of oligonucleotides used in this study****List of oligonucleotides to screen deletion/DAmP mutants:**

<b>Gene</b>	<b>Primer name</b>	<b>Sequence</b>
Kanamycin	KANMX-FW	5'-AGATGCGAAGTTAAGTGCGC-3'
<i>ARO7</i>	ARO7dR	5'-GAGAGAAGGTCATGGATGTG-3'
<i>CUE1</i>	CUE1dR	5'-GTAAGGGGAGAAGAACGTTTC-3'
<i>DER1</i>	DER1dR	5'-TCTGCAAACGGACACCAAGT-3'
<i>EMC1</i>	EMC1dR	5'-GCACATCATTTCCAGACGAG-3'
<i>EMC3</i>	EMC3dR	5'-GCGAGGACTTTTTGCCATAC-3'
<i>GCS1</i>	GCS1dR	5'-GTGGTAGTTCTCTCTCCTTG-3'
<i>HAC1</i>	HAC1dR	5'-AGAGCCGTGAGAGTGAGAGT-3'
<i>HRD1</i>	HRD1dR	5'-TATGTCACCTTCCTATGCCG-3'
<i>HRD3</i>	HRD3dR	5'-ATGAACGGCAATTTGAGACC-3'
<i>IRE1</i>	IRE1dR	5'-TCTTGCACTTTTTCGCCATGC-3'
<i>PDR1</i>	PDR1dR	5'-TGGCAACTATGTGGTGCAAT-3'
<i>PDR5</i>	PDR5dR	5'-GCATCTTGCTCTTTCCTCTC-3'
<i>RPN4</i>	RPN4dR	5'-CTGGGTACGAATTCAAGGAG-3'
<i>SBH2</i>	SBH2dR	5'-CATGCACCCTTAACATCGTC-3'
<i>SEC65</i>	SEC65-DAmP	5'-GGAAGTTGTGAGTACTGACG-3'
<i>SLG1</i>	SLG1dR	5'-TATATCGTCTTTC AACGCGG-3'
<i>SSH1</i>	SSH1dR	5'-CCACGAAGCAAGGTAACAAG-3'
<i>SSM4</i>	SSM4dR	5'-GACGAGGGCTAAGCAGTTTG-3'
<i>TRP2</i>	TRP2dR	5'-CCAAACCACATTGGTCTAGG-3'
<i>UBC7</i>	UBC7dR	5'-TACTGTACGGCTTGGAAGAG-3'
<i>UFD2</i>	UFD2dR	5'-ACCGTCATCAACGAACAACA-3'
<i>YPK1</i>	YPK1dR	5'-CCGTTTCGTGGTTAAGGTAAG-3'

**List of oligonucleotides to screen MoBY plasmids:**

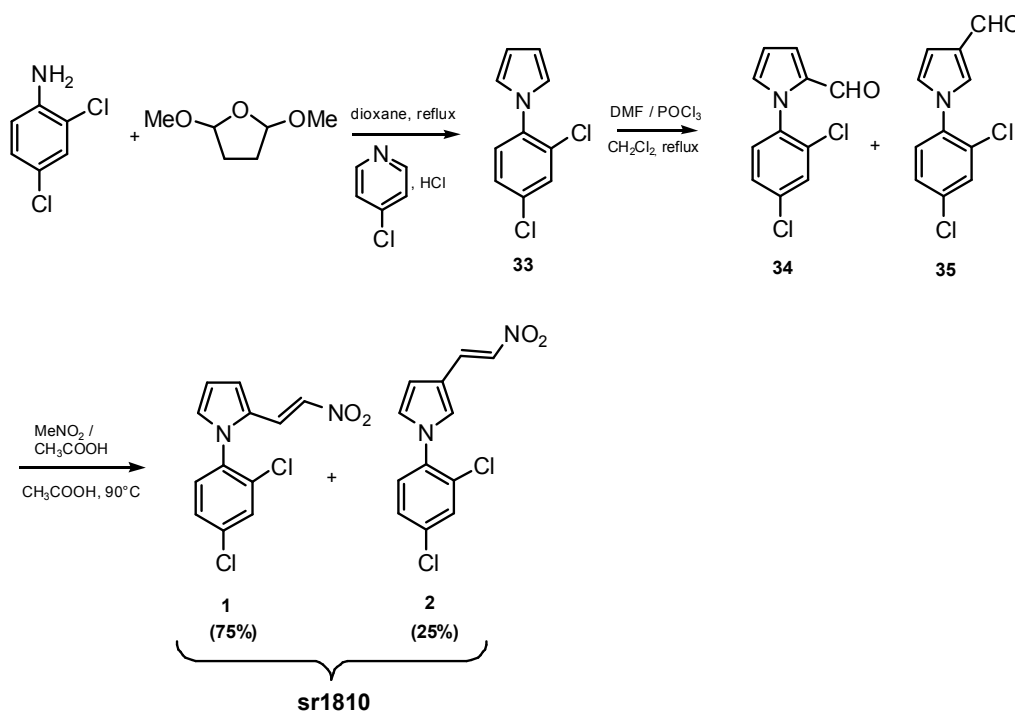
<b>Gene</b>	<b>Primer name</b>	<b>Sequence</b>
<i>ARO7</i>	ARO7iF	5'-TCGCCACATGTCCTTCAGTT-3'
	ARO7iR	5'-GCAAGTATTCCACCTCAACTTCC-3'
<i>CUE1</i>	CUE1iF	5'-ATGGAGGATTCGAGATTGCTT-3'
	CUE1iR	5'-CTGGCTTGCCAAACCAACAA-3'
<i>EMC1</i>	EMC1iF	5'-TGCCCCTTCTACGACCATTT-3'
	EMC1iR	5'-TGCCATTTCGTGTCATGCTCT-3'
<i>EMC3</i>	EMC3iF	5'-ACCAGCTGAAGTATTGGGTCC-3'
	EMC3iR	5'-TATCCCGGCCTGAATACCCA-3'
<i>HRD1</i>	HRD1iF	5'-TGCGTGTATTTCAGCCACCAA-3'
	HRD1iR	5'-GCCAAGATATCCCACACCACA-3'
<i>RPN4</i>	RPN4iF	5'-GCGAAACCCATTGCAGAAG-3'
	RPN4iR	5'-TGGTGATGCAGTCGAAGGTT-3'
<i>SSH1</i>	SSH1iF	5'-TTGGTTCGGTGCTGGCATATT-3'
	SSH1iR	5'-GGATGCACCCGTAACAGCT-3'
<i>UBC7</i>	UBC7iF	5'-CGAAAACCGCTCAGAAACGT-3'
	UBC7iR	5'-GCATCAATGTTGGCACC ACT-3'

## Supporting information (S1) - Synthesis of sr7575-related compounds.

### General Methods

All chemical reagents and solvents were purchased from commercial sources and used without further purification. Thin-layer chromatography (TLC) was performed on silica gel plates. Silica gel 0.06–0.2 mm, 60 Å was used for all column chromatography. Melting points were determined on a Kofler melting point apparatus. NMR spectra were recorded on a BRUKER AVANCE III 400 MHz ( $^1\text{H}$  NMR at 399.8 MHz and  $^{13}\text{C}$  NMR at 100 MHz) with the solvents indicated. Chemical shifts are reported in parts per million (ppm) on the  $\delta$  scale and referenced to the appropriate solvent peak. High-resolution mass spectral (HRMS) were performed on a BRUKER maxis mass spectrometer by the “fédération de Recherche” ICOA / CBM (FR2708) platform. LC-MS Analysis was performed on a Waters alliance 2695 using the following gradient: A (95%)/B (5%) to A (5%)/B (95%) in 4 min. This ratio was held for 1.5 min before returning to initial conditions in 0.5 min. Initial conditions were then maintained for 2 min (A,  $\text{H}_2\text{O}$ ; B, MeCN; each containing 0.1% HCOOH; column, C18 Xbridge 4.6 x 50 mm / 2.5  $\mu\text{m}$ ). MS detection was performed with a SQDetector.

### Compound sr1810: Mixture of (*E*) 1-(2,4-Dichlorophenyl)-2-(2-nitrovinyl)-1*H*-pyrrole [75%] and (*E*) 1-(2,4-Dichlorophenyl)-3-(2-nitrovinyl)-1*H*-pyrrole [25%].



1-(2,4-Dichlorophenyl)-1*H*-pyrrole ( 33).<sup>1</sup> 4-chloropyridine, hydrochloride (9.25 g, 0.0617 mol) and 2,5-dimethoxytetrahydrofuran (8.15 g, 0.0617 mol) were stirred in 150 mL of dioxane at room temperature for 30 min. 2,4-dichloroaniline (10 g, 0.0617 mol) was then added and the mixture was stirred at reflux for 4 h. The reaction was cooled down to room temperature and concentrated under vacuum. 150 mL of water were added to the residue, followed by 200 mL of Et<sub>2</sub>O. The aqueous layer was extracted with Et<sub>2</sub>O (2x 100 mL). The

<sup>1</sup> Azizi, N. *et al.* Iron-catalyzed inexpensive and practical synthesis of *N*-substituted pyrroles in water. *Synlett*, **14**, 2245-2248 (2009).

combined organic layers were washed with HCl 1N (200 mL) and water (2x 200 mL), dried over MgSO<sub>4</sub> and concentrated under vacuum. The resulting residue was purified by chromatography on silica gel using CH<sub>2</sub>Cl<sub>2</sub> as eluant to give compound **33** as a brown oil (11.4 g, 87%). <sup>1</sup>H NMR (400 MHz, CDCl<sub>3</sub>) δ 7.56 (d, *J* = 2.2 Hz, 1H), 7.35 (dd, *J* = 8.7 and 2.3 Hz, 1H), 7.31 (d, *J* = 8.6 Hz, 1H), 6.92 (t, *J* = 2.1 Hz, 2H), 6.39 (t, *J* = 1.9 Hz, 2H). <sup>13</sup>C NMR (100 MHz, CDCl<sub>3</sub>) δ 137.5, 133.3, 130.5, 130.4, 128.5, 127.9, 122.1, 109.7.

Mixture of 1-(2,4-Dichlorophenyl)-1-*H*-pyrrole-2-carbaldehyde (**34**) and 1-(2,4-Dichlorophenyl)-1*H*-pyrrole-3-carbaldehyde (**35**). Dimethylformamide (2.20 mL, 0.0283 mol) was stirred at 0°C. Phosphorus oxychloride (2.7 mL, 0.0283 mol) was then added dropwise and the white solid obtained was stayed cold for 30 min. After this time, a solution of compound **33** (6 g, 0.0283 mol) in 120 mL of CH<sub>2</sub>Cl<sub>2</sub> was slowly added dropwise to the reaction mixture. The reaction was refluxed for 20 h. After cooling, 120 mL of water were added and the mixture was stirred at room temperature for 30 min. Then, the layers were separated and the aqueous layer was alkalinized with 20% sodium hydroxide solution. This aqueous layer was extracted with Et<sub>2</sub>O (2x 120 mL). The combined organic layers were dried over MgSO<sub>4</sub> and concentrated under vacuum. The mixture of compound **34** and **35** was engaged in the next step without further purification and was obtained as brown solid (4.4 g, 65%). LC-MS (ESI): *t*<sub>R</sub> = 4.66 and 4.79 min; [M+H]<sup>+</sup> 240.35. HRMS for C<sub>11</sub>H<sub>8</sub>Cl<sub>2</sub>NO [M+H]<sup>+</sup> calculated mass: 239.9977, measured: 239.9974.

Compound **34**: <sup>1</sup>H NMR (400 MHz, CDCl<sub>3</sub>) δ 9.44 (s, 1H), 7.44 (d, *J* = 2.3 Hz, 1H), 7.26 (dd, *J* = 8.6 and 2.0 Hz, 1H), 7.20 (d, *J* = 8.4 Hz, 1H), 7.04 (dd, *J* = 1.4 and 4.0 Hz, 1H), 6.86 (m, 1H), 6.37 (dd, *J* = 4.0 and 2.8 Hz, 1H). <sup>13</sup>C NMR (100 MHz, CDCl<sub>3</sub>) δ 178.5, 136.0, 135.2, 132.9, 132.9, 131.1, 130.0, 129.6, 127.7, 123.2, 111.2.

Compound **35**: <sup>1</sup>H NMR (400 MHz, CDCl<sub>3</sub>) δ 9.79 (s, 1H), 7.50 (d, *J* = 2.3 Hz, 1H), 7.40 (t, *J* = 1.7 Hz, 1H), 7.31 (dd, *J* = 8.5 and 2.3 Hz, 1H), 7.25 (d, *J* = 8.4 Hz, 1H), 6.80 (t, *J* = 2.8 Hz, 1H), 6.73 (m, 1H). <sup>13</sup>C NMR (100 MHz, CDCl<sub>3</sub>) δ 185.4, 136.1, 135.0, 130.8, 130.7, 130.0, 128.4, 128.2, 127.8, 124.8, 108.8.

**sr1810**: Mixture of (*E*) 1-(2,4-Dichlorophenyl)-2-(2-nitrovinyl)-1-*H*-pyrrole (**1**) and (*E*) 1-(2,4-Dichlorophenyl)-3-(2-nitrovinyl)-1*H*-pyrrole (**2**). Nitromethane (54 mL, 1 mol) and ammonium acetate (15.4 g, 0.2 mol) were stirred in 100 mL of acetic acid at 30°C for 30 min. Then, the mixture of compounds **34** and **35** (12 g, 0.05 mol) was added and the solution was heated at 90°C for 24 h. Then, the reaction was concentrated under vacuum. A saturated solution of sodium hydrogenocarbonate (100 mL) was added to the residue. This aqueous layer was extracted with EtOAc (2x 100mL). The organic layers were washed with water (2x 100 mL), dried over MgSO<sub>4</sub> and concentrated under vacuum. The mixture of compound **1** and **2** was obtained as a yellow solid (8.7 g, 61%). Mp: 114 °C. LC-MS (ESI): *t*<sub>R</sub> = 5.22 and 5.32 min; [M+H]<sup>+</sup> 283.31. HRMS for C<sub>12</sub>H<sub>9</sub>Cl<sub>2</sub>N<sub>2</sub>O<sub>2</sub> [M+H]<sup>+</sup> calculated mass: 283.0035, measured: 283.0035.

Compound **1**: <sup>1</sup>H NMR (400 MHz, CDCl<sub>3</sub>) δ 7.62 (d, *J* = 2.3 Hz, 1H), 7.56 (d, *J* = 13.3 Hz, 1H), 7.45 (dd, *J* = 8.4 and 2.3 Hz, 1H), 7.33 (d, *J* = 8.4 Hz, 1H), 7.17 (d, *J* = 13.4 Hz, 1H), 7.00 (m, 1H), 6.95 (m, 1H), 6.49 (m, 1H). <sup>13</sup>C NMR (100 MHz, CDCl<sub>3</sub>) δ 136.4, 134.3, 133.4, 132.6, 130.8, 130.3, 130.0, 128.4, 127.4, 125.8, 116.7, 112.3.

Compound **2**: <sup>1</sup>H NMR (400 MHz, CDCl<sub>3</sub>) δ 8.04 (d, *J* = 13.4 Hz, 1H), 7.58 (d, *J* = 2.3 Hz, 1H), 7.47 (d, *J* = 13.2 Hz, 1H), 7.39 (dd, *J* = 8.4 and 2.3 Hz, 1H), 7.30-7.26 (m, 2H), 6.92 (m, 1H), 6.56 (m, 1H). <sup>13</sup>C NMR (100 MHz, CDCl<sub>3</sub>) δ 136.0, 134.9, 134.2, 133.2, 130.9, 130.8, 128.3, 128.2, 127.9, 125.5, 116.8, 108.3.

**(E) 1-(2,4-Dichlorophenyl)-2-(2-nitrovinyl)-1H-pyrrole (1 or sr7575).** See **Supplementary Fig.1a**.

1-(2,4-Dichlorophenyl)-1H-pyrrole-2-carbaldehyde (**34**). Dimethylformamide (2.20 mL, 0.0283 mol) was stirred at 0°C. Phosphorus oxychloride (2.7 mL, 0.0283 mol) was then added dropwise and the white solid obtained was cooled for 30 min. After this time, a solution of compound **33** (6 g, 0.0283 mol) in 120 mL of CH<sub>2</sub>Cl<sub>2</sub> was added dropwise to the reaction mixture. The reaction was refluxed for 20 h. After cooling to room temperature, 120 mL of water were added and the mixture was stirred at room temperature for 30 min. Then, the layers were separated and the aqueous layer was alkalinized with 20% sodium hydroxide solution. This aqueous layer was extracted with Et<sub>2</sub>O (2x 120 mL) and the organic layers were dried over MgSO<sub>4</sub> and concentrated under vacuum. The residue was purified by chromatography on silica gel using cyclohexane and CH<sub>2</sub>Cl<sub>2</sub> as eluants (50/50) to afford compound **34** as a beige solid (2.1 g, 30%). <sup>1</sup>H NMR (400 MHz, CDCl<sub>3</sub>) δ 9.44 (s, 1H), 7.44 (d, *J* = 2.3 Hz, 1H), 7.26 (dd, *J* = 8.6 and 2.0 Hz, 1H), 7.20 (d, *J* = 8.4 Hz, 1H), 7.04 (dd, *J* = 4.0 and 1.4 Hz, 1H), 6.86 (m, 1H), 6.37 (dd, *J* = 4.0 and 2.8 Hz, 1H). <sup>13</sup>C NMR (100 MHz, CDCl<sub>3</sub>) δ 178.5, 136.0, 135.2, 132.9, 132.9, 131.1, 130.0, 129.6, 127.7, 123.2, 111.2. LC-MS (ESI): *t*<sub>R</sub> = 4.79 min; [M+H]<sup>+</sup> 240.35. HRMS for C<sub>11</sub>H<sub>8</sub>Cl<sub>2</sub>NO [M+H]<sup>+</sup> calculated mass: 239.9977, measured: 239.9974.

**(E) 1-(2,4-Dichlorophenyl)-2-(2-nitrovinyl)-1H-pyrrole (1).** Nitromethane (54 mL, 1 mol) and ammonium acetate (15.4 g, 0.2 mol) were stirred in 100 mL of acetic acid at 30°C for 30 min. Then, 1-(2,4-dichlorophenyl)-1H-pyrrole-2-carbaldehyde (12 g, 0.05 mol) was added and the mixture was heated at 90°C for 24 h. Then, the reaction was concentrated under vacuum. A saturated solution of sodium hydrogenocarbonate (100 mL) was added to the residue. The aqueous layer was extracted with EtOAc (2x 100 mL). The combined organic layers were washed with water (2x 100 mL), dried over MgSO<sub>4</sub> and concentrated under vacuum. The resulting residue was purified by chromatography on silica gel using cyclohexane and CH<sub>2</sub>Cl<sub>2</sub> as eluant (50/50) to obtain compound **1** as a yellow solid (6.6 g, 47%). Mp: 118°C. <sup>1</sup>H NMR (400 MHz, CDCl<sub>3</sub>) δ 7.62 (d, *J* = 2.3 Hz, 1H), 7.56 (d, *J* = 13.3 Hz, 1H), 7.45 (dd, *J* = 2.3 and 8.3 Hz, 1H), 7.33 (d, *J* = 8.4 Hz, 1H), 7.17 (d, *J* = 13.4 Hz, 1H), 7.00 (m, 1H), 6.95 (m, 1H), 6.49 (m, 1H). <sup>13</sup>C NMR (100 MHz, CDCl<sub>3</sub>) δ 136.4, 134.3, 133.4, 132.6, 130.8, 130.3, 130.0, 128.4, 127.4, 125.8, 116.7, 112.3. LC-MS (ESI): *t*<sub>R</sub> = 5.20 min; [M+H]<sup>+</sup> 283.44. HRMS for C<sub>12</sub>H<sub>9</sub>Cl<sub>2</sub>N<sub>2</sub>O<sub>2</sub> [M+H]<sup>+</sup> calculated mass: 283.0035, measured: 283.0036.

**(E) 1-(2,4-Dichlorophenyl)-3-(2-nitrovinyl)-1H-pyrrole (2 or sr7576).** See **Supplementary Fig.1b**.

1-(2,4-Dichlorophenyl)-1H-pyrrole-3-carbaldehyde (**35**).<sup>2</sup> 4-chloropyridine, hydrochloride (9.88 g, 0.0617 mol) and 2,5-Dimethoxy-3-tetrahydrofuran-carboxaldehyde (8.15 g, 0.0617 mol) were stirred in 150 mL of dioxane at room temperature for 30 min. 2,4-dichloroaniline (10 g, 0.0617 mol) was then added and the mixture was stirred at reflux for 4 h. The reaction was cooled to room temperature and concentrated under vacuum. 150 mL of water were added to the residue, followed by 200 mL of Et<sub>2</sub>O. The aqueous layer was extracted with Et<sub>2</sub>O (2x 100 mL). The combined organic layers were washed with 1N HCl (200 mL) and water (2x 200 mL), dried over MgSO<sub>4</sub> and concentrated under vacuum. The resulting residue was purified by chromatography on silica gel using CH<sub>2</sub>Cl<sub>2</sub> as eluant to afford compound **35** as a

<sup>2</sup> Dallemagne, P. *et al.* A convenient rearrangement of 1-phenylpyrrole-2-carboxaldehydes into their 3-isomers. *Synthetic Communications*. **13**, 1855-1857 (1994).

beige solid (5.2 g, 35%). Mp: 186°C. <sup>1</sup>H NMR (400 MHz, CDCl<sub>3</sub>) δ 9.79 (s, 1H), 7.50 (d, *J* = 2.3 Hz, 1H), 7.40 (t, *J* = 1.7 Hz, 1H), 7.31 (dd, *J* = 8.5 and 2.3 Hz, 1H), 7.25 (d, *J* = 8.4 Hz, 1H), 6.80 (t, *J* = 2.8 Hz, 1H), 6.73 (m, 1H). <sup>13</sup>C NMR (100 MHz, CDCl<sub>3</sub>) δ 185.4, 136.1, 135.0, 130.8, 130.7, 130.0, 128.4, 128.2, 127.8, 124.8, 108.8. LC-MS (ESI): t<sub>R</sub> = 4.66 min; [M+H]<sup>+</sup> 240.35.

(*E*) 1-(2,4-Dichlorophenyl)-3-(2-nitrovinyl)-1*H*-pyrrole (**2**). Nitromethane (54 mL, 1 mol) and ammonium acetate (15.4 g, 0.2 mol) were stirred in 100 mL of acetic acid at 30°C for 30 minutes. Then, 1-(2,4-dichloro-phenyl)-1*H*-pyrrole-2-carbaldehyde (12 g, 0.05 mol) was added and the mixture was heated at 90°C for 24 h. The reaction was concentrated under vacuum. A saturated solution of sodium hydrogenocarbonate (100 mL) was added to the residue. This aqueous layer was extracted with EtOAc (2x 100 mL). The organic layers were washed with water (2x 100 mL), dried over MgSO<sub>4</sub> and concentrated under vacuum. The solid resulting residue was purified by chromatography on silica gel using cyclohexane and CH<sub>2</sub>Cl<sub>2</sub> as eluant (50/50) to give compound **2** as a yellow solid (6.1 g, 43%). Mp: 186 °C. <sup>1</sup>H NMR (400 MHz, DMSO-*d*<sub>6</sub>) δ 8.11 (d, *J* = 13.3 Hz, 1H), 7.95 (d, *J* = 13.3 Hz, 1H), 7.90 (d, *J* = 2.3 Hz, 1H), 7.78 (m, 1H), 7.60 (dd, *J* = 6.4 and 8.5 Hz, 1H), 7.58 (d, *J* = 8.7 Hz, 1H), 7.19 (m, 1H), 6.86 (m, 1H). <sup>13</sup>C NMR (100 MHz, DMSO-*d*<sub>6</sub>) δ 136.5, 134.8, 134.6, 134.0, 130.6, 130.2, 130.0, 129.7, 129.0, 126.3, 117.5, 109.3. LC-MS (ESI): t<sub>R</sub> = 5.34 min; [M+H]<sup>+</sup> 283.40. HRMS for C<sub>12</sub>H<sub>9</sub>Cl<sub>2</sub>N<sub>2</sub>O<sub>2</sub> [M+H]<sup>+</sup> calculated mass: 283.0035, measured: 283.0036.

(*E*) 1-(2,4-dichlorophenyl)-2-methyl-5-(2-nitrovinyl)-1*H*-pyrrole (**3**). See **Supplementary Fig.1c**.

1-(2,4-Dichlorophenyl)-2-methyl-1*H*-pyrrole (**36**). A mixture of 1-(2,4-Dichlorophenyl)-1*H*-pyrrole-2-carbaldehyde (**34**) (1g, 0.02 mol), potassium hydroxide (0.7g, 0.06 mol) and hydrazine monohydrate (0.61 ml, 0.06 mol) in ethylene glycol (20 ml) was stirred at room temperature for 30 min, then slowly heated to 150°C and maintained for 2 h. The reaction mixture was allowed to cool to room temperature, poured into ice-water and extracted with Et<sub>2</sub>O (2x 20 ml). The combined organic layers were washed with water, brine, dried over MgSO<sub>4</sub>, filtered and concentrated under vacuum. The crude compound was purified by chromatography on silica gel using cyclohexane and CH<sub>2</sub>Cl<sub>2</sub> as eluant (90/10) to afford compound **36** as an orange oil (0.78 g, 70%). <sup>1</sup>H NMR (400 MHz, CDCl<sub>3</sub>) δ 7.53 (d, *J* = 2.2 Hz, 1H), 7.33 (dd, *J* = 8.5 and 2.3 Hz, 1H), 7.26 (d, *J* = 8.3 Hz, 1H), 6.60 (dd, *J* = 2.8 and 1.9 Hz, 1H), 6.22 (t, *J* = 3.0 Hz, 1H), 6.04 (m, 1H), 2.04 (s, 3H). <sup>13</sup>C NMR (100 MHz, CDCl<sub>3</sub>) δ 136.7, 134.6, 133.7, 130.5, 130.1, 130.0, 127.7, 121.3, 108.5, 107.4, 12.1. HRMS for C<sub>11</sub>H<sub>10</sub>Cl<sub>2</sub>N [M+H]<sup>+</sup> calculated mass: 226.0184, measured: 226.0185.

Synthetic procedure for the compound (**3**) is the similar as that described for the compound (**1**) and spectra data are shown below.

1-(2,4-Dichlorophenyl)-5-methyl-1*H*-pyrrole-2-carbaldehyde (**37**). Yellow oil (61%). <sup>1</sup>H NMR (400 MHz, CDCl<sub>3</sub>) δ 9.37 (s, 1H), 7.55 (d, *J* = 2.4 Hz, 1H), 7.38 (dd, *J* = 8.5 and 2.4 Hz, 1H), 7.25 (d, *J* = 8.5 Hz, 1H), 7.03 (d, *J* = 3.9 Hz, 1H), 6.22 (d, *J* = 3.9 Hz, 1H), 2.04 (s, 3H). <sup>13</sup>C NMR (100 MHz, CDCl<sub>3</sub>) δ 177.6, 140.1, 135.4, 134.8, 133.7, 132.7, 130.4, 130.1, 128.0, 123.8, 110.4, 12.1. LC-MS (ESI): t<sub>R</sub> = 4.52 min; [M+H]<sup>+</sup> 254.37. HRMS for C<sub>12</sub>H<sub>10</sub>Cl<sub>2</sub>NO [M+H]<sup>+</sup> calculated mass: 254.0133, measured: 254.0133.

(*E*) 1-(2,4-Dichlorophenyl)-2-methyl-5-(2-nitrovinyl)-1*H*-pyrrole (**3**). Orange solid (50%). Mp: 90°C. <sup>1</sup>H NMR (400 MHz, CDCl<sub>3</sub>) δ 7.65 (d, *J* = 2.4 Hz, 1H), 7.47 (m, 2H), 7.28 (m,

1H), 6.99 (d,  $J = 13.4$  Hz, 1H), 6.90 (d,  $J = 4.0$  Hz, 1H), 6.27 (d,  $J = 4.0$  Hz, 1H), 2.06 (s, 3H).  $^{13}\text{C}$  NMR (100 MHz,  $\text{CDCl}_3$ )  $\delta$  139.8, 136.8, 134.5, 133.1, 131.1, 130.9, 130.6, 128.7, 127.7, 125.3, 118.0, 111.7, 12.8. LC-MS (ESI):  $t_{\text{R}} = 5.35$  min;  $[\text{M}+\text{H}]^+ 297.42$ . HRMS for  $\text{C}_{13}\text{H}_{11}\text{Cl}_2\text{N}_2\text{O}_2$   $[\text{M}+\text{H}]^+$  calculated mass: 297.0192, measured: 297.0193.

**(E) 3-[1-(2,4-Dichlorophenyl)-1H-pyrrol-2-yl]-acrylonitrile (4).** See Supplementary Fig.1d.

2-Cyano-3-(1-(2,4-dichlorophenyl)-1H-pyrrol-2-yl)-acrylic acid ethyl ester (**38**). To a solution of 1-(2,4-dichlorophenyl)-1H-pyrrole-2-carbaldehyde (**34**) (1g, 4.16 mmol) in ethanol (10 ml), were added ethylcyanoacetate (0.49 ml, 4.58 mmol) and triethylamine (0.58 ml, 4.16 mmol). The mixture was refluxed for 4 h. After removal of the solvent under vacuum,  $\text{CH}_2\text{Cl}_2$  was added to the residue and the organic layer was washed with water, dried over  $\text{MgSO}_4$ , filtered and concentrated in vacuo. The crude compound was purified by chromatography on silica gel using  $\text{CH}_2\text{Cl}_2$  as eluant to obtain compound **34** as a yellow solid (1.2 g, 86%). Mp: 138 °C.  $^1\text{H}$  NMR (400 MHz,  $\text{CDCl}_3$ )  $\delta$  7.86 (d,  $J = 4.2$  Hz, 1H), 7.59 (d,  $J = 1.6$  Hz, 1H), 7.52 (s, 1H), 7.41 (dd,  $J = 8.3$  and 1.5 Hz, 1H), 7.28 (d,  $J = 8.5$  Hz, 1H), 7.07 (m, 1H), 6.59 (m, 1H), 4.26 (q,  $J = 7.1$  Hz, 2H), 1.32 (t,  $J = 7.1$  Hz, 3H).  $^{13}\text{C}$  NMR (100 MHz,  $\text{CDCl}_3$ )  $\delta$  163.5, 140.1, 136.5, 133.6, 133.5, 130.7, 130.7, 130.6, 128.3, 128.3, 119.4, 116.6, 113.3, 95.2, 62.2, 14.2. HRMS for  $\text{C}_{16}\text{H}_{13}\text{Cl}_2\text{N}_2\text{O}_2$   $[\text{M}+\text{H}]^+$  calculated mass: 335.0348, measured: 335.0346.

2-Cyano-3-(1-(2,4-dichlorophenyl)-1H-pyrrol-2-yl)-acrylic acid (**39**). To a solution of lithium hydroxyde (340 mg, 0.014 mol) in water (50 ml) was added a solution of 2-cyano-3-(1-(2,4-dichlorophenyl)-1H-pyrrol-2-yl)-acrylic acid ethyl ester (**38**) (3.2 g, 9.54 mmol) in THF (50 ml) and the mixture was heated at 50°C for 5h. After removing THF under vacuum, the aqueous layer was acidified with 6N HCl and then extracted with EtOAc (2x 50 mL). The organic layers were washed with water (2x 50 mL), dried over  $\text{MgSO}_4$  and concentrated in vacuo. The product was purified by recrystallization in  $\text{CH}_2\text{Cl}_2$  to obtain compound **39** as a yellow solid (1.1 g, 37%). Mp: 110°C.  $^1\text{H}$  NMR (400 MHz,  $\text{CDCl}_3$ )  $\delta$  7.95 (d,  $J = 4.1$  Hz, 1H), 7.64 (d,  $J = 2.2$  Hz, 1H), 7.56 (s, 1H), 7.46 (dd,  $J = 8.3$  and 2.2 Hz, 1H), 7.31 (d,  $J = 8.3$  Hz, 1H), 7.15 (m, 1H), 6.65 (m, 1H).  $^{13}\text{C}$  NMR (100 MHz,  $\text{CDCl}_3$ )  $\delta$  168.8, 141.2, 136.7, 133.5, 133.2, 131.8, 130.8, 130.6, 128.4, 128.3, 120.7, 116.0, 113.8, 93.8. LC-MS (ESI):  $t_{\text{R}} = 4.55$  min;  $[\text{M}+\text{H}]^+ 307.32$ . HRMS for  $\text{C}_{14}\text{H}_9\text{Cl}_2\text{N}_2\text{O}_2$   $[\text{M}+\text{H}]^+$  calculated 307.0035, measured: 307.0034.

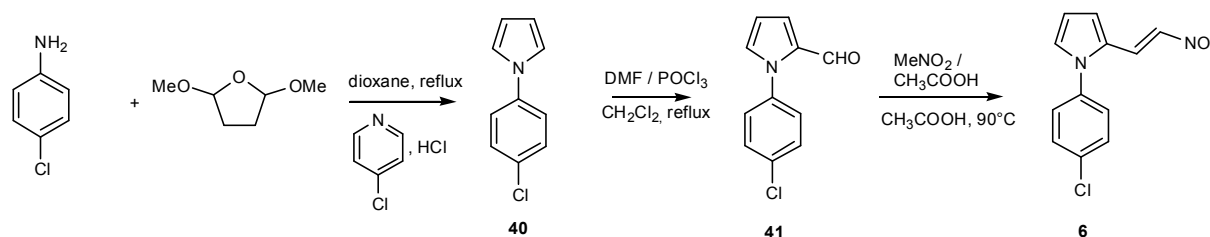
3-(1-(2,4-Dichlorophenyl)-1H-pyrrol-2-yl)-acrylonitrile (**4**). To a solution of copper (155 mg, 2.44 mmol) in quinoline (10 ml), heated at 190°C, was added 2-cyano-3-(1-(2,4-dichlorophenyl)-1H-pyrrol-2-yl)-acrylic acid (**39**) (500 mg, 1.62 mmol). The mixture was stirred vigorously. After the carbon dioxide evolution stopped and TLC indicated complete consumption of the starting material, the reaction was cooled to room temperature and 1N HCl (10 ml) was added. The aqueous layer was extracted with  $\text{CH}_2\text{Cl}_2$  (2x 15 mL). The combined organic layers were washed with water (2x 20 mL), dried over  $\text{MgSO}_4$  and concentrated under vacuum. The resulting residue was purified by chromatography on silica gel using cyclohexane and  $\text{CH}_2\text{Cl}_2$  as eluant (50/50 to 30/70) to obtain compound **4** as a white solid (150 mg, 36%). Mp: 108 °C.  $^1\text{H}$  NMR (400 MHz,  $\text{CDCl}_3$ )  $\delta$  7.58 (d,  $J = 2.3$  Hz, 1H), 7.53 (m, 1H), 7.39 (dd,  $J = 8.4$  and 2.3 Hz, 1H), 7.28 (d,  $J = 8.5$  Hz, 1H), 6.86 (m, 1H), 6.49 (t,  $J = 3.2$  Hz, 1H), 6.44 (d,  $J = 12.1$  Hz, 1H), 5.01 (d,  $J = 12.1$  Hz, 1H).  $^{13}\text{C}$  NMR (100 MHz,  $\text{CDCl}_3$ )  $\delta$  135.8, 135.1, 134.5, 133.7, 130.8, 130.4, 129.3, 128.1, 126.4, 118.2, 114.3, 111.6,

88.7. LC-MS (ESI):  $t_R = 5.18$  min;  $[M+H]^+ 263.51$ . HRMS for  $C_{13}H_9Cl_2N_2$   $[M+H]^+$  calculated mass: 263.0137, measured: 263.0136.

**1-(2,4-Dichlorophenyl)-2-(2-nitroethyl)-1H-pyrrole (5).** See Supplementary Fig.1e.

1-(2,4-Dichlorophenyl)-2-(2-nitroethyl)-1H-pyrrole (5). To a solution of (*E*) 1-(2,4-Dichlorophenyl)-2-(2-nitrovinyl)-1H-pyrrole (1) (200 mg, 0.70 mmol) in methanol (7 ml) was added portionwise sodium borohydride (53 mg, 1.41 mmol) at 0°C. After the addition, the reaction mixture was stirred at 0°C for 1 h. Then a mixture of ice / water (10 ml) was added and the aqueous layer was extracted with EtOAc (2x 20 ml). The combined organic layers were washed with water (2x 30 ml), dried over  $MgSO_4$ , filtered and concentrated under vacuum to give compound 5 as a brown oil (0.1 g, 50%).  $^1H$  NMR (400 MHz,  $CDCl_3$ )  $\delta$  7.57 (d,  $J = 2.4$  Hz, 1H), 7.39 (dd,  $J = 8.4$  and 2.3 Hz, 1H), 7.30 (d,  $J = 8.5$  Hz, 1H), 6.64 (dd,  $J = 2.9$  and 1.7 Hz, 1H), 6.27 (t,  $J = 3.2$  Hz, 1H), 6.13 (m, 1H), 4.48 (dd,  $J = 15.2$  and 7.7 Hz, 2H), 3.09 (dd,  $J = 15.4$  and 7.5 Hz, 2H).  $^{13}C$  NMR (100 MHz,  $CDCl_3$ )  $\delta$  135.7, 135.4, 133.7, 130.6, 130.3, 128.1, 127.6, 122.8, 109.2, 108.0, 74.1, 24.3. HRMS for  $C_{12}H_{11}Cl_2N_2O_2$   $[M+H]^+$  calculated mass: 285.0192, measured: 285.0189.

**(E) 1-(4-Chlorophenyl)-2-(2-nitrovinyl)-1H-pyrrole (6).**



Synthetic procedure for compound (6) is similar as that described for compound (1) and spectra data are shown below.

1-(4-chlorophenyl)-1H-pyrrole (40).<sup>3</sup> Beige solid (85%). Mp: 90 °C.  $^1H$  NMR (400 MHz,  $CDCl_3$ )  $\delta$  7.28 (d,  $J = 9.2$  Hz, 2H), 7.21 (d,  $J = 9.1$  Hz, 2H), 6.94 (t,  $J = 2.2$  Hz, 2H), 6.35 (t,  $J = 2.2$  Hz, 2H).  $^{13}C$  NMR (100 MHz,  $CDCl_3$ )  $\delta$  139.4, 131.1, 129.8, 121.6, 119.3, 110.8.

1-(4-chlorophenyl)-1H-pyrrole-2-carbaldehyde (41).<sup>4</sup> Orange solid (30%). Mp: 98°C.  $^1H$  NMR (400 MHz,  $CDCl_3$ )  $\delta$  9.49 (s, 1H), 7.35 (d,  $J = 8.8$  Hz, 2H), 7.21 (d,  $J = 8.7$  Hz, 2H), 7.07 (dd,  $J = 4.0$  and 1.7 Hz, 1H), 6.97 (m, 1H), 6.34 (dd,  $J = 4.1$  and 2.7 Hz, 1H).  $^{13}C$  NMR (100 MHz,  $CDCl_3$ )  $\delta$  178.7, 137.5, 134.1, 132.4, 131.3, 129.2, 127.2, 123.7, 111.1. LC-MS (ESI):  $t_R = 4.52$  min;  $[M+H]^+ 206.39$ .

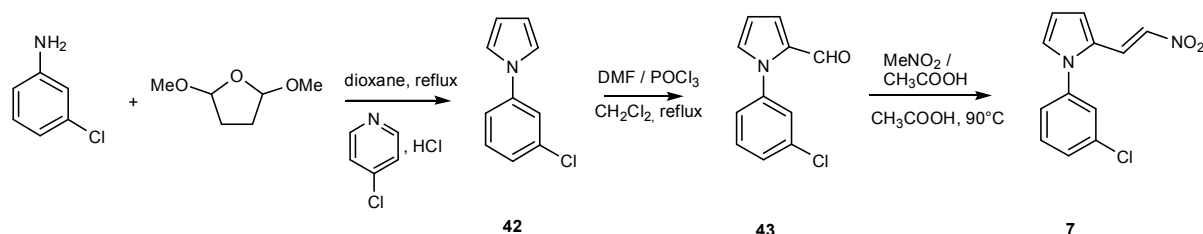
(*E*) 1-(4-chlorophenyl)-2-(2-nitrovinyl)-1H-pyrrole (6). Yellow solid (54%). Mp: 124 °C.  $^1H$  NMR (400 MHz,  $CDCl_3$ )  $\delta$  7.74 (d,  $J = 13.3$  Hz, 1H), 7.49 (d,  $J = 8.6$  Hz, 2H), 7.24 (d,  $J =$

<sup>3</sup> Das, B. *et al.* Novel approach for the synthesis of N-substituted pyrroles starting directly from nitro compounds in water. *Synthetic Communications*. **4**, 548-553 (2012)

<sup>4</sup> Pina, M. *et al.* Synthesis and spectral data of 1-aryl-2-formylpyrroles. *Khimiya Geterotsiklicheskikh Soedinenii*. **2**, 180-184, (1989). *Khimiya*

13.4 Hz, 1H), 7.22 (d,  $J = 8.6$  Hz, 2H), 7.07 (m, 1H), 6.91 (d,  $J = 3.8$  Hz, 1H), 6.42 (t,  $J = 3.6$  Hz, 1H).  $^{13}\text{C}$  NMR (100 MHz,  $\text{CDCl}_3$ )  $\delta$  136.5, 134.9, 132.8, 130.0, 129.9, 127.8, 127.6, 125.2, 116.5, 112.1. LC-MS (ESI):  $t_{\text{R}} = 5.07$  min;  $[\text{M}+\text{H}]^+ 249.44$ . HRMS for  $\text{C}_{12}\text{H}_{10}\text{ClN}_2\text{O}_2$   $[\text{M}+\text{H}]^+$  calculated mass: 249.0425, measured: 249.0425.

**(E) 1-(3-Chlorophenyl)-2-(2-nitrovinyl)-1H-pyrrole (7).**



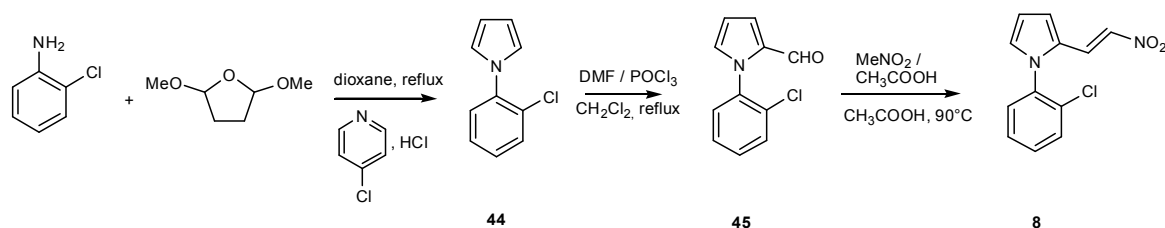
Synthetic procedure for compound ( 7) is similar as that described for compound ( 1) and spectra data are shown below.

1-(3-chlorophenyl)-1H-pyrrole (**42**).<sup>5</sup> Brown solid (90%). Mp: 54 °C.  $^1\text{H}$  NMR (400 MHz,  $\text{CDCl}_3$ )  $\delta$  7.30 (t,  $J = 2.0$  Hz, 1H), 7.22 (d,  $J = 7.9$  Hz, 1H), 7.18 (ddd,  $J = 8.1, 2.1$  and 1.2 Hz, 1H), 7.11 (ddd,  $J = 7.9, 2.0$  and 1.2 Hz, 1H), 6.97 (t,  $J = 2.2$  Hz, 2H), 6.26 (t,  $J = 2.2$  Hz, 2H).  $^{13}\text{C}$  NMR (100 MHz,  $\text{CDCl}_3$ )  $\delta$  141.8, 135.2, 130.6, 125.6, 120.6, 119.2, 118.4, 111.1.

1-(3-chlorophenyl)-1H-pyrrole-2-carbaldehyde (**43**).<sup>4</sup> Brown solid (50%). Mp: 68°C.  $^1\text{H}$  NMR (400 MHz,  $\text{CDCl}_3$ )  $\delta$  9.49 (s, 1H), 7.31-7.27 (m, 3H), 7.18-7.15 (m, 1H), 7.06 (dd,  $J = 4.0$  and 1.7 Hz, 1H), 6.97 (m, 1H), 6.33 (dd,  $J = 3.9$  and 2.7 Hz, 1H).  $^{13}\text{C}$  NMR (100 MHz,  $\text{CDCl}_3$ )  $\delta$  178.7, 140.0, 134.6, 132.4, 131.2, 130.0, 128.4, 126.3, 124.4, 123.5, 111.2. LC-MS (ESI):  $t_{\text{R}} = 4.42$  min;  $[\text{M}+\text{H}]^+ 206.34$ .

(E) 1-(3-Chlorophenyl)-2-(2-nitrovinyl)-1H-pyrrole (**7**). Red oil (50%).  $^1\text{H}$  NMR (400 MHz,  $\text{CDCl}_3$ )  $\delta$  7.78 (d,  $J = 13.3$  Hz, 1H), 7.50-7.48 (m, 2H), 7.35 (m, 1H), 7.32 (d,  $J = 13.3$  Hz, 1H), 7.20-7.23 (m, 1H), 7.12 (dd,  $J = 2.6$  and 1.1 Hz, 1H), 6.95 (dd,  $J = 4.0$  and 2.6 Hz, 1H), 6.45 (dd,  $J = 3.8$  and 0.9 Hz, 1H).  $^{13}\text{C}$  NMR (100 MHz,  $\text{CDCl}_3$ )  $\delta$  139.1, 135.5, 132.9, 130.7, 129.8, 129.1, 127.7, 126.6, 125.2, 124.7, 116.5, 112.2. LC-MS (ESI):  $t_{\text{R}} = 5.06$  min;  $[\text{M}+\text{H}]^+ 249.40$ . HRMS for  $\text{C}_{12}\text{H}_{10}\text{ClN}_2\text{O}_2$   $[\text{M}+\text{H}]^+$  calculated mass: 249.0425, measured: 249.0425.

**(E) 1-(2-Chlorophenyl)-2-(2-nitrovinyl)-1H-pyrrole (8).**



<sup>5</sup> Corsi, C. *et al.* Preparation of pyrrole derivatives as plant growth regulators. PCT Int. Appl., 2010069879, 24 Jun 2010.



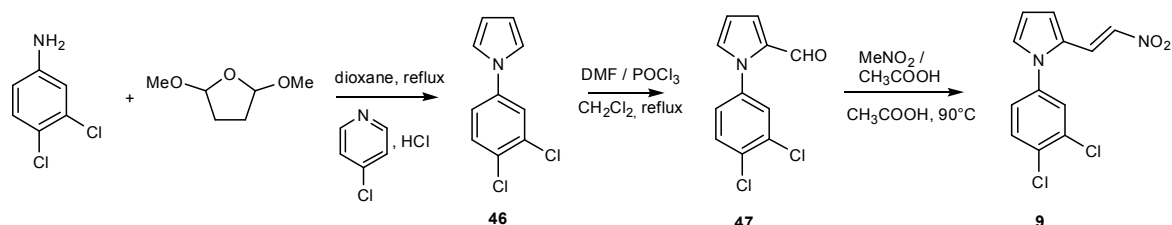
Synthetic procedure for compound ( **8** ) is similar as that described for compound ( **1** ) and spectra data are shown below.

1-(2-Chlorophenyl)-1*H*-pyrrole (**44**)<sup>1</sup>. Brown oil (87%). <sup>1</sup>H NMR (400 MHz, CDCl<sub>3</sub>) δ 7.47 (m, 1H), 7.32-7.22 (m, 3H), 6.88 (t, *J* = 2.2 Hz, 2H), 6.31 (t, *J* = 2.2 Hz, 2H). <sup>13</sup>C NMR (100 MHz, CDCl<sub>3</sub>) δ 138.8, 130.7, 129.7, 128.3, 127.9, 127.6, 122.2, 109.3.

1-(2-Chlorophenyl)-1*H*-pyrrole-2-carbaldehyde (**45**)<sup>4</sup> Beige solid (29%). Mp: 94°C. <sup>1</sup>H NMR (400 MHz, CDCl<sub>3</sub>) δ 9.42 (d, *J* = 0.5 Hz, 1H), 7.44 (m, 1H), 7.35-7.27 (m, 2H), 7.05 (dd, *J* = 4.0 and 1.7 Hz, 1H), 7.07 (dd, *J* = 4.0 and 1.8 Hz, 1H), 6.89 (m, 1H), 6.37 (dd, *J* = 4.0 and 2.5 Hz, 1H). <sup>13</sup>C NMR (100 MHz, CDCl<sub>3</sub>) δ 178.6, 137.1, 133.0, 132.0, 131.0, 130.2, 130.0, 129.0, 127.4, 122.2, 110.9. LC-MS (ESI): *t*<sub>R</sub> = 4.38 min; [M+H]<sup>+</sup> 206.39.

(*E*) 1-(2-Chlorophenyl)-2-(2-nitrovinyl)-1*H*-pyrrole (**8**). Brown oil (50%). <sup>1</sup>H NMR (400 MHz, CDCl<sub>3</sub>) δ 7.62-7.57 (m, 2H), 7.51 (dt, *J* = 7.5 and 1.7 Hz, 1H), 7.46 (dt, *J* = 7.6 and 1.5 Hz, 1H), 7.38 (dd, *J* = 7.6 and 1.7 Hz, 1H), 7.09 (d, *J* = 13.3 Hz, 1H), 7.04 (dd, *J* = 2.5 and 0.9 Hz, 1H), 6.95 (dd, *J* = 2.6 and 1.1 Hz, 1H), 6.49 (dd, *J* = 2.7 and 0.9 Hz, 1H). <sup>13</sup>C NMR (100 MHz, CDCl<sub>3</sub>) δ 135.7, 132.5, 132.3, 131.0, 130.9, 130.3, 129.6, 128.0, 127.8, 125.8, 116.9, 112.0. LC-MS (ESI): *t*<sub>R</sub> = 4.95 min; [M+H]<sup>+</sup> 249.44. HRMS for C<sub>12</sub>H<sub>10</sub>ClN<sub>2</sub>O<sub>2</sub> [M+H]<sup>+</sup> calculated mass: 249.0425, measured: 249.0425.

### (*E*) 1-(3,4-Dichlorophenyl)-2-(2-nitrovinyl)-1*H*-pyrrole (**9**).



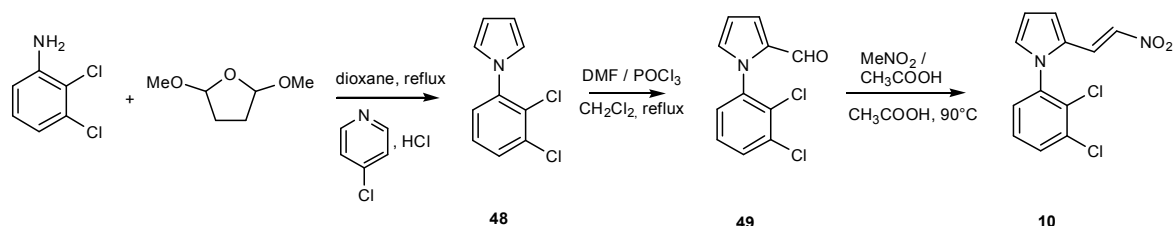
Synthetic procedure for compound ( **9** ) is similar as that described for compound ( **1** ) and spectra data are shown below.

1-(3,4-Dichlorophenyl)-1*H*-pyrrole (**46**). Brown solid (77%). Mp: 56 °C. <sup>1</sup>H NMR (400 MHz, CDCl<sub>3</sub>) δ 7.51-7.48 (m, 2H), 7.24 (dd, *J* = 8.7 and 2.6 Hz, 1H), 7.05 (t, *J* = 2.1 Hz, 2H), 6.39 (t, *J* = 2.2 Hz, 2H). <sup>13</sup>C NMR (100 MHz, CDCl<sub>3</sub>) δ 140.0, 133.5, 131.2, 129.2, 122.1, 119.4, 119.2, 111.4.

1-(3,4-Dichlorophenyl)-1*H*-pyrrole-2-carbaldehyde (**47**). Brown solid (40%). Mp: 104°C. <sup>1</sup>H NMR (400 MHz, CDCl<sub>3</sub>) δ 9.50 (d, *J* = 0.7 Hz, 1H), 7.44 (d, *J* = 8.4 Hz, 1H), 7.39 (d, *J* = 2.5 Hz, 1H), 7.14 (dd, *J* = 8.5 and 2.5 Hz, 1H), 7.07 (dd, *J* = 4.0 and 1.8 Hz, 1H), 6.97 (m, 1H), 6.35 (dd, *J* = 4.0 and 2.6 Hz, 1H). <sup>13</sup>C NMR (100 MHz, CDCl<sub>3</sub>) δ 178.6, 138.3, 132.9, 132.5, 132.2, 131.6, 130.6, 127.8, 125.5, 124.6, 111.4. LC-MS (ESI): *t*<sub>R</sub> = 4.81 min; [M+H]<sup>+</sup> 240.30. HRMS for C<sub>11</sub>H<sub>8</sub>Cl<sub>2</sub>NO [M+H]<sup>+</sup> calculated mass: 239.9977, measured: 239.9975.

(*E*) 1-(3,4-Dichlorophenyl)-2-(2-nitrovinyl)-1*H*-pyrrole (**9**): yellow solid (65%). Mp: 128 °C. <sup>1</sup>H NMR (400 MHz, CDCl<sub>3</sub>) δ 7.75 (d, *J* = 13.3 Hz, 1H), 7.64 (d, *J* = 8.5 Hz, 1H), 7.46 (d, *J* = 2.4 Hz, 1H), 7.34 (d, *J* = 13.3 Hz, 1H), 7.17 (dd, *J* = 8.5 and 2.4 Hz, 1H), 7.10 (dd, *J* = 2.6 and 1.1 Hz, 1H), 6.95 (dd, *J* = 4.0 and 1.3 Hz, 1H), 6.49 (dd, *J* = 3.9 and 2.8 Hz, 1H). <sup>13</sup>C NMR (100 MHz, CDCl<sub>3</sub>) δ 135.7, 132.5, 132.3, 131.0, 130.9, 130.3, 129.6, 128.0, 127.8, 125.8, 116.9, 112.0. LC-MS (ESI): t<sub>R</sub> = 5.29 min; [M+H]<sup>+</sup> 283.44. HRMS for C<sub>12</sub>H<sub>9</sub>Cl<sub>2</sub>N<sub>2</sub>O<sub>2</sub> [M+H]<sup>+</sup> calculated mass: 283.0035, measured: 283.0035.

**(*E*) 1-(2,3-Dichlorophenyl)-2-(2-nitrovinyl)-1*H*-pyrrole (**10**).**



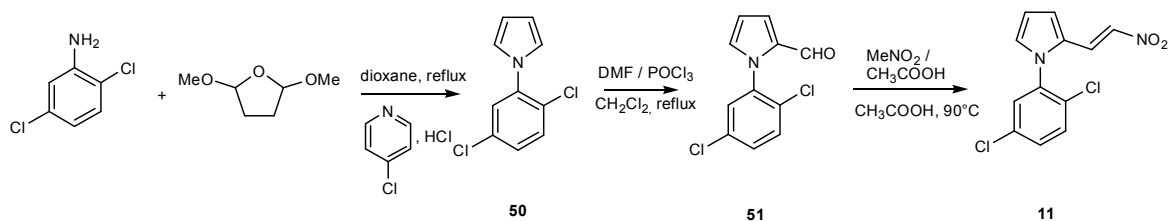
Synthetic procedure for compound (**10**) is similar as that described for compound (**1**) and spectra data are shown below.

1-(2,3-Dichlorophenyl)-1*H*-pyrrole (**48**).<sup>3</sup> Pink oil (78%). <sup>1</sup>H NMR (400 MHz, CDCl<sub>3</sub>) δ 7.49-7.47 (m, 1H), 7.27 (m, 2H), 6.90 (t, *J* = 2.1 Hz, 2H), 6.36 (t, *J* = 2.1 Hz, 2H). <sup>13</sup>C NMR (100 MHz, CDCl<sub>3</sub>) δ 140.5, 134.4, 129.2, 129.0, 127.5, 126.2, 122.2, 109.6.

1-(2,3-Dichlorophenyl)-1*H*-pyrrole-2-carbaldehyde (**49**). Yellow solid (32%). Mp: 92°C. <sup>1</sup>H NMR (400 MHz, CDCl<sub>3</sub>) δ 9.54 (s, 1H), 7.59 (dd, *J* = 7.6 and 2.1 Hz, 1H), 7.35-7.28 (m, 2H), 7.15 (dd, *J* = 4.0 and 1.6 Hz, 1H), 6.98 (m, 1H), 6.48 (dd, *J* = 4.1 and 2.5 Hz, 1H). <sup>13</sup>C NMR (100 MHz, CDCl<sub>3</sub>) δ 178.5, 139.0, 134.0, 132.9, 131.3, 131.0, 130.8, 127.3, 127.2, 122.9, 111.1. LC-MS (ESI): t<sub>R</sub> = 4.69 min; [M+H]<sup>+</sup> 240.30. HRMS for C<sub>11</sub>H<sub>8</sub>Cl<sub>2</sub>NO [M+H]<sup>+</sup> calculated mass: 239.9977, measured: 239.9975.

(*E*) 1-(2,3-Dichlorophenyl)-2-(2-nitrovinyl)-1*H*-pyrrole (**10**). Yellow solid (53%). Mp: 122 °C. <sup>1</sup>H NMR (400 MHz, CDCl<sub>3</sub>) δ 7.69 (dd, *J* = 8.1 and 1.5 Hz, 1H), 7.56 (d, *J* = 13.3 Hz, 1H), 7.40 (t, *J* = 8.0 Hz, 1H), 7.32 (dd, *J* = 7.9 and 1.5 Hz, 1H), 7.17 (d, *J* = 13.3 Hz, 1H), 7.03 (dd, *J* = 2.5 and 1.5 Hz, 1H), 6.96 (m, 1H), 6.50 (m, 1H). <sup>13</sup>C NMR (100 MHz, CDCl<sub>3</sub>) δ 137.3, 134.8, 132.6, 131.9, 131.8, 130.0, 128.0, 127.9, 127.4, 125.7, 116.7, 112.3. LC-MS (ESI): t<sub>R</sub> = 5.11 min; [M+H]<sup>+</sup> 283.44. HRMS for C<sub>12</sub>H<sub>9</sub>Cl<sub>2</sub>N<sub>2</sub>O<sub>2</sub> [M+H]<sup>+</sup> calculated mass: 283.0035, measured: 283.0035.

**(*E*) 1-(2,5-Dichlorophenyl)-2-(2-nitrovinyl)-1*H*-pyrrole (**11**).**



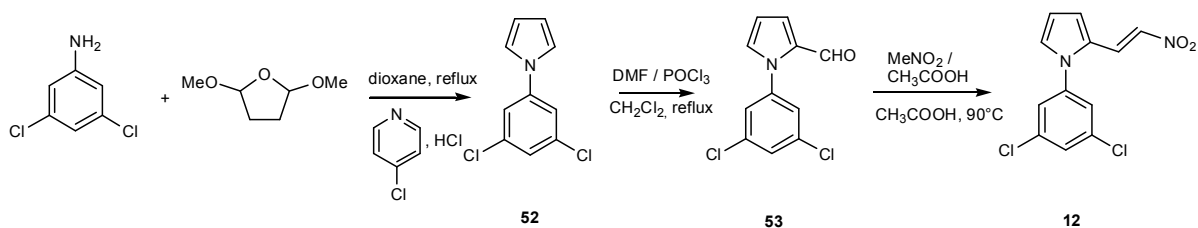
Synthetic procedure for compound (**11**) is similar as that described for compound (**1**) and spectra data are shown below.

1-(2,5-Dichlorophenyl)-1*H*-pyrrole (**50**). Brown oil (79%). <sup>1</sup>H NMR (400 MHz, CDCl<sub>3</sub>) δ 7.35 (d, *J* = 8.4 Hz, 1H), 7.27 (d, *J* = 2.4 Hz, 1H), 7.17 (dd, *J* = 8.6 and 2.4 Hz, 1H), 6.82 (t, *J* = 2.2 Hz, 2H), 6.26 (t, *J* = 2.2 Hz, 2H). <sup>13</sup>C NMR (100 MHz, CDCl<sub>3</sub>) δ 139.5, 133.1, 131.6, 128.1, 127.8, 127.7, 122.0, 109.9. HRMS for C<sub>10</sub>H<sub>9</sub>Cl<sub>2</sub>N [M+H]<sup>+</sup> calculated mass: 212.0028, measured: 212.0030.

1-(2,5-Dichlorophenyl)-1*H*-pyrrole-2-carbaldehyde (**51**). Orange solid (45%). Mp: 126°C. <sup>1</sup>H NMR (400 MHz, CDCl<sub>3</sub>) δ 9.54 (s, 1H), 7.45 (d, *J* = 8.5 Hz, 1H), 7.40 (m, 1H), 7.37 (m, 1H), 7.13 (dd, *J* = 4.0 and 1.8 Hz, 1H), 6.95 (m, 1H), 6.46 (dd, *J* = 3.9 and 2.6 Hz, 1H). <sup>13</sup>C NMR (100 MHz, CDCl<sub>3</sub>) δ 178.5, 138.2, 132.9, 132.8, 130.9, 130.8, 130.6, 130.0, 129.0, 123.1, 111.2. LC-MS (ESI): t<sub>R</sub> = 4.72 min; [M+H]<sup>+</sup> 240.35. HRMS for C<sub>11</sub>H<sub>8</sub>Cl<sub>2</sub>NO [M+H]<sup>+</sup> calculated mass: 239.9977, measured: 239.9972.

(*E*) 1-(2,5-Dichlorophenyl)-2-(2-nitrovinyl)-1*H*-pyrrole (**11**) Yellow solid (59%). Mp: 124 °C. <sup>1</sup>H NMR (400 MHz, CDCl<sub>3</sub>) δ 7.55 (d, *J* = 13.2 Hz, 1H), 7.53 (s, 1H), 7.51 (d, *J* = 2.4 Hz, 1H), 7.41 (d, *J* = 2.3 Hz, 1H), 7.16 (d, *J* = 13.4 Hz, 1H), 7.01 (dd, *J* = 2.7 and 1.5 Hz, 1H), 6.95 (dd, *J* = 4.0 and 1.3 Hz, 1H), 6.50 (m, 1H). <sup>13</sup>C NMR (100 MHz, CDCl<sub>3</sub>) δ 136.6, 133.7, 132.8, 131.6, 131.2, 131.1, 129.9, 129.8, 127.4, 125.8, 116.8, 112.5. LC-MS (ESI): t<sub>R</sub> = 5.13 min; [M+H]<sup>+</sup> 283.49. HRMS for C<sub>12</sub>H<sub>9</sub>Cl<sub>2</sub>N<sub>2</sub>O<sub>2</sub> [M+H]<sup>+</sup> calculated mass: 283.0035, measured: 283.0035.

### (*E*) 1-(3,5-Dichlorophenyl)-2-(2-nitrovinyl)-1*H*-pyrrole (**12**).



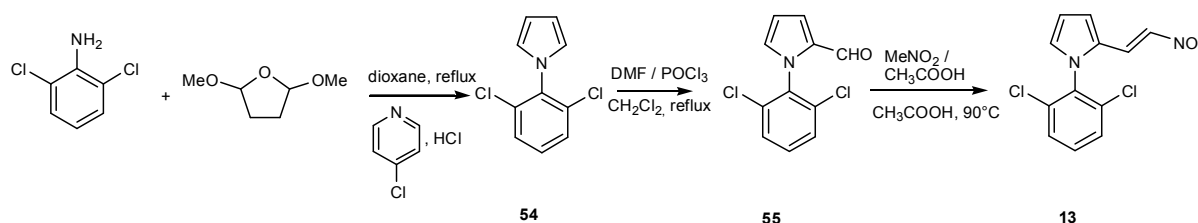
Synthetic procedure for compound (**12**) is similar as that described for compound (**1**) and spectra data are shown below.

1-(3,5-Dichlorophenyl)-1*H*-pyrrole (**52**). Brown solid (79%). Mp: 60 °C. <sup>1</sup>H NMR (400 MHz, CDCl<sub>3</sub>) δ 7.29 (d, *J* = 1.8 Hz, 2H), 7.23 (t, *J* = 1.8 Hz, 1H), 7.05 (t, *J* = 2.2 Hz, 2H), 6.38 (t, *J* = 2.2 Hz, 2H). <sup>13</sup>C NMR (100 MHz, CDCl<sub>3</sub>) δ 142.2, 135.9, 125.4, 119.1, 118.7, 111.6. HRMS for C<sub>10</sub>H<sub>8</sub>Cl<sub>2</sub>N [M+H]<sup>+</sup> calculated mass: 212.0028, measured: 212.0032.

1-(3,5-Dichlorophenyl)-1*H*-pyrrole-2-carbaldehyde (**53**). Yellow solid (50%). Mp: 144°C. <sup>1</sup>H NMR (400 MHz, CDCl<sub>3</sub>) δ 9.52 (s, 1H), 7.34 (t, *J* = 1.8 Hz, 1H), 7.20 (d, *J* = 1.8 Hz, 2H), 7.07 (dd, *J* = 3.9 and 1.6 Hz, 1H), 6.98 (m, 1H), 6.35 (dd, *J* = 3.9 and 2.7 Hz, 1H). <sup>13</sup>C NMR (100 MHz, CDCl<sub>3</sub>) δ 178.5, 140.7, 135.1, 132.2, 131.3, 128.4, 124.8, 124.6, 111.5. LC-MS (ESI): *t*<sub>R</sub> = 4.69 min; [M+H]<sup>+</sup> 240.26. HRMS for C<sub>11</sub>H<sub>8</sub>Cl<sub>2</sub>NO [M+H]<sup>+</sup> calculated mass: 239.9975, measured: 239.9977.

(*E*) 1-(3,5-Dichlorophenyl)-2-(2-nitrovinyl)-1*H*-pyrrole (**12**). Orange solid (65%). Mp: 120°C. <sup>1</sup>H NMR (400 MHz, CDCl<sub>3</sub>) δ 7.76 (d, *J* = 13.3 Hz, 1H), 7.52 (t, *J* = 1.8 Hz, 1H), 7.46 (d, *J* = 2.4 Hz, 1H), 7.34 (d, *J* = 13.3 Hz, 1H), 7.25 (d, *J* = 1.8 Hz, 1H), 7.10 (dd, *J* = 2.6 and 1.5 Hz, 1H), 6.95 (dd, *J* = 4.0 and 1.3 Hz, 1H), 6.46 (m, 1H). <sup>13</sup>C NMR (100 MHz, CDCl<sub>3</sub>) δ 139.8, 136.2, 133.4, 129.6, 129.2, 127.2, 125.2, 125.1, 116.7, 112.5. LC-MS (ESI): *t*<sub>R</sub> = 5.33 min; [M+H]<sup>+</sup> 283.44. HRMS for C<sub>12</sub>H<sub>9</sub>Cl<sub>2</sub>N<sub>2</sub>O<sub>2</sub> [M+H]<sup>+</sup> calculated mass: 283.0035, measured: 283.0036.

**(*E*) 1-(2,6-Dichlorophenyl)-2-(2-nitrovinyl)-1*H*-pyrrole (**13**)**



Synthetic procedure for compound (**13**) is similar as that described for compound (**1**) and spectra data are shown below.

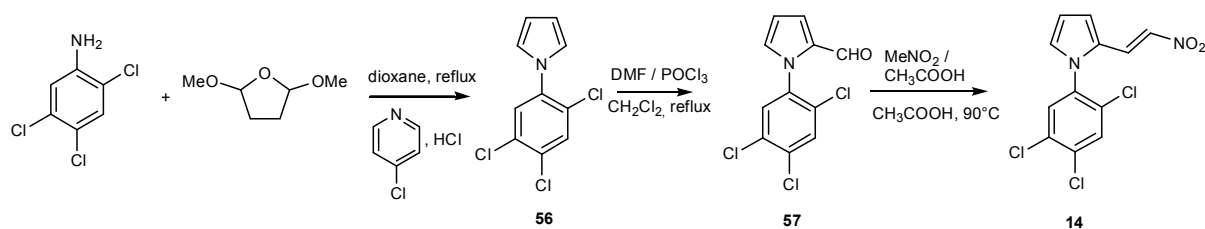
1-(2,6-Dichlorophenyl)-1*H*-pyrrole (**54**).<sup>6</sup> Orange solid (83%). Mp: 90 °C. <sup>1</sup>H NMR (400 MHz, CDCl<sub>3</sub>) δ 7.47 (m, 2H), 7.33-7.29 (m, 1H), 6.76 (t, *J* = 2.3 Hz, 2H), 6.43 (t, *J* = 2.2 Hz, 2H). <sup>13</sup>C NMR (100 MHz, CDCl<sub>3</sub>) δ 137.0, 134.5, 129.6, 128.7, 121.9, 109.4.

1-(2,6-Dichlorophenyl)-1*H*-pyrrole-2-carbaldehyde (**55**).<sup>6</sup> Orange solid (45%). Mp: 94°C. <sup>1</sup>H NMR (400 MHz, CDCl<sub>3</sub>) δ 9.53 (s, 1H), 7.45 (m, 2H), 7.34 (dd, *J* = 9.0 and 7.3 Hz, 1H), 7.16 (dd, *J* = 3.8 and 1.6 Hz, 1H), 6.92 (m, 1H), 6.52 (dd, *J* = 3.9 and 2.7 Hz, 1H). <sup>13</sup>C NMR (100 MHz, CDCl<sub>3</sub>) δ 178.4, 135.6, 134.2, 132.3, 130.4, 130.2, 128.4, 123.1, 111.4. LC-MS (ESI): *t*<sub>R</sub> = 4.61 min; [M+H]<sup>+</sup> 240.35.

(*E*) 1-(2,6-Dichlorophenyl)-2-(2-nitrovinyl)-1*H*-pyrrole (**13**). Orange solid (60%). Mp: 120°C. <sup>1</sup>H NMR (400 MHz, CDCl<sub>3</sub>) δ 7.54 (m, 2H), 7.53 (d, *J* = 12.9 Hz, 1H), 7.46 (m, 1H), 7.03-7.01 (d, *J* = 13.1 Hz, 1H), 6.99 (dd, *J* = 4.0 and 1.4 Hz, 1H), 6.96 (dd, *J* = 2.7 and 1.4 Hz, 1H), 6.55 (dd, *J* = 3.9 and 2.8 Hz, 1H). <sup>13</sup>C NMR (100 MHz, CDCl<sub>3</sub>) δ 135.1, 133.8, 132.3, 131.4, 129.5, 129.1, 127.2, 125.1, 117.5, 112.7. LC-MS (ESI): *t*<sub>R</sub> = 5.05 min; [M+H]<sup>+</sup> 283.40. HRMS for C<sub>12</sub>H<sub>9</sub>Cl<sub>2</sub>N<sub>2</sub>O<sub>2</sub> [M+H]<sup>+</sup> calculated mass: 283.0035, measured: 283.0035.

**(*E*) 1-(2,4,5-Trichlorophenyl)- 2-(2-nitrovinyl)-1*H*-pyrrole (**14**).**

<sup>6</sup> Ikegami, H. *et al.* Hydrazide compound and their preparation, formulation and pesticidal use. PCT Int. Appl., 2007043677, 19 Apr 2007



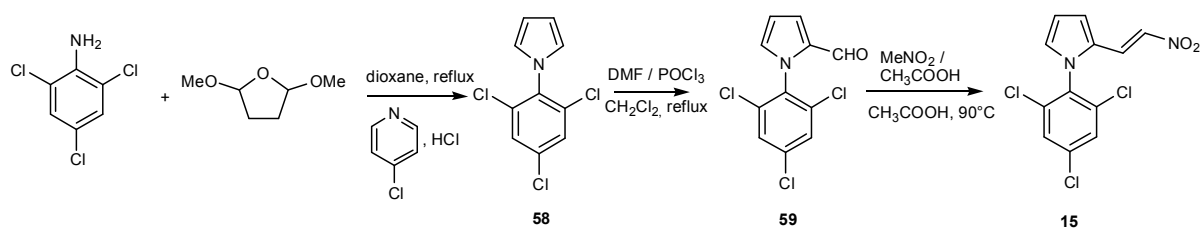
Synthetic procedure for compound ( **14** ) is similar as that described for compound ( **1** ) and spectra data are shown below.

1-(2,4,5-Trichlorophenyl)-1*H*-pyrrole (**56**).<sup>7</sup> Brown solid (79%). Mp: 102 °C. <sup>1</sup>H NMR (400 MHz, CDCl<sub>3</sub>) δ 7.54 (s, 1H), 7.38 (s, 1H), 6.80 (t, *J* = 2.2 Hz, 2H), 6.27 (t, *J* = 2.2 Hz, 2H). <sup>13</sup>C NMR (100 MHz, CDCl<sub>3</sub>) δ 138.0, 131.7, 131.7, 131.6, 128.8, 128.2, 122.0, 110.2.

1-(2,4,5-Trichlorophenyl)-1*H*-pyrrole-2-carbaldehyde (**57**). Beige solid (32%). Mp: 96°C. <sup>1</sup>H NMR (400 MHz, CDCl<sub>3</sub>) δ 9.55 (s, 1H), 7.62 (s, 1H), 7.46 (s, 1H), 7.13 (dd, *J* = 4.0 and 1.5 Hz, 1H), 6.94 (m, 1H), 6.47 (dd, *J* = 3.9 and 2.5 Hz, 1H). <sup>13</sup>C NMR (100 MHz, CDCl<sub>3</sub>) δ 178.5, 136.7, 133.7, 132.9, 131.4, 131.1, 131.0, 130.9, 130.0, 123.7, 111.4. LC-MS (ESI): *t*<sub>R</sub> = 5.07 min; [M+H]<sup>+</sup> 274.26. HRMS for C<sub>11</sub>H<sub>7</sub>Cl<sub>3</sub>NO [M+H]<sup>+</sup> calculated mass: 273.9587, measured: 273.9587.

(*E*) 1-(2,4,5-Trichlorophenyl)- 2-(2-nitrovinyl)-1*H*-pyrrole (**14**). Yellow solid (62%). Mp: 166 °C. <sup>1</sup>H NMR (400 MHz, CDCl<sub>3</sub>) δ 7.65 (s, 1H), 7.46-7.43 (m, 2H), 7.14 (d, *J* = 13.3 Hz, 1H), 6.91 (dd, *J* = 2.7 and 1.5 Hz, 1H), 6.88 (dd, *J* = 4.0 and 1.3 Hz 1H), 6.42 (dd, *J* = 3.8 and 2.8 Hz, 1H). <sup>13</sup>C NMR (100 MHz, CDCl<sub>3</sub>) δ 135.1, 134.9, 133.0, 132.3, 131.8, 131.5, 130.8, 129.7, 127.1, 125.8, 116.6, 112.7. LC-MS (ESI): *t*<sub>R</sub> = 5.42 min; [M+H]<sup>+</sup> 317.27. HRMS for C<sub>12</sub>H<sub>8</sub>Cl<sub>3</sub>N<sub>2</sub>O<sub>2</sub> [M+H]<sup>+</sup> calculated mass: 316.9645, measured: 316.9645.

**(*E*) 1-(2,4,6-Trichlorophenyl)- 2-(2-nitrovinyl)-1*H*-pyrrole (**15**).**



Synthetic procedure for compound ( **15** ) is similar as that described for compound ( **1** ) and spectra data are shown below.

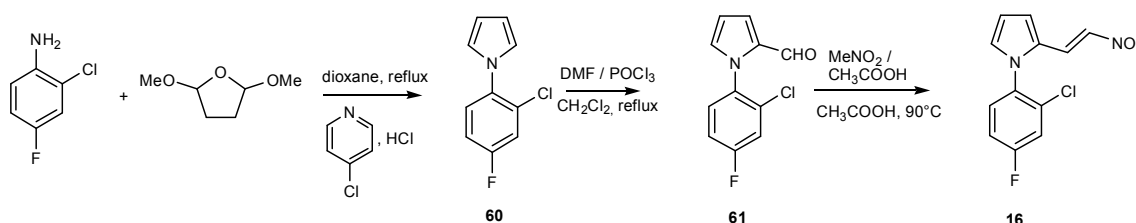
1-(2,4,6-Trichlorophenyl)-1*H*-pyrrole (**58**). Beige solid (88%). Mp: 90 °C. <sup>1</sup>H NMR (400 MHz, CDCl<sub>3</sub>) δ 7.37 (s, 2H), 6.60 (t, *J* = 2.2 Hz, 2H), 6.30 (t, *J* = 2.2 Hz, 2H). <sup>13</sup>C NMR (100 MHz, CDCl<sub>3</sub>) δ 135.8, 135.1, 134.6, 128.6, 121.8, 109.7. HRMS for C<sub>10</sub>H<sub>7</sub>Cl<sub>3</sub>N [M+H]<sup>+</sup> calculated mass: 245.9638, measured: 245.9642.

<sup>7</sup> Ma, F *et al.* A recyclable magnetic nanoparticles supported antimony catalyst for the synthesis of N-substituted pyrroles in water. *Applied Catalysis , A: General* , **457**, 34-41 (2013)

1-(2,4,6-Trichlorophenyl)-1*H*-pyrrole-2-carbaldehyde (**59**). Yellow solid (30%). Mp: 100 °C. <sup>1</sup>H NMR (400 MHz, CDCl<sub>3</sub>) δ 9.54 (s, 1H), 7.46 (s, 2H), 7.15 (dd, *J* = 4.0 and 1.5 Hz, 1H), 6.89 (m, 1H), 6.52 (dd, *J* = 4.0 and 2.8 Hz, 1H). <sup>13</sup>C NMR (100 MHz, CDCl<sub>3</sub>) δ 178.4, 135.3, 134.8, 134.6, 132.2, 130.4, 128.5, 123.6, 111,7. LC-MS (ESI): t<sub>R</sub> = 4.97 min; [M+H]<sup>+</sup> 274.31. HRMS for C<sub>11</sub>H<sub>7</sub>Cl<sub>3</sub>NO [M+H]<sup>+</sup> calculated mass: 273.9587, measured: 273.9587.

(*E*) 1-(2,4,6-Trichlorophenyl)-2-(2-nitrovinyl)-1 *H*-pyrrole (**15**). Light brown solid (50%). Mp: 114 °C. <sup>1</sup>H NMR (400 MHz, CDCl<sub>3</sub>) δ 7.56 (s, 2H), 7.47 (d, *J* = 13.3 Hz, 1H), 7.10 (d, *J* = 13.3 Hz, 1H), 6.98 (dd, *J* = 4.0 and 1.3 Hz, 1H), 6.92 (dd, *J* = 2.7 and 1.4 Hz 1H), 6.55 (dd, *J* = 3.8 and 2.9 Hz, 1H). <sup>13</sup>C NMR (100 MHz, CDCl<sub>3</sub>) δ 136.8, 135.7, 132.7, 132.6, 129.3, 129.2, 126.8, 125.1, 117.3, 113.0. LC-MS (ESI): t<sub>R</sub> = 5.32 min; [M+H]<sup>+</sup> 317.32. HRMS for C<sub>12</sub>H<sub>8</sub>Cl<sub>3</sub>N<sub>2</sub>O<sub>2</sub> [M+H]<sup>+</sup> calculated mass: 316.9645, measured: 316.9645.

**(*E*) 1-(2-Chloro-4-fluorophenyl)-2-(2-nitrovinyl)-1*H*-pyrrole (**16**).**



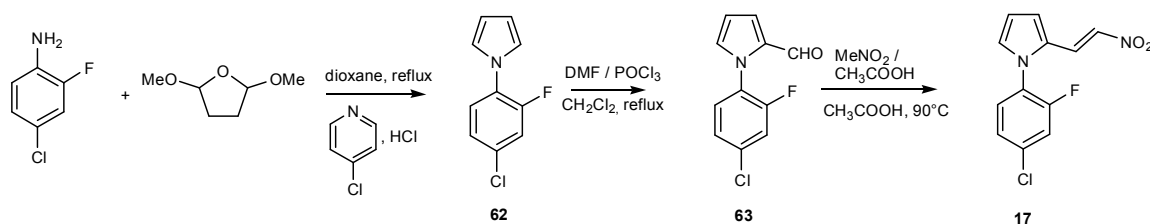
Synthetic procedure for compound ( **16**) is similar as that described for compound ( **1**) and spectra data are shown below.

1-(2-Chloro-4-fluorophenyl)-1*H*-pyrrole (**60**). Orange oil (80%). <sup>1</sup>H NMR (400 MHz, CDCl<sub>3</sub>) δ 7.47 (d, *J* = 8.0 Hz, 2H), 7.31 (dd, *J* = 8.6 and 7.6 Hz, 1H), 6.76 (t, *J* = 2.3 Hz, 2H), 6.43 (t, *J* = 2.2 Hz, 2H). <sup>13</sup>C NMR (100 MHz, CDCl<sub>3</sub>) δ 161.1 (d, *J* = 250.7 Hz), 135.3 (d, *J* = 3.9 Hz), 131.0 (d, *J* = 10.7 Hz), 129.0 (d, *J* = 10.7 Hz), 122.3 (s), 117.7 (d, *J* = 25.8 Hz), 114.6 (d, *J* = 21.9 Hz), 109.5 (s). HRMS for C<sub>10</sub>H<sub>8</sub>ClFN [M+H]<sup>+</sup> calculated mass: 196.0323, measured: 196.0326.

1-(2-Chloro-4-fluorophenyl)-1*H*-pyrrole-2-carbaldehyde (**61**). White solid (61%). Mp: 104°C. <sup>1</sup>H NMR (400 MHz, CDCl<sub>3</sub>) δ 9.43 (s, 1H), 7.25 (dd, *J* = 8.7 and 5.4 Hz, 1H), 7.18 (dd, *J* = 8.0 and 2.8 Hz, 1H), 7.04 (dd, *J* = 4.0 and 1.6 Hz, 1H), 7.02-6.97 (m, 1H), 6.86 (m, 1H), 6.37 (dd, *J* = 4.0 and 2.6 Hz, 1H). <sup>13</sup>C NMR (100 MHz, CDCl<sub>3</sub>) δ 178.6 (s), 162.1 (d, *J* = 250.9 Hz), 133.6 (d, *J* = 3.7 Hz), 133.1 (d, *J* = 10.5 Hz), 133.0 (s), 131.2 (s), 129.9 (d, *J* = 9.2 Hz), 123.0 (bs), 117.5 (d, *J* = 25.9 Hz), 114,6 (d, *J* = 21.6 Hz), 111.0 (s). LC-MS (ESI): t<sub>R</sub> = 4.49 min; [M+H]<sup>+</sup> 224.40. HRMS for C<sub>11</sub>H<sub>8</sub>ClFNO [M+H]<sup>+</sup> calculated mass: 224.0272, measured: 224.0272.

(*E*) 1-(2-Chloro-4-fluorophenyl)-2-(2-nitrovinyl)-1 *H*-pyrrole (**16**). Orange solid (55%). Mp: 102 °C. <sup>1</sup>H NMR (400 MHz, CDCl<sub>3</sub>) δ 7.54 (d, *J* = 13.4 Hz, 1H), 7.40-7.34 (m, 2H), 7.20-7.15 (m, 1H), 7.12 (d, *J* = 13.3 Hz, 1H), 7.01 (dd, *J* = 2.6 and 1.5 Hz, 1H), 6.95 (dd, *J* = 4.0 and 1.3 Hz, 1H), 6.49 (dd, *J* = 3.8 and 2.8 Hz, 1H). <sup>13</sup>C NMR (100 MHz, CDCl<sub>3</sub>) δ 162.6 (d, *J* = 257.9 Hz), 133.9 (d, *J* = 10.9 Hz), 132.5 (s), 132.0 (d, *J* = 3.7 Hz), 130.8 (d, *J* = 9.5 Hz), 130.3 (s), 127.5 (s), 125.9 (s), 118.3 (d, *J* = 25.7 Hz), 116.8 (s), 115.4 (d, *J* = 22.3 Hz), 112.3 (s). LC-MS (ESI): t<sub>R</sub> = 4.95 min; [M+H]<sup>+</sup> 267.41. HRMS for C<sub>12</sub>H<sub>9</sub>ClFN<sub>2</sub>O<sub>2</sub> [M+H]<sup>+</sup> calculated mass: 267.0331, measured: 267.0329.

**(E) 1-(4-Chloro-2-fluorophenyl)-2-(2-nitrovinyl)-1H-pyrrole (17).**



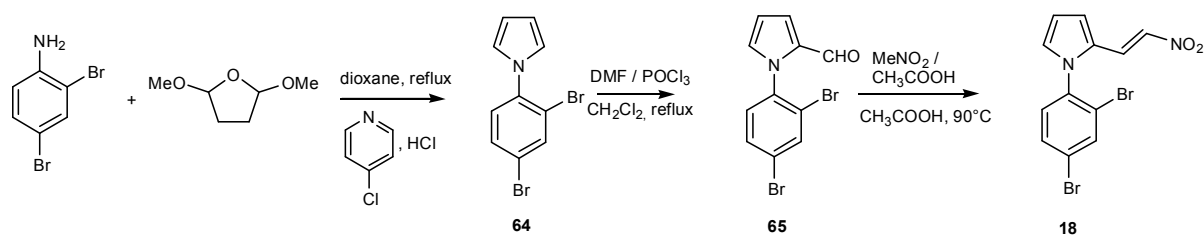
Synthetic procedure for compound ( 17) is similar as that described for compound ( 1) and spectra data are shown below.

1-(4-Chloro-2-fluorophenyl)-1H-pyrrole (**62**). Orange oil (75%). <sup>1</sup>H NMR (400 MHz, CDCl<sub>3</sub>) δ 7.34 (t, *J* = 8.5 Hz, 1H), 7.27 (m, 1H), 7.21 (ddd, *J* = 8.4, 2.2 and 1.2 Hz, 1H), 7.03 (q, *J* = 2.1 Hz, 2H), 6.38 (t, *J* = 2.2 Hz, 2H). <sup>13</sup>C NMR (100 MHz, CDCl<sub>3</sub>) δ 154.7 (d, *J* = 255.7 Hz), 131.9 (d, *J* = 9.8 Hz), 127.8 (d, *J* = 10.5 Hz), 125.5 (d, *J* = 2.0 Hz), 125.1 (d, *J* = 4.1 Hz), 121.2 (d, *J* = 4.8 Hz), 117.8 (d, *J* = 23.7 Hz), 110.3 (s). HRMS for C<sub>10</sub>H<sub>8</sub>ClFN [M+H]<sup>+</sup> calculated mass: 196.0323, measured: 196.0329.

1-(4-Chloro-2-fluorophenyl)-1H-pyrrole-2-carbaldehyde (**63**). White solid (60%). Mp: 82 °C. <sup>1</sup>H NMR (400 MHz, CDCl<sub>3</sub>) δ 9.58 (s, 1H), 7.32-7.23 (m, 3H), 7.15 (m, 1H), 7.01 (m, 1H), 6.47 (m, 1H). <sup>13</sup>C NMR (100 MHz, CDCl<sub>3</sub>) δ 178.6 (s), 156.9 (d, *J* = 253.8 Hz), 135.0 (d, *J* = 9.2 Hz), 132.8 (s), 131.5 (s), 128.9 (s), 126.3 (d, *J* = 12.9 Hz), 124.7 (d, *J* = 3.7 Hz), 124.0 (bs), 117.2 (d, *J* = 22.8 Hz), 111.3 (s). LC-MS (ESI): t<sub>R</sub> = 4.55 min; [M+H]<sup>+</sup> 224.35. HRMS for C<sub>11</sub>H<sub>8</sub>ClFNO [M+H]<sup>+</sup> calculated mass: 224.0272, measured: 224.0272.

(E) 1-(4-Chloro-2-fluorophenyl)-2-(2-nitrovinyl)-1H-pyrrole (**17**). Yellow solid (60%). Mp: 134 °C. <sup>1</sup>H NMR (400 MHz, CDCl<sub>3</sub>) δ 7.60 (dt, *J* = 13.4 and 0.6 Hz, 1H), 7.34 (dd, *J* = 1.9 and 0.5 Hz, 1H), 7.32 (m, 1H), 7.29 (m, 1H), 7.26-7.23 (m, 1H), 7.03 (m, 1H), 6.94 (dd, *J* = 4.0 and 1.4 Hz, 1H), 6.49 (dd, *J* = 3.8 and 2.8 Hz, 1H). <sup>13</sup>C NMR (100 MHz, CDCl<sub>3</sub>) δ 156.9 (d, *J* = 257.9 Hz), 136.2 (d, *J* = 9.6 Hz), 133.0 (s), 130.2 (s), 129.7 (s), 127.3 (s), 125.8 (s), 125.7 (d, *J* = 3.7 Hz), 124.6 (d, *J* = 12.3 Hz), 118.1 (d, *J* = 22.7 Hz), 116.5 (s), 112.5 (s). LC-MS (ESI): t<sub>R</sub> = 5.02 min; [M+H]<sup>+</sup> 267.45. HRMS for C<sub>12</sub>H<sub>9</sub>ClFN<sub>2</sub>O<sub>2</sub> [M+H]<sup>+</sup> calculated mass: 267.0331, measured: 267.0330.

**(E) 1-(2,4-Dibromophenyl)-2-(2-nitrovinyl)-1H-pyrrole (18).**



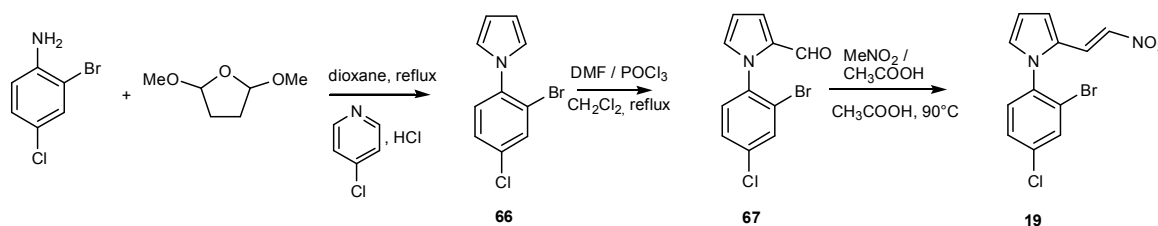
Synthetic procedure for compound ( 18) is similar as that described for compound ( 1) and spectra data are shown below.

1-(2,4-Dibromophenyl)-1*H*-pyrrole (**64**). Orange oil (94%). <sup>1</sup>H NMR (400 MHz, CDCl<sub>3</sub>) δ 7.86 (d, *J* = 2.2 Hz, 1H), 7.52 (dd, *J* = 8.1 and 1.9 Hz, 1H), 7.21 (d, *J* = 8.3 Hz, 1H), 6.85 (t, *J* = 2.4 Hz, 2H), 6.35 (t, *J* = 2.3 Hz, 2H). <sup>13</sup>C NMR (100 MHz, CDCl<sub>3</sub>) δ 139.6, 136.1, 131.3, 129.2, 122.1, 121.4, 120.6, 109.6. HRMS for C<sub>10</sub>H<sub>8</sub>Br<sub>2</sub>N [M+H]<sup>+</sup> calculated mass: 299.9018, measured: 299.9017.

1-(2,4-Dibromophenyl)-1*H*-pyrrole-2-carbaldehyde (**65**). White solid (30%). Mp: 88 °C. <sup>1</sup>H NMR (400 MHz, CDCl<sub>3</sub>) δ 9.52 (s, 1H), 7.55 (d, *J* = 2.3 Hz, 1H), 7.54 (dd, *J* = 8.4 and 2.3 Hz, 1H), 7.22 (d, *J* = 8.5 Hz, 1H), 7.12 (dd, *J* = 3.9 and 1.7 Hz, 1H), 6.93 (m, 1H), 6.45 (dd, *J* = 3.8 and 2.5 Hz, 1H). <sup>13</sup>C NMR (100 MHz, CDCl<sub>3</sub>) δ 178.2, 138.1, 135.7, 132.7, 131.3, 130.9, 130.0, 123.2, 123.0, 122.9, 111.1. LC-MS (ESI): t<sub>R</sub> = 4.92 min; [M+H]<sup>+</sup> 328.25. HRMS for C<sub>11</sub>H<sub>8</sub>Br<sub>2</sub>NO [M+H]<sup>+</sup> calculated mass: 327.8967, measured: 327.8963.

(*E*) 1-(2,4-Dibromophenyl)-2-(2-nitrovinyl)-1*H*-pyrrole (**18**). Orange solid (60%). Mp: 122 °C. <sup>1</sup>H NMR (400 MHz, CDCl<sub>3</sub>) δ 7.93 (d, *J* = 2.1 Hz, 1H), 7.63 (dd, *J* = 8.4 and 2.2 Hz, 1H), 7.53 (d, *J* = 13.4 Hz, 1H), 7.26 (d, *J* = 8.3 Hz, 1H), 7.13 (d, *J* = 13.5 Hz, 1H), 7.00 (dd, *J* = 2.7 and 1.5 Hz, 1H), 6.95 (dd, *J* = 4.0 and 1.4 Hz, 1H), 6.49 (m, 1H). <sup>13</sup>C NMR (100 MHz, CDCl<sub>3</sub>) δ 136.4, 134.3, 133.4, 132.6, 130.8, 130.3, 130.0, 128.4, 127.4, 125.8, 116.7, 112.3. LC-MS (ESI): t<sub>R</sub> = 5.30 min; [M+H]<sup>+</sup> 371.30. HRMS for C<sub>12</sub>H<sub>9</sub>Br<sub>2</sub>N<sub>2</sub>O<sub>2</sub> [M+H]<sup>+</sup> calculated mass: 370.9025, measured: 370.9023.

**(*E*) 1-(2-Bromo-4-chlorophenyl)-2-(2-nitrovinyl)-1*H*-pyrrole (**19**).**



Synthetic procedure for compound (**19**) is similar as that described for compound (**1**) and spectra data are shown below.

1-(2-Bromo-4-chlorophenyl)-1*H*-pyrrole (**66**).<sup>8</sup> Orange oil (89%). <sup>1</sup>H NMR (400 MHz, CDCl<sub>3</sub>) δ 7.60 (d, *J* = 2.3 Hz, 1H), 7.25 (dd, *J* = 8.4 and 2.3 Hz, 1H), 7.15 (d, *J* = 8.4 Hz, 1H), 6.74 (t, *J* = 2.2 Hz, 2H), 6.24 (t, *J* = 2.3 Hz, 2H). <sup>13</sup>C NMR (100 MHz, CDCl<sub>3</sub>) δ 139.2, 134.6, 133.6, 128.9, 128.5, 122.2, 120.4, 109.6.

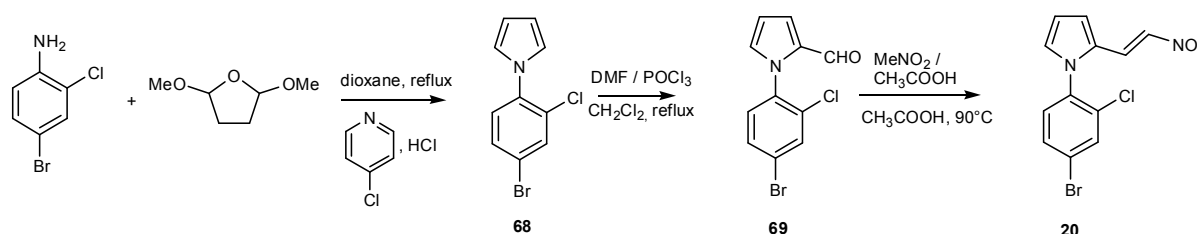
1-(2-Bromo-4-chlorophenyl)-1*H*-pyrrole-2-carbaldehyde (**67**). White solid (30%). Mp: 102 °C. <sup>1</sup>H NMR (400 MHz, CDCl<sub>3</sub>) δ 9.43 (s, 1H), 7.61 (d, *J* = 2.4 Hz, 1H), 7.31 (dd, *J* = 8.4 and 2.3 Hz, 1H), 7.20 (d, *J* = 8.3 Hz, 1H), 7.04 (dd, *J* = 4.1 and 1.7 Hz, 1H), 6.85 (m, 1H), 6.38 (dd, *J* = 3.9 and 2.6 Hz, 1H). <sup>13</sup>C NMR (100 MHz, CDCl<sub>3</sub>) δ 178.5, 137.6, 135.4, 133.0, 132.8, 131.0, 129.6, 128.3, 123.0, 122.6, 111.1. LC-MS (ESI): t<sub>R</sub> = 4.80 min; [M+H]<sup>+</sup> 284.30. HRMS for C<sub>11</sub>H<sub>8</sub>BrClNO [M+H]<sup>+</sup> calculated mass: 283.9472, measured: 283.9470.

<sup>8</sup> Sugita, K *et al*. Preparation of tricyclic compounds such as pyrrolobenzoxazepine derivatives and analogs thereof for treatment of hypercholesteremia, hyperlipemia, and arteriosclerosis. Jpn. Kokai Tokkyo Koho, 2008291018, 04 Dec 2008



(*E*) 1-(2-Bromo-4-chlorophenyl)-2-(2-nitrovinyl)-1*H*-pyrrole (**19**). Yellow solid (53%). Mp: 98 °C. <sup>1</sup>H NMR (400 MHz, CDCl<sub>3</sub>) δ 7.79 (d, *J* = 2.2 Hz, 1H), 7.53 (d, *J* = 13.3 Hz, 1H), 7.48 (dd, *J* = 8.3 and 2.3 Hz, 1H), 7.32 (d, *J* = 8.3 Hz, 1H), 7.12 (d, *J* = 13.3 Hz, 1H), 6.99 (dd, *J* = 2.5 and 1.5 Hz, 1H), 6.95 (dd, *J* = 4.0 and 1.3 Hz, 1H), 6.49 (dd, *J* = 3.8 and 2.7 Hz, 1H). <sup>13</sup>C NMR (100 MHz, CDCl<sub>3</sub>) δ 136.6, 136.0, 133.7, 132.6, 130.4, 130.0, 129.0, 127.4, 125.7, 123.3, 116.9, 112.3. LC-MS (ESI): *t*<sub>R</sub> = 5.23 min; [M+H]<sup>+</sup> 327.35. HRMS for C<sub>12</sub>H<sub>9</sub>BrClN<sub>2</sub>O<sub>2</sub> calculated mass: 326.9530, measured: 326.9529

**(*E*) 1-(4-Bromo-2-chlorophenyl)-2-(2-nitrovinyl)-1*H*-pyrrole (**20**).**



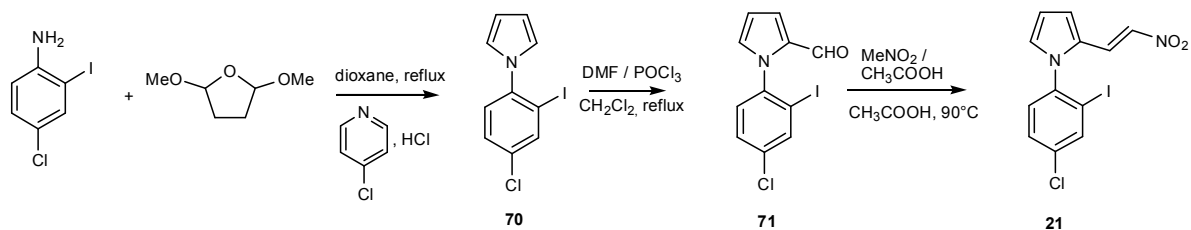
Synthetic procedure for compound (**20**) is similar as that described for compound (**1**) and spectra data are shown below.

1-(4-Bromo-2-chlorophenyl)-1*H*-pyrrole (**68**). Orange oil (90%). <sup>1</sup>H NMR (400 MHz, CDCl<sub>3</sub>) δ 7.68 (d, *J* = 2.3 Hz, 1H), 7.47 (dd, *J* = 8.4 and 2.3 Hz, 1H), 7.22 (d, *J* = 8.4 Hz, 1H), 6.89 (t, *J* = 2.1 Hz, 2H), 6.35 (t, *J* = 2.2 Hz, 2H). <sup>13</sup>C NMR (100 MHz, CDCl<sub>3</sub>) δ 137.9, 133.3, 130.8, 130.6, 128.8, 122.0, 120.8, 109.7. HRMS for C<sub>10</sub>H<sub>8</sub>BrClN [M+H]<sup>+</sup> calculated mass: 255.9523, measured: 255.9523.

1-(4-Bromo-2-chlorophenyl)-1*H*-pyrrole-2-carbaldehyde (**69**). Beige solid (31%). Mp: 92 °C. <sup>1</sup>H NMR (400 MHz, CDCl<sub>3</sub>) δ 9.52 (s, 1H), 7.68 (d, *J* = 2.1 Hz, 1H), 7.50 (dd, *J* = 8.4 and 2.2 Hz, 1H), 7.22 (d, *J* = 8.3 Hz, 1H), 7.13 (dd, *J* = 4.0 and 1.7 Hz, 1H), 6.94 (m, 1H), 6.46 (dd, *J* = 3.9 and 2.6 Hz, 1H). <sup>13</sup>C NMR (100 MHz, CDCl<sub>3</sub>) δ 178.5, 136.5, 133.1, 132.9, 132.8, 131.1, 130.7, 129.9, 123.2, 122.9, 111.2. LC-MS (ESI): *t*<sub>R</sub> = 4.83 min; [M+H]<sup>+</sup> 284.25. HRMS for C<sub>11</sub>H<sub>8</sub>BrClNO [M+H]<sup>+</sup> calculated mass: 283.9472, measured: 283.9468.

(*E*) 1-(4-Bromo-2-chlorophenyl)-2-(2-nitrovinyl)-1*H*-pyrrole (**20**). Orange solid (57%). Mp: 124 °C. <sup>1</sup>H NMR (400 MHz, CDCl<sub>3</sub>) δ 7.77 (d, *J* = 2.1 Hz, 1H), 7.59 (dd, *J* = 8.3 and 2.1 Hz, 1H), 7.54 (d, *J* = 13.3 Hz, 1H), 7.25 (d, *J* = 8.3 Hz, 1H), 7.16 (d, *J* = 13.3 Hz, 1H), 7.00 (dd, *J* = 2.7 and 1.4 Hz, 1H), 6.95 (dd, *J* = 4.0 and 1.4 Hz, 1H), 6.49 (m, 1H). <sup>13</sup>C NMR (100 MHz, CDCl<sub>3</sub>) δ 134.8, 133.6, 133.7, 132.6, 131.4, 130.6, 130.0, 127.4, 125.7, 124.1, 116.7, 112.4. LC-MS (ESI): *t*<sub>R</sub> = 5.26 min; [M+H]<sup>+</sup> 327.35. HRMS for C<sub>12</sub>H<sub>9</sub>BrClN<sub>2</sub>O<sub>2</sub> calculated mass: 326.9530, measured: 326.9529.

**(*E*) 1-(4-Chloro-2-iodophenyl)-2-(2-nitrovinyl)-1*H*-pyrrole (**21**).**



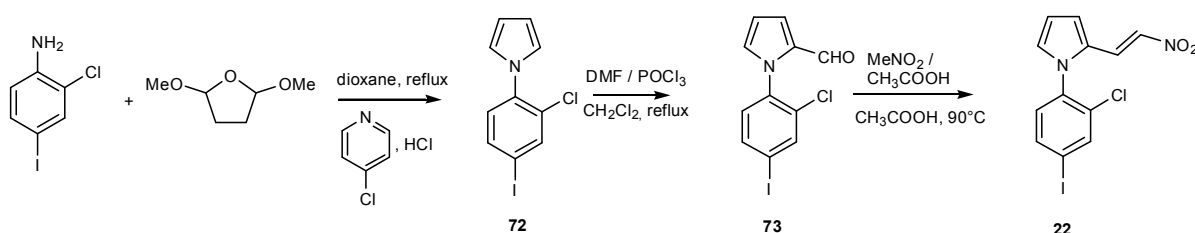
Synthetic procedure for compound ( **21** ) is similar as that described for compound ( **1** ) and spectra data are shown below.

1-(4-Chloro-2-iodophenyl)-1*H*-pyrrole (**70**).<sup>9</sup> Yellow solid (88%). Mp: 72 °C. <sup>1</sup>H NMR (400 MHz, CDCl<sub>3</sub>) δ 7.84 (d, *J* = 2.3 Hz, 1H), 7.31 (dd, *J* = 8.4 and 2.2 Hz, 1H), 7.13 (d, *J* = 8.5 Hz, 1H), 6.74 (t, *J* = 2.2 Hz, 2H), 6.26 (t, *J* = 2.2 Hz, 2H). <sup>13</sup>C NMR (100 MHz, CDCl<sub>3</sub>) δ 142.7, 139.2, 134.2, 129.1, 128.4, 122.1, 109.5, 96.0.

1-(4-Chloro-2-iodophenyl)-1*H*-pyrrole-2-carbaldehyde (**71**). Pink solid (30%). Mp: 62 °C. <sup>1</sup>H NMR (400 MHz, CDCl<sub>3</sub>) δ 9.51 (s, 1H), 7.91 (d, *J* = 2.3 Hz, 1H), 7.42 (dd, *J* = 8.3 and 2.2 Hz, 1H), 7.24 (d, *J* = 8.3 Hz, 1H), 7.12 (dd, *J* = 4.0 and 1.7 Hz, 1H), 6.90 (m, 1H), 6.46 (dd, *J* = 4.0 and 2.6 Hz, 1H). <sup>13</sup>C NMR (100 MHz, CDCl<sub>3</sub>) δ 178.5, 141.2, 138.8, 135.3, 132.5, 130.8, 129.1, 128.8, 122.9, 111.2, 97.8. LC-MS (ESI): *t*<sub>R</sub> = 4.86 min; [M+H]<sup>+</sup> 332.23. HRMS for C<sub>11</sub>H<sub>8</sub>ClINO [M+H]<sup>+</sup> calculated mass: 331.9333, measured: 331.9329.

(*E*) 1-(4-Chloro-2-iodophenyl)-2-(2-nitrovinyl)-1*H*-pyrrole (**21**). Orange solid (57%). Mp: 100 °C. <sup>1</sup>H NMR (400 MHz, CDCl<sub>3</sub>) δ 7.99 (d, *J* = 2.0 Hz, 1H), 7.52 (m, 2H), 7.28 (d, *J* = 8.2 Hz, 1H), 7.07 (d, *J* = 13.3 Hz, 1H), 6.94 (m, 2H), 6.49 (m, 1H). <sup>13</sup>C NMR (100 MHz, CDCl<sub>3</sub>) δ 139.6, 136.5, 132.6, 132.5, 129.9, 129.8, 129.5, 127.5, 125.4, 117.2, 112.4, 98.6. LC-MS (ESI): *t*<sub>R</sub> = 5.35 min; [M+H]<sup>+</sup> 375.29. HRMS for C<sub>12</sub>H<sub>9</sub>ClIN<sub>2</sub>O<sub>2</sub> calculated mass: 374.9391, measured: 374.9391

### (*E*) 1-(2-Chloro-4-iodophenyl)-2-(2-nitrovinyl)-1*H*-pyrrole (**22**).



Synthetic procedure for compound ( **22** ) is similar as that described for compound ( **1** ) and spectra data are shown below.

1-(2-Chloro-4-iodophenyl)-1*H*-pyrrole (**72**). Orange oil (95%). <sup>1</sup>H NMR (400 MHz, CDCl<sub>3</sub>) δ 7.78 (d, *J* = 2.0 Hz, 1H), 7.57 (dd, *J* = 8.3 and 1.9 Hz, 1H), 6.99 (d, *J* = 8.3 Hz, 1H), 6.80 (t, *J* = 2.3 Hz, 2H), 6.27 (t, *J* = 2.3 Hz, 2H). <sup>13</sup>C NMR (100 MHz, CDCl<sub>3</sub>) δ 139.0, 138.6, 137.8,

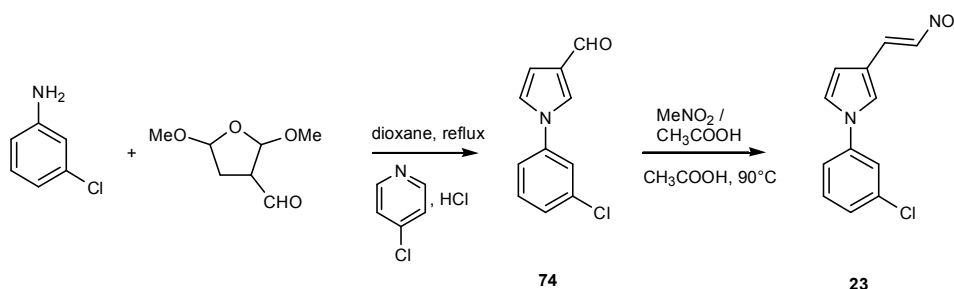
<sup>9</sup> Chai, D. *et al*. Mechanistic Studies of Pd-Catalyzed Regioselective Aryl C-H Bond Functionalization with Strained Alkenes: Origin of Regioselectivity. *Chemistry - A European Journal*, **29**, 8175-8188, S8175/1-S8175/54 (2011).

130.5, 129.0, 122.0, 109.8, 91.6. HRMS for C<sub>10</sub>H<sub>8</sub>ClIN [M+H]<sup>+</sup> calculated mass: 303.9384, measured: 303.9384.

1-(2-Chloro-4-iodophenyl)-1*H*-pyrrole-2-carbaldehyde (**73**). Yellow solid (32%). Mp: 92 °C. <sup>1</sup>H NMR (400 MHz, CDCl<sub>3</sub>) δ 9.52 (s, 1H), 7.87 (d, *J* = 2.0 Hz, 1H), 7.69 (dd, *J* = 8.3 and 2.0 Hz, 1H), 7.13 (dd, *J* = 3.8 and 1.6 Hz, 1H), 7.07 (d, *J* = 8.3 Hz, 1H), 6.94 (m, 1H), 6.46 (dd, *J* = 3.9 and 2.7 Hz, 1H). <sup>13</sup>C NMR (100 MHz, CDCl<sub>3</sub>) δ 178.5, 138.5, 137.2, 136.6, 133.0, 132.8, 131.0, 130.1, 123.2, 111.2, 94.1. LC-MS (ESI): t<sub>R</sub> = 4.98 min; [M+H]<sup>+</sup> 332.28. HRMS for C<sub>11</sub>H<sub>8</sub>ClINO [M+H]<sup>+</sup> calculated mass: 331.9333, measured: 331.9329.

(*E*) 1-(2-Chloro-4-iodophenyl)-2-(2-nitrovinyl)-1*H*-pyrrole (**22**). Orange solid (57%). Mp: 96 °C. <sup>1</sup>H NMR (400 MHz, CDCl<sub>3</sub>) δ 7.96 (d, *J* = 2.0 Hz, 1H), 7.78 (dd, *J* = 8.2 and 1.9 Hz, 1H), 7.56 (d, *J* = 13.4 Hz, 1H), 7.17 (d, *J* = 13.3 Hz, 1H), 7.09 (d, *J* = 8.3 Hz, 1H), 7.00 (dd, *J* = 2.1 and 1.3 Hz, 1H), 6.95 (m, 1H), 6.49 (t, *J* = 3.3 Hz, 1H). <sup>13</sup>C NMR (100 MHz, CDCl<sub>3</sub>) δ 139.3, 137.3, 135.5, 133.4, 132.6, 130.8, 130.0, 127.4, 125.7, 116.8, 112.4, 95.4. LC-MS (ESI): t<sub>R</sub> = 5.35 min; [M+H]<sup>+</sup> 375.29. HRMS for C<sub>12</sub>H<sub>9</sub>ClIN<sub>2</sub>O<sub>2</sub> calculated mass: 374.9391, measured: 374.9391.

**(*E*) 1-(3-Chlorophenyl)-3-(2-nitrovinyl)-1*H*-pyrrole (**23**).**



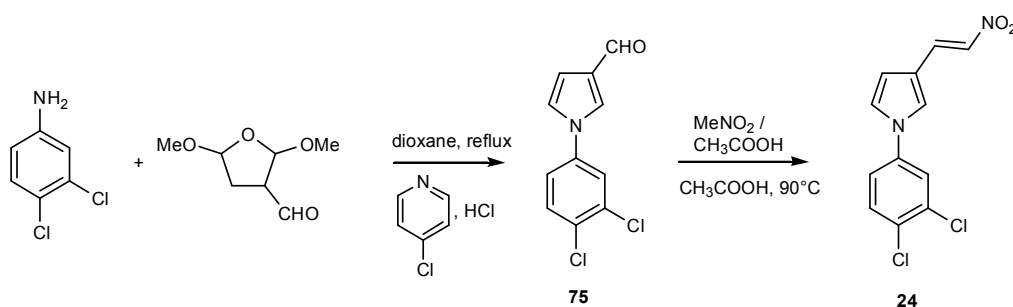
Synthetic procedure for compound (**23**) is similar as that described for compound (**2**) and spectra data are shown below.

1-(3-Chlorophenyl)-1*H*-pyrrole-3-carbaldehyde (**74**).<sup>10</sup> Brown solid (50%). Mp: 68 °C. <sup>1</sup>H NMR (400 MHz, CDCl<sub>3</sub>) δ 9.86 (s, 1H), 7.66 (t, *J* = 2.0 Hz, 1H), 7.44 (t, *J* = 2.0 Hz, 1H), 7.41 (d, *J* = 8.0 Hz, 1H), 7.37-7.31 (m, 2H), 7.07 (m, 1H), 6.81 (dd, *J* = 3.1 and 1.6 Hz, 1H). <sup>13</sup>C NMR (100 MHz, CDCl<sub>3</sub>) δ 185.4, 140.5, 135.6, 131.0, 128.5, 127.4, 127.0, 122.2, 121.4, 119.2, 110.0. LC-MS (ESI): t<sub>R</sub> = 4.42 min; [M+H]<sup>+</sup> 206.34.

(*E*) 1-(3-chlorophenyl)-3-(2-nitrovinyl)-1*H*-pyrrole (**23**). Brown solid (50%). Mp: 104 °C. <sup>1</sup>H NMR (400 MHz, CDCl<sub>3</sub>) δ 8.01 (d, *J* = 13.3 Hz, 1H), 7.46 (d, *J* = 13.3 Hz, 1H), 7.43-7.40 (m, 3H), 7.33 (dt, *J* = 8.1 and 1.0 Hz, 1H), 7.39 (dt, *J* = 8.0 and 1.0 Hz, 1H), 7.11 (t, *J* = 2.7 Hz, 1H), 6.57 (dd, *J* = 3.0 and 1.6 Hz, 1H). <sup>13</sup>C NMR (100 MHz, CDCl<sub>3</sub>) δ 140.4, 135.7, 134.3, 133.1, 131.0, 127.2, 124.9, 122.7, 121.1, 118.8, 118.2, 109.5. LC-MS (ESI): t<sub>R</sub> = 5.15 min; [M+H]<sup>+</sup> 249.40. HRMS for C<sub>12</sub>H<sub>10</sub>ClN<sub>2</sub>O<sub>2</sub> [M+H]<sup>+</sup> calculated mass: 249.0425, measured: 249.0424.

<sup>10</sup> McInnes, Campbell and Liu, Shu. Cyclin based inhibitors of CDK2 and CDK4. U.S. Pat. Appl. Publ., 20130289240, 31 Oct 2013.

**(E) 1-(3,4-Dichlorophenyl)-3-(2-nitrovinyl)-1H-pyrrole (24).**

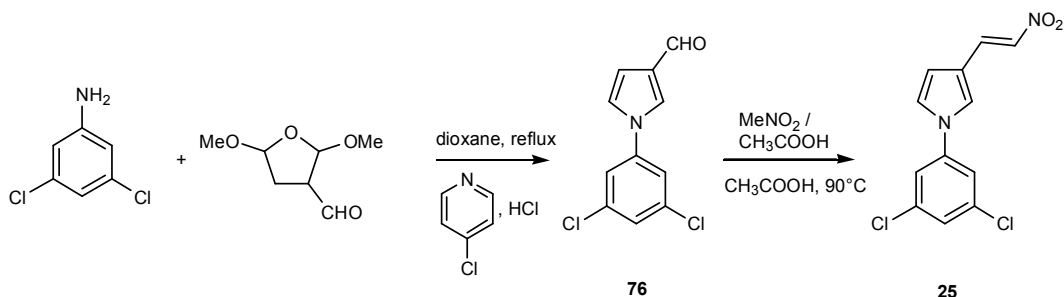


Synthetic procedure for compound ( 24) is similar as that described for compound ( 2) and spectra data are shown below.

1-(3,4-Dichlorophenyl)-1H-pyrrole-3-carbaldehyde (**75**).<sup>11</sup> Orange solid (30%). Mp: 112 °C. <sup>1</sup>H NMR (400 MHz, CDCl<sub>3</sub>) δ 9.78 (s, 1H), 7.56 (t, *J* = 1.9 Hz, 1H), 7.48 (m, 2H), 7.21 (dd, *J* = 8.6 and 2.6 Hz, 1H), 6.98 (t, *J* = 2.6 Hz, 1H), 6.74 (dd, *J* = 3.0 and 1.7 Hz, 1H). <sup>13</sup>C NMR (100 MHz, CDCl<sub>3</sub>) δ 185.4, 138.8, 134.0, 131.6, 131.4, 128.7, 126.8, 123.0, 122.1, 120.2, 110.0. LC-MS (ESI): *t*<sub>R</sub> = 4.92 min; [M+H]<sup>+</sup> 240.26.

(*E*) 1-(3,4-Dichlorophenyl)-3-(2-nitrovinyl)-1H-pyrrole (**24**). Brown solid (40%). Mp: 128 °C. <sup>1</sup>H NMR (400 MHz, CDCl<sub>3</sub>) δ 8.01 (d, *J* = 13.2 Hz, 1H), 7.58 (d, *J* = 8.6 Hz, 1H), 7.54 (d, *J* = 2.9 Hz, 1H), 7.47 (d, *J* = 13.4 Hz, 1H), 7.41 (t, *J* = 2.0 Hz, 1H), 7.27 (dd, *J* = 8.6 and 2.6 Hz, 1H), 7.10 (t, *J* = 2.5 Hz, 1H), 6.59 (dd, *J* = 3.1 and 1.8 Hz, 1H). <sup>13</sup>C NMR (100 MHz, CDCl<sub>3</sub>) δ 138.6, 134.6, 134.0, 132.8, 131.6, 131.2, 124.7, 122.7, 122.6, 119.9, 118.4, 109.8. LC-MS (ESI): *t*<sub>R</sub> = 5.37 min; [M+H]<sup>+</sup> 283.44. HRMS for C<sub>12</sub>H<sub>9</sub>Cl<sub>2</sub>N<sub>2</sub>O<sub>2</sub> [M+H]<sup>+</sup> calculated mass: 283.0035, measured: 283.0036.

**(E) 1-(3,5-Dichlorophenyl)-3-(2-nitrovinyl)-1H-pyrrole (25).**



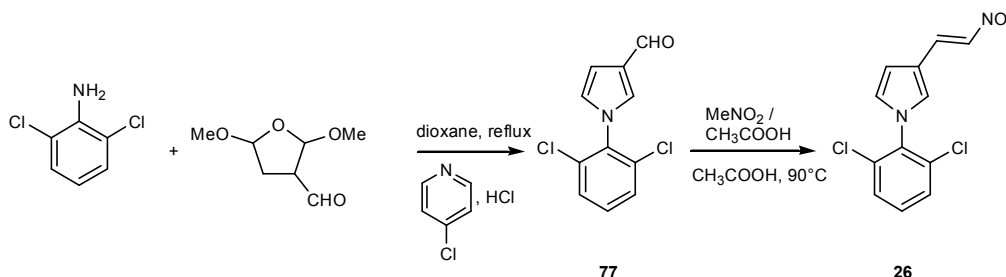
Synthetic procedure for compound ( 25) is similar as that described for compound ( 2) and spectra data are shown below.

1-(3,5-Dichlorophenyl)-1H-pyrrole-3-carbaldehyde (**76**). Brown solid (35%). Mp: 154 °C. <sup>1</sup>H NMR (400 MHz, CDCl<sub>3</sub>) δ 9.86 (s, 1H), 7.65 (t, *J* = 2.1 Hz, 1H), 7.36-7.34 (m, 3H), 7.07 (t, *J* = 2.8 Hz, 1H), 6.83 (dd, *J* = 3.0 and 1.6 Hz, 1H). <sup>13</sup>C NMR (100 MHz, CDCl<sub>3</sub>) δ 185.3, 141.1, 136.3, 128.8, 127.3, 126.7, 122.0, 119.7, 110.4. LC-MS (ESI): *t*<sub>R</sub> = 4.85 min; [M+H]<sup>+</sup> 240.35. HRMS for C<sub>11</sub>H<sub>8</sub>Cl<sub>2</sub>NO [M+H]<sup>+</sup> calculated mass: 239.9975, measured: 239.9977.

<sup>11</sup> Halder, P. *et al.* Sodium borohydride-iodine mediated reduction of  $\gamma$ -lactam carboxylic acids followed by DDQ mediated oxidative aromatization: a simple approach towards N-aryl-formylpyrroles and 1,3-diaryl-formylpyrroles. *Tetrahedron*, **14**, 3049-3056 (2007)

(*E*) 1-(3,5-Dichlorophenyl)-3-(2-nitrovinyl)-1*H*-pyrrole (**25**). Brown solid (40%). Mp: 190°C. <sup>1</sup>H NMR (400 MHz, CDCl<sub>3</sub>) δ 7.99 (d, *J* = 13.3 Hz, 1H), 7.45 (d, *J* = 13.4 Hz, 1H), 7.41 (t, *J* = 1.9 Hz, 1H), 7.34 (t, *J* = 1.7 Hz, 1H), 7.31 (d, *J* = 1.8 Hz, 2H), 7.10 (t, *J* = 2.7 Hz, 1H), 6.58 (dd, *J* = 3.0 and 1.6 Hz, 1H). <sup>13</sup>C NMR (100 MHz, CDCl<sub>3</sub>) δ 140.9, 136.3, 134.7, 132.6, 127.1, 124.5, 122.6, 119.3, 118.6, 109.9. LC-MS (ESI): t<sub>R</sub> = 5.49 min; [M+H]<sup>+</sup> 283.40. HRMS for C<sub>12</sub>H<sub>9</sub>Cl<sub>2</sub>N<sub>2</sub>O<sub>2</sub> [M+H]<sup>+</sup> calculated mass: 283.0035, measured: 283.0035.

**(*E*) 1-(2,6-Dichlorophenyl)-3-(2-nitrovinyl)-1*H*-pyrrole (**26**).**

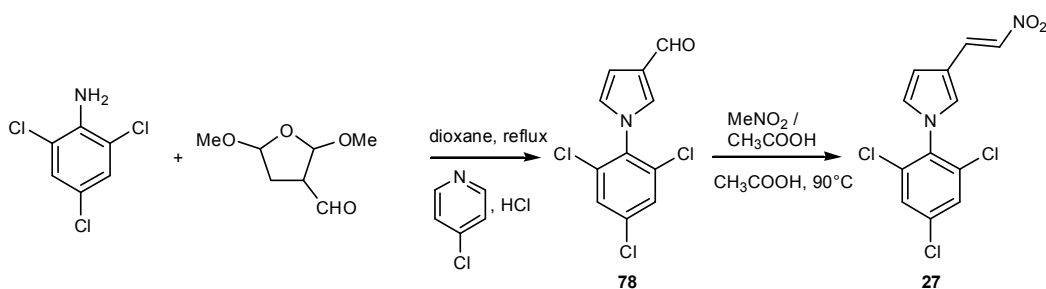


Synthetic procedure for compound (**26**) is similar as that described for compound (**2**) and spectra data are shown below.

1-(2,6-Dichlorophenyl)-1*H*-pyrrole-3-carbaldehyde (**77**).<sup>6</sup> White solid (30%). Mp: 92°C. <sup>1</sup>H NMR (400 MHz, CDCl<sub>3</sub>) δ 9.79 (s, 1H), 7.42-7.39 (m, 2H), 7.30 (m, 1H), 7.27 (dd, *J* = 3.7 and 1.1 Hz, 1H), 6.75 (dd, *J* = 3.1 and 1.5 Hz, 1H), 6.66 (m, 1H). <sup>13</sup>C NMR (100 MHz, CDCl<sub>3</sub>) δ 185.4, 135.5, 133.9, 130.6, 130.4, 128.9, 127.7, 124.7, 108.5. LC-MS (ESI): t<sub>R</sub> = 4.85 min; [M+H]<sup>+</sup> 240.39.

(*E*) 1-(2,6-Dichlorophenyl)-3-(2-nitrovinyl)-1*H*-pyrrole (**26**). Yellow solid (50%). Mp: 108°C. <sup>1</sup>H NMR (400 MHz, CDCl<sub>3</sub>) δ 8.04 (d, *J* = 13.2 Hz, 1H), 7.49-7.46 (m, 3H), 7.37 (dd, *J* = 8.8 and 7.3 Hz, 1H), 7.12 (m, 1H), 6.77 (m, 1H), 6.61-6.58 (m, 1H). <sup>13</sup>C NMR (100 MHz, CDCl<sub>3</sub>) δ 134.1, 133.9, 133.4, 130.5, 129.9, 128.9, 128.1, 125.3, 117.1, 108.0. LC-MS (ESI): t<sub>R</sub> = 5.08 min; [M+H]<sup>+</sup> 283.40. HRMS for C<sub>12</sub>H<sub>9</sub>Cl<sub>2</sub>N<sub>2</sub>O<sub>2</sub> [M+H]<sup>+</sup> calculated mass: 283.0035, measured: 283.0035.

**(*E*) 3-(2-Nitrovinyl)-1-(2,4,6-trichlorophenyl)-1*H*-pyrrole (**27**).**

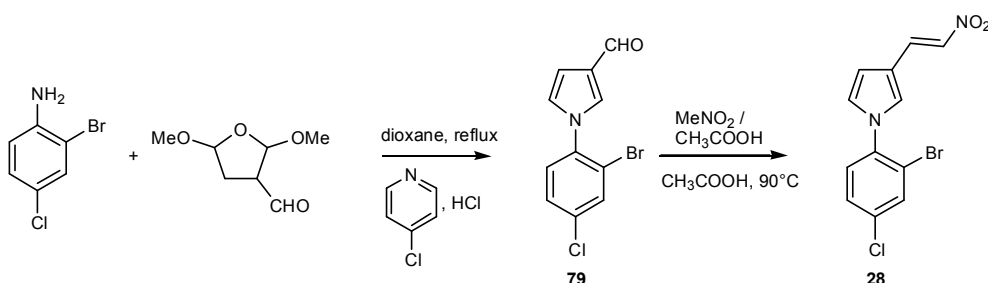


Synthetic procedure for compound ( **27**) is similar as that described for compound ( **2**) and spectra data are shown below.

1-(2,4,6-Trichlorophenyl)-1*H*-pyrrole-3-carbaldehyde (**78**). Beige solid (30%). Mp: 74°C. <sup>1</sup>H NMR (400 MHz, CDCl<sub>3</sub>) δ 9.87 (s, 1H), 7.50 (s, 2H), 7.31 (t, *J* = 2.0 Hz, 1H), 6.83 (dd, *J* = 3.1 and 1.5 Hz, 1H), 6.71-6.69 (m, 1H). <sup>13</sup>C NMR (100 MHz, CDCl<sub>3</sub>) δ 185.3, 135.8, 134.6, 134.3, 130.1, 128.9, 127.9, 124.6, 108.8. LC-MS (ESI): t<sub>R</sub> = 4.86 min; [M+H]<sup>+</sup> 274.31. HRMS for C<sub>11</sub>H<sub>7</sub>Cl<sub>3</sub>NO [M+H]<sup>+</sup> calculated mass: 273.9587, measured: 273.9582.

(*E*) 3-(2-Nitrovinyl)-1-(2,4,6-trichlorophenyl)-1*H*-pyrrole (**27**). Yellow solid (50%). Mp: 90 °C. <sup>1</sup>H NMR (400 MHz, CDCl<sub>3</sub>) δ 8.02 (d, *J* = 13.2 Hz, 1H), 7.50 (s, 2H), 7.47 (d, *J* = 13.3 Hz, 1H), 7.08 (t, *J* = 1.7 Hz, 1H), 6.73 (t, *J* = 6.7 Hz, 1H), 6.58 (m, 1H). <sup>13</sup>C NMR (100 MHz, CDCl<sub>3</sub>) δ 135.8, 134.5, 134.3, 134.2, 133.1, 128.9, 127.9, 125.2, 117.3, 108.3. LC-MS (ESI): t<sub>R</sub> = 5.39 min; [M-H]<sup>-</sup> 315.31. HRMS for C<sub>12</sub>H<sub>8</sub>Cl<sub>3</sub>N<sub>2</sub>O<sub>2</sub> [M+H]<sup>+</sup> calculated mass: 316.9645, measured: 316.9645.

**(E) 1-(2-Bromo-4-chlorophenyl)-3-(2-nitrovinyl)-1*H*-pyrrole (**28**).**



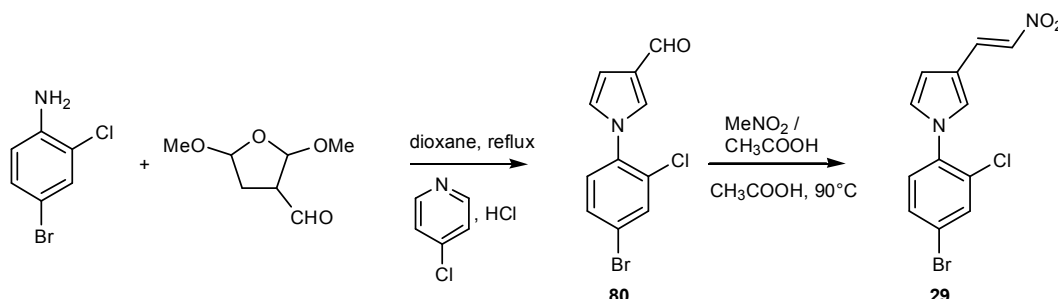
Synthetic procedure for compound ( **28**) is similar as that described for compound ( **2**) and spectra data are shown below.

1-(2-Bromo-4-chlorophenyl)-1*H*-pyrrole-3-carbaldehyde (**79**). Rose solid (32%). Mp: 86 °C. <sup>1</sup>H NMR (400 MHz, CDCl<sub>3</sub>) δ 9.85 (s, 1H), 7.74 (d, *J* = 2.3 Hz, 1H), 7.44 (t, *J* = 1.8 Hz, 1H), 7.42 (dd, *J* = 8.4 and 2.2 Hz, 1H), 7.30 (d, *J* = 8.3 Hz, 1H), 6.83 (m, 1H), 6.78 (dd, *J* = 3.0 and 1.7 Hz, 1H). <sup>13</sup>C NMR (100 MHz, CDCl<sub>3</sub>) δ 185.4, 137.8, 135.3, 133.7, 130.1, 128.7, 128.7, 127.7, 124.9, 120.4, 108.7. LC-MS (ESI): t<sub>R</sub> = 4.72 min; [M+H]<sup>+</sup> 284.25. HRMS for C<sub>11</sub>H<sub>8</sub>BrClNO [M+H]<sup>+</sup> calculated mass: 283.9472, measured: 283.9470.

(*E*) 1-(2-Bromo-4-chlorophenyl)-3-(2-nitrovinyl)-1*H*-pyrrole (**28**). Yellow solid (53%). <sup>1</sup>H NMR (400 MHz, CDCl<sub>3</sub>) δ 8.08 (d, *J* = 13.2 Hz, 1H), 8.00 (d, *J* = 2.4 Hz, 1H), 7.93 (d, *J* = 13.1 Hz, 1H), 7.72 (t, *J* = 1.8 Hz, 1H), 7.61 (dd, *J* = 8.5 and 2.4 Hz, 1H), 7.53 (d, *J* = 8.6 Hz, 1H), 7.13 (t, *J* = 1.8 Hz, 1H), 6.82 (dd, *J* = 2.8 and 1.6 Hz, 1H). <sup>13</sup>C NMR (100 MHz, CDCl<sub>3</sub>)

$\delta$  138.2, 134.9, 134.5, 134.3, 133.3, 130.3, 130.0, 129.4, 126.4, 120.4, 117.4, 109.2. LC-MS (ESI):  $t_R = 5.36$  min;  $[M+H]^+$  327.35. HRMS for  $C_{12}H_9BrClN_2O_2$   $[M+H]^+$  calculated mass: 326.9530, measured: 326.9529.

**(E) 1-(4-Bromo-2-chlorophenyl)-3-(2-nitrovinyl)-1H-pyrrole (29).**

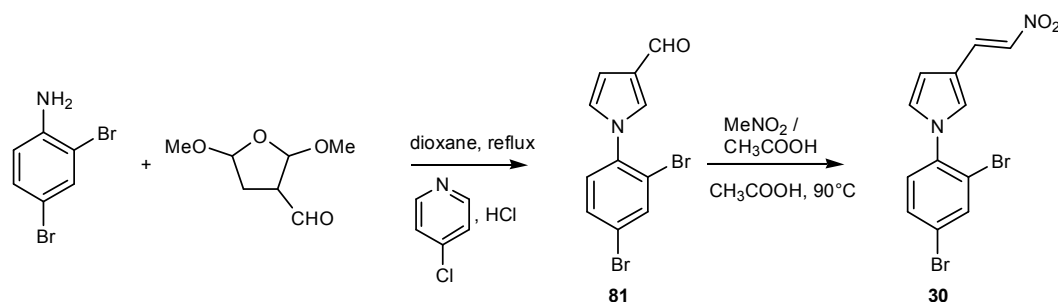


Synthetic procedure for compound ( **29** ) is similar as that described for compound ( **2** ) and spectra data are shown below.

1-(4-Bromo-2-chlorophenyl)-1H-pyrrole-3-carbaldehyde (**80**). Orange solid (34%). Mp: 100 °C.  $^1H$  NMR (400 MHz,  $CDCl_3$ )  $\delta$  9.88 (s, 1H), 7.75 (d,  $J = 2.1$  Hz, 1H), 7.55 (dd,  $J = 8.4$  and 2.1 Hz, 1H), 7.50 (t,  $J = 1.7$  Hz, 1H), 7.28 (d,  $J = 8.3$  Hz, 1H), 6.89 (t,  $J = 2.7$  Hz, 1H), 6.82 (dd,  $J = 2.9$  and 1.5 Hz, 1H).  $^{13}C$  NMR (100 MHz,  $CDCl_3$ )  $\delta$  185.4, 136.6, 133.6, 131.2, 130.8, 130.0, 128.7, 127.8, 124.8, 122.5, 108.9. LC-MS (ESI):  $t_R = 4.76$  min;  $[M+H]^+$  284.21. HRMS for  $C_{11}H_8BrClNO$   $[M+H]^+$  calculated mass: 283.9472, measured: 283.9470.

(E) 1-(4-Bromo-2-chlorophenyl)-3-(2-nitrovinyl)-1H-pyrrole (**29**). Yellow solid (55%). Mp: 182 °C.  $^1H$  NMR (400 MHz,  $DMSO-d_6$ )  $\delta$  8.09 (d,  $J = 13.3$  Hz, 1H), 8.00 (dd,  $J = 2.1$  and 0.9 Hz, 1H), 7.93 (d,  $J = 13.3$  Hz, 1H), 7.76 (bs, 1H), 7.71 (ddd,  $J = 8.5$ , 2.1, and 0.9 Hz, 1H), 7.49 (dd,  $J = 8.4$  and 0.8 Hz, 1H), 7.17 (m, 1H), 6.83 (m, 2.8 and 1.6 Hz, 1H).  $^{13}C$  NMR (100 MHz,  $DMSO-d_6$ )  $\delta$  136.9, 134.8, 134.6, 133.3, 132.0, 130.2, 130.1, 130.0, 126.3, 122.1, 117.6, 109.3. LC-MS (ESI):  $t_R = 5.38$  min;  $[M+H]^+$  327.35. HRMS for  $C_{12}H_9BrClN_2O_2$   $[M+H]^+$  calculated mass: 326.9530, measured: 326.9528.

**(E) 1-(2,4-Dibromophenyl)-2-(2-nitrovinyl)-1H-pyrrole (30).**

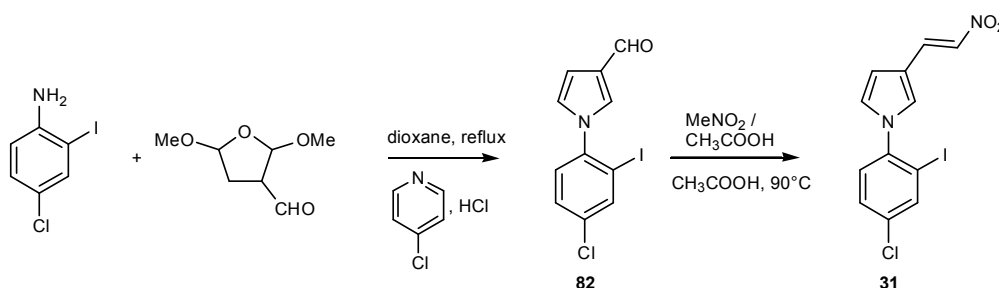


Synthetic procedure for compound ( **30** ) is similar as that described for compound ( **2** ) and spectra data are shown below.

1-(2,4-Dibromophenyl)-1*H*-pyrrole-3-carbaldehyde (**81**). Pink solid (32%). Mp: 86 °C. <sup>1</sup>H NMR (400 MHz, CDCl<sub>3</sub>) δ 9.85 (s, 1H), 7.89 (d, *J* = 2.1 Hz, 1H), 7.57 (dd, *J* = 8.5 and 2.1 Hz, 1H), 7.45 (t, *J* = 1.8 Hz, 1H), 7.24 (d, *J* = 8.4 Hz, 1H), 6.84 (m, 1H), 6.78 (m, 1H). <sup>13</sup>C NMR (100 MHz, CDCl<sub>3</sub>) δ 185.4, 138.2, 136.4, 131.7, 130.0, 129.1, 127.7, 124.8, 123.0, 120.6, 108.7. LC-MS (ESI): t<sub>R</sub> = 4.81 min; [M+H]<sup>+</sup> 328.25.

(*E*) 1-(2,4-Dibromophenyl)-2-(2-nitrovinyl)-1*H*-pyrrole (**30**). Yellow solid (52%). Mp: 190 °C. <sup>1</sup>H NMR (400 MHz, DMSO-*d*<sub>6</sub>) δ 8.10 (s, 1H), 8.08 (d, *J* = 13.2 Hz, 1H), 7.92 (d, *J* = 13.1 Hz, 1H), 7.73 (dd, *J* = 8.4 and 2.1 Hz, 1H), 7.45 (d, *J* = 8.5 Hz, 1H), 7.12 (m, 1H), 7.17 (m, 1H), 6.80 (dd, 3.0 and 1.6 Hz, 1H). <sup>13</sup>C NMR (100 MHz, DMSO-*d*<sub>6</sub>) δ 138.6, 136.0, 134.9, 134.5, 132.4, 130.3, 130.2, 126.4, 122.6, 120.6, 117.4, 109.2. LC-MS (ESI): t<sub>R</sub> = 5.44 min; [M+H]<sup>+</sup> 369.37. HRMS for C<sub>12</sub>H<sub>9</sub>Br<sub>2</sub>N<sub>2</sub>O<sub>2</sub> [M+H]<sup>+</sup> calculated mass: 370.9025, measured: 370.9023.

**(*E*) 1-(4-Chloro-2-iodophenyl)-3-(2-nitrovinyl)-1*H*-pyrrole (**31**).**



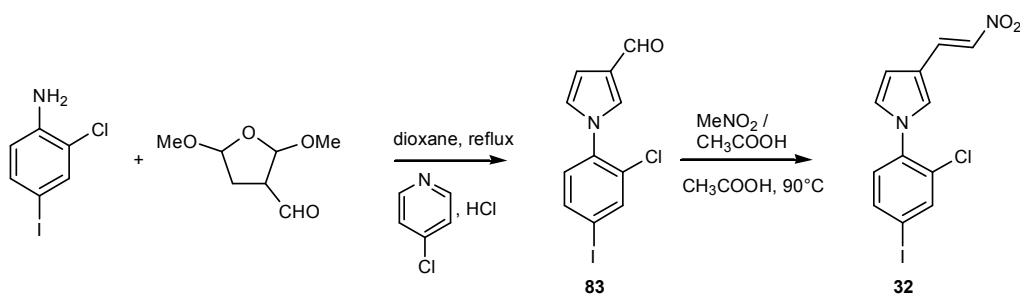
Synthetic procedure for compound (**31**) is similar as that described for compound (**2**) and spectra data are shown below.

1-(4-Chloro-2-iodophenyl)-1*H*-pyrrole-3-carbaldehyde (**82**). Yellow solid (31%). Mp: 102 °C. <sup>1</sup>H NMR (400 MHz, CDCl<sub>3</sub>) δ 9.79 (s, 1H), 7.89 (d, *J* = 2.4 Hz, 1H), 7.38 (dd, *J* = 8.4 and 2.3 Hz, 1H), 7.31 (t, *J* = 1.8 Hz, 1H), 7.18 (d, *J* = 8.4 Hz, 1H), 6.71 (m, 2H). <sup>13</sup>C NMR (100 MHz, CDCl<sub>3</sub>) δ 185.4, 141.3, 139.5, 135.5, 130.0, 129.5, 128.2, 127.7, 124.8, 108.8, 95.6. LC-MS (ESI): t<sub>R</sub> = 4.81 min; [M+H]<sup>+</sup> 332.23. HRMS for C<sub>11</sub>H<sub>8</sub>ClINO [M+H]<sup>+</sup> calculated mass: 331.9333, measured: 331.9328.

(*E*) 1-(4-Chloro-2-iodophenyl)-3-(2-nitrovinyl)-1*H*-pyrrole (**31**). Yellow solid (53%). <sup>1</sup>H NMR (400 MHz, CDCl<sub>3</sub>) δ 8.03 (d, *J* = 13.3 Hz, 1H), 7.96 (d, *J* = 2.3 Hz, 1H), 7.47 (d, *J* = 13.3 Hz, 1H), 7.45 (dd, *J* = 2.3 and 8.3 Hz, 1H), 7.24 (d, *J* = 8.4 Hz, 1H), 7.16 (t, *J* = 1.8 Hz, 1H), 6.82 (t, *J* = 2.8 Hz, 1H), 6.55 (dd, *J* = 2.9 and 1.6 Hz, 1H). <sup>13</sup>C NMR (100 MHz, CDCl<sub>3</sub>) δ 139.3, 138.9, 137.2, 137.1, 134.2, 133.2, 130.5, 128.7, 127.8, 125.3, 117.3, 108.3. LC-MS (ESI): t<sub>R</sub> = 5.40 min; [M-H]<sup>-</sup> 373.32. HRMS for C<sub>12</sub>H<sub>9</sub>ClIN<sub>2</sub>O<sub>2</sub> [M+H]<sup>+</sup> calculated mass: 374.9391, measured: 374.9390.

**(*E*) 1-(2-Chloro-4-iodophenyl)-3-(2-nitrovinyl)-1*H*-pyrrole (**32**).**





Synthetic procedure for compound ( **32** ) is similar as that described for compound ( **2** ) and spectra data are shown below.

1-(4-Chloro-2-iodophenyl)-1*H*-pyrrole-3-carbaldehyde (**83**). Beige solid (35%). Mp: 118 °C. <sup>1</sup>H NMR (400 MHz, CDCl<sub>3</sub>) δ 9.85 (s, 1H), 7.91 (d, *J* = 1.8 Hz, 1H), 7.72 (dd, *J* = 8.3 and 1.8 Hz, 1H), 7.48 (t, *J* = 1.8 Hz, 1H), 7.10 (d, *J* = 8.3 Hz, 1H), 6.87 (m, 1H), 6.79 (dd, *J* = 3.2 and 1.7 Hz, 1H). <sup>13</sup>C NMR (100 MHz, CDCl<sub>3</sub>) δ 185.4, 139.3, 137.2, 137.1, 130.6, 130.0, 128.9, 127.8, 124.7, 108.8, 93.5. LC-MS (ESI): *t*<sub>R</sub> = 4.87 min; [M+H]<sup>+</sup> 332.28. HRMS for C<sub>11</sub>H<sub>8</sub>ClINO [M+H]<sup>+</sup> calculated mass: 331.9333, measured: 331.9328.

(*E*) 1-(2-Chloro-4-iodophenyl)-3-(2-nitrovinyl)-1*H*-pyrrole (**32**). Yellow solid (53%). <sup>1</sup>H NMR (400 MHz, CDCl<sub>3</sub>) δ 8.02 (d, *J* = 13.4 Hz, 1H), 7.91 (d, *J* = 1.9 Hz, 1H), 7.72 (dd, *J* = 8.2 and 2.0 Hz, 1H), 7.46 (d, *J* = 13.5 Hz, 1H), 7.25 (t, 1.9 Hz, 1H), 7.08 (d, *J* = 8.4 Hz, 1H), 6.91 (m, 1H), 6.55 (m, 1H). <sup>13</sup>C NMR (100 MHz, CDCl<sub>3</sub>) δ 139.3, 138.9, 137.2, 137.1, 134.2, 133.2, 130.5, 128.7, 127.8, 125.3, 117.3, 108.3. LC-MS (ESI): *t*<sub>R</sub> = 5.47 min; [M-H]<sup>-</sup> 373.27. HRMS for C<sub>12</sub>H<sub>9</sub>ClIN<sub>2</sub>O<sub>2</sub> [M+H]<sup>+</sup> calculated mass: 374.9391, measured: 374.9390.